

ENHANCED ELECTROKINETIC REMEDICATION FOR THE REMOVAL OF PFOA FROM CONTAMINATED KAOLINITE SOIL

by Namuun Ganbat

Thesis submitted in fulfilment of the requirements for
the degree of

Doctor of Philosophy

under the supervision of Dr Ali Altaee and Prof John Zhou

University of Technology Sydney
Faculty of Engineering and Information Technology

October 2023

CERTIFICATE OF ORIGINAL AUTHORSHIP

I, **Namuun Ganbat**, declare that this thesis, is submitted in fulfilment of the requirements for the award of *Doctor of Philosophy*, in the *School of Civil and Environmental Engineering/ Faculty of Engineering and Information Technology* at the **University of Technology Sydney**.

This thesis is wholly my own work unless otherwise referenced or acknowledged. In addition, I certify that all information sources and literature used are indicated in the thesis.

This document has not been submitted to any other academic institution for qualification.

This research has been supported by the Australian Government Research Training Program (RTP).

Signature

Production Note:
Signature removed prior to publication.

16/10/2023

ACKNOWLEDGEMENT

First and foremost, I would like to express my sincere appreciation to my principal supervisor, Ali Altaee, for his unwavering support, guidance, and encouragement throughout my PhD journey. Ali's exceptional mentorship has allowed me to grow as a scholar and an individual. His faith in my abilities, patience, and mentorship have been invaluable in helping me to grow academically. I would also like to express my gratitude to my co-supervisor, John Zhou, for his insightful feedback, direction, and assistance. Moreover, I would like to acknowledge the exceptional support and understanding of both Ali and John during the unprecedented outbreak of COVID-19. Despite the significant challenges posed by the pandemic, their support and encouragement were cooperative for me to continue working on my project.

I am sincerely grateful to my brother, Barsbold, and sister-in-law, Zoljargal, for their invaluable support and unconditional love. Without their help, I would not have been able to reach where I am today. Their unwavering support in caring for Anand and Anu-Ujin has been essential, and I am infinitely thankful for their kindness. My deepest gratitude to my loving parents, Bolormaa and Ganbat, for their unconditional love and support. Their persistent encouragement and motivation have always brought out the best in me. I also want to express my appreciation to my husband, Erdenemunkh, for your love and support of our family, who have been my pillars of strength during the challenging times. Anand and Anu-Ujin have been my constant motivation, inspiration, and source of joy. My children are the biggest accomplishment in my life, my source of strength; I hope to inspire them to pursue their passions and achieve their dreams, as they have inspired me to pursue mine. Finally, this thesis is dedicated to my late grandfather Samdan, the greatest person I have ever known, also the first person to inspire me to become a scientist.

TABLE OF CONTENTS

CERTIFICATE OF ORIGINAL AUTHORSHIP	i
ACKNOWLEDGEMENT	ii
TABLE OF CONTENTS.....	iii
LIST OF FIGURES	vii
LIST OF TABLES	ix
PUBLICATIONS	x
ABSTRACT	xi
CHAPTER 1: INTRODUCTION	1
1.1 SOIL CONTAMINATION	1
1.1.1 Impacts of PFAS on environmental quality and human health	5
1.1.2 Techniques for the remediation of PFAS-contaminated soil.....	6
1.1.3 Electrokinetic process for the removal of PFAS	8
1.2 RESEARCH HYPOTHESIS	10
1.3 RESEARCH SIGNIFICANCE.....	12
1.4 RESEARCH OBJECTIVES	12
1.5 THESIS STRUCTURE	13
CHAPTER 2 : LITERATURE REVIEW	17
2.1 CONVENTIONAL APPROACHES TO SOIL REMEDIATION	17
2.1.1 Bioremediation.....	17
2.1.2 Phytoremediation	18
2.1.3 Thermal treatment	21
2.1.4 Soil washing.....	23
2.1.5 Immobilization	25
2.1.6 Mechanical treatment.....	26
2.1.7 Encapsulation	26
2.1.8 Electron beam technology.....	27
2.2 PHYSICAL-CHEMICAL REMEDIATION METHODS	27
2.2.1 Solvent extraction.....	28

2.2.2 Supercritical fluid extraction	28
2.3 ELECTROKINETIC REMEDIATION METHOD (EK)	29
2.3.1 Fundamentals of electrokinetic remediation.....	30
2.4 INFLUENCE OF FACTORS ON THE ELECTROKINETIC PROCESS.	32
2.4.1 Soil properties	32
2.4.2 Influence of the electrode type	33
2.4.3 Impact of contamination type.....	33
2.5 ELECTROKINETIC ENHANCEMENT	37
2.5.1 Surfactants aided electrokinetic remediation.....	37
2.5.2 Permeable reactive barrier.....	38
2.5.3 Activated carbon	39
2.5.4 Chitosan	40
2.5.5 Biochar	40
2.5.6 Carbon nanotubes.....	41
2.5.7 Nanoscale zero-valent iron.....	42
CHAPTER 3 : MATERIALS AND METHOD	44
3.1 MATERIALS.....	44
3.2 METHODS.....	45
3.2.1 Soil Preparation.....	45
3.2.2 Surfactants.....	46
3.2.3 Permeable reactive barrier (PRB).....	46
3.2.4 Electrokinetic cell set-up.....	47
3.2.5 Extraction procedure for PFOA	48
3.2.6 PFOA removal	49
3.2.7 Specific energy consumption (SEC)	50
3.2.8 Analytical approach.....	50
CHAPTER 4 : INVESTIGATION OF THE EFFECT OF SURFACTANT ON	
ELECTROKINETIC TREATMENT OF PFOA CONTAMINATED SOIL	53
4.1 BACKGROUND.....	53

4.2 MATERIALS AND METHODS	58
4.2.1 Materials and preparation of the soil	58
4.3 ANALYTICAL PROCEDURE	59
4.3.1 Extraction of PFOA from soil	59
4.3.2 Soil pH measurement	60
4.3.3 Soil conductivity measurement	60
4.3.4 LC-MS analysis.....	60
4.4 EXPERIMENTAL SET-UP	61
4.5 RESULTS AND DISCUSSION.....	63
4.5.1 Change in current and voltage.....	63
4.5.2 Change in pH of the soil.....	67
4.5.3 Change in the soil's electric conductivity	69
4.5.4 Performance of EK and different types of surfactants.....	70
4.5.5 Impact of PFOA concentration.....	79
4.5.6 Energy Consumption and mass balance	82
4.6 CONCLUSIONS	84
CHAPTER 5 : PFOA REMEDIATION FROM KAOLINITE SOIL BY ELECTROKINETIC PROCESS COUPLED WITH AC/FEAC- PERMEABLE REACTIVE BARRIER	87
5.1 BACKGROUND	87
5.2 MATERIALS AND METHODS	91
5.2.1 Experimental set-up and analysis	91
5.2.2 Iron coating of AC.....	92
5.2.3 Electrokinetic cell setup	92
5.2.4 PFOA extraction.....	94
5.3 RESULTS AND DISCUSSION	95
5.3.1 Change in the current and voltage.....	95
5.3.2 Change in pH and electric conductivity of the soil	98
5.3.3 Removal of PFOA from soil	101
5.3.4 Characterisation of PRB.....	106
5.3.5 PERFORMANCE OF ACTIVATED CARBON AND IRON LOADED ACTIVATED CARBON PRBS	109

5.3.6 ENERGY CONSUMPTION AND ELECTROSMOTIC FLOW	111
5.4 CONCLUSIONS	114
CHAPTER 6 : IRON SLAG PERMEABLE REACTIVE BARRIER FOR PFOA REMOVAL BY THE ELECTROKINETIC PROCESS	115
6.1 BACKGROUND	115
6.2 MATERIALS AND METHODS	119
6.2.1 EXPERIMENTAL SET-UP AND ANALYSIS	119
6.2.2 ELECTROKINETIC CELL SETUP AND TEST DESIGN.....	120
6.2.3 PFOA ANALYSIS	122
6.3 RESULTS AND DISCUSSION	123
6.3.1 CHANGE IN THE CURRENT AND VOLTAGE.....	123
6.3.2 SOIL pH AND ELECTRIC CONDUCTIVITY	127
6.3.3 Removal efficiency	132
6.3.4 Characteristics of PRB	138
6.3.5 Specific energy consumption	145
6.4 CONCLUSION.....	147
CHAPTER 7 : CONCLUSIONS AND FUTURE RESEARCH RECCOMENDATIONS	145
7.1 CONCLUSIONS	145
7.2 THE IMPORTANCE OF THE RESEARCH AND ITS IMPACT ON THE FIELD	148
7.3 FUTURE STUDIES	149
REFERENCES.....	152

LIST OF FIGURES

Figure 2.1: Advantages and disadvantages of phytoremediation.	19
Figure 2.2: electroosmosis and electromigration of ions (adapted from Virkutyte (2002)).	31
Figure 4.1:Electrokinetic cell set up scheme.....	59
Figure 4.2: (a) Change in electric current and voltage over time in EK tests E1-E3-E5 and E7 (b) Change in electric current in E2, E4, E6, E8 and E9-E10 (c) Voltage during EK test in E2, E4, E6, E8 and E9-E10	67
Figure 4.3: (a) pH across soil sections after all EK tests (b) electric conductivity across soil sections after all EK tests	70
Figure 4.4: residual PFOA concentration (mg/kg) in the soil sections after EK tests (a) E1-E2; (b) E3; (c) E4; (d) E5; (e) E6; (f) E7; (g) E8; (h) E9; (i) E10.....	77
Figure 4.5: (a) removal rate (%) in soil sections after EK tests; (b) overall removal rate of PFOA after EK tests (c) PFOA's chemical structure.....	78
Figure 4.6: (a) change in voltage over time (b) change in current (c) pH through soil sections (d) PFOA removal rate through soil sections.....	81
Figure 4.7: Total PFOA removal and specific energy consumption.....	83
Figure 5.1: change in current of all experiments after 2 weeks.	98
Figure 5.2:(a) pH across the soil section of different EK tests (b) electric conductivity of the soil sections for all EK tests	100
Figure 5.3:(a) PFOA distribution in soil sections after remediation (b) PFOA removal rate in soil sections post-treatment.....	105
Figure 5.4: (a) AC EDS (b) FeAC EDS after iron loading (c) FeAC PRB after EK test (d) Recycled FeAC PRB after EK test (e) Zeta Potential of AC and FeAC PRB before and after EK tests (f) FTIR results of AC, FeAC before and after EK.....	109

Figure 5.5: (a) AC-PRB EK test; (b)AC PRB EK test.....	111
Figure 5.6: Specific Energy Consumption (kWh kg^{-1}), total PFOA removal of all EK tests and variation of EOF.....	114
Figure 6.1: Electrokinetic test set-up of slag/AC PRB enhanced EK test.	121
Figure 6.2. (a) change in current (b) change in voltage during the EK experiment.....	127
Figure 6.3: (a) the soil pH in all EK experiments (b) the soil EC in the soil section in all EK tests.	132
Figure 6.4: (a) E1 (b)E2 (c) E3 (d) E4 (e)E5 (f) E6 residual PFOA concentration(g) Removal Rate in all EK tests.	138
Figure 6.5: (a) Slag XRD spectrum (b) FTIR results of PRB before and after EK tests (c) Pseudo Second-order kinetic model (d) EDS results of PRB before EK tests (e) EDS results of PRB after EK test (E3) (f) EDS of PRB after E4 (g) EDS of PRB after E6.	144

LIST OF TABLES

Table 2.1: Microbes used in remediation for various soil contaminants	20
Table 2.2: Performance studies for various soil contaminants using electrokinetic treatment.....	35
Table 2.3 Soil remediation through the application of nzvi for the Removal of heavy metals and organic pollutants.....	43
Table 3.1: Physical properties of Kaolin soil	45
Table 4.1: Experimental design.....	62
Table 4.2: Total removal rate and the mass balance of EK tests	81
Table 5.1: Physicochemical properties of PRB.....	92
Table 5.2: Biosurfactant enhanced EK test design.....	94
Table 5.3: Mass balance, residual PFOA concentration and removal efficiency	106
Table 6.1: Biosurfactant enhanced EK tests coupled with Slag/AC PRB.	122
Table 6.2: Mass Balance and Removal efficiency of EK tests	138

PUBLICATIONS

I have contributed to the publication of the following peer-reviewed articles derived from this thesis: These articles contribute to the scientific literature by presenting novel findings and insights on the electrokinetic process for the removal of PFOA from kaolinite soil.

- Ganbat, N., et al. (2022). "Investigation of the effect of surfactant on the electrokinetic treatment of PFOA contaminated soil." Environmental Technology & Innovation: 102938.
- Ganbat, N., et al. (2023) "Iron slag permeable reactive barrier for PFOA removal by the electrokinetic process" Journal of Hazardous Material
- Ganbat, N., et al. (2023). "Remediation of PFOA contaminated kaolinite soil by biosurfactant enhanced electrokinetic coupled with AC/FeAC permeable reactive barrier" - under review in Journal of Technology and Biotechnology JCTB-23-0224

I have also co-authored the following peer-reviewed publications and made contributions to scientific forums during my PhD study:

- Yadav, S., Ibrar, I., Al-Juboori, R., Singh, L., Ganbat, N., Kazwini, T., Karbassiyazdi, E., Samal, A., Subbiah, S. and Altaee, A., 2022. Updated review on emerging technologies for PFAS contaminated water treatment. *Chemical Engineering Research and Design*, 182, pp.667-700.
- Khanafer, D., Yadav, S., Ganbat, N., Altaee, A., Zhou, J., & Hawari, A. (2021). Performance of the Pressure Assisted Forward Osmosis-MSF Hybrid Desalination Plant. *Water*, 13(9), 1245. doi: 10.3390/w13091245
- Ghobadi, R., Altaee, A., Zhou, J., Karbassiyazdi, E., & Ganbat, N. (2021). Effective remediation of heavy metals in contaminated soil by electrokinetic technology incorporating reactive filter media. *Science Of The Total Environment*, 794, 148668. doi: 10.1016/j.scitotenv.2021.148668
- Ibrar, I., Yadav, S., Ganbat, N., Samal, A., Altaee, A., Zhou, J., & Nguyen, T. (2021). Feasibility of H₂O₂ cleaning for forward osmosis membrane treating landfill leachate. *Journal Of Environmental Management*, 294, 113024. doi: 10.1016/j.jenvman.2021.113024
- Ghobadi, R., Altaee, A., Zhou, J., McLean, P., Ganbat, N. and Li, D., 2020. Enhanced copper removal from contaminated kaolinite soil by electrokinetic process using compost reactive filter media. *Journal of Hazardous Materials*, 402, p.123891.
- Ibrar, I., Yadav, S., Altaee, A., Samal, A.K., Zhou, J.L., Nguyen, T.V. and Ganbat, N., 2020. Treatment of biologically treated landfill leachate with forward osmosis: Investigating membrane performance and cleaning protocols. *Science of The Total Environment*, p.140901.
- Karbassiyazdi, E., Altaee, A., Ibrar, I., Razmjou, A., Alsaka, L., Ganbat, N., Malekizadeh, A., Ghobadi, R. and Khabbaz, H., 2023. Fabrication of carbon-based hydrogel membrane for landfill leachate wastewater treatment. *Desalination*, p.116783.

ABSTRACT

Perfluorooctanoic acid (PFOA) belongs to the class of per- and poly-fluoroalkyl substances (PFAS), an emerged contamination with adverse impacts on human health and the ecosystem (Ko et al., 2000). There is mounting concern regarding water and soil pollution with PFOA. The unique physicochemical properties of PFOA enable it to infiltrate soil pores and contaminate groundwater.

Conventional electrokinetic (EK) remediation, hinder the effectiveness in removing PFOA from the soil. This study examines the feasibility of different surfactants and permeable reactive barriers (PRBs) as enhancing agents to increase the removal efficiency of PFOA during EK process. The experiments evaluated using three surfactants: sodium dodecyl sulfate (SDS), Tween 80, and sodium cholate (NaC). The findings reveal that the NaC-EK remediation achieved a removal efficiency of 75.58% after two weeks. The surfactant enhanced EK tests, demonstrated removal efficiencies as follows: NaC>SDS>TW80.

Applying a standalone EK process for PFOA removal from soil has been hampered by the concurrent occurrence of electromigration and electroosmosis transportation mechanisms, leading to PFOA accumulation in the soil. A PRB has been proposed in response to this challenge as an effective strategy to capture and extract contaminants from the soil in the EK process. Activated carbon and iron loaded AC PRBs, in conjunction with the NaC biosurfactant, were evaluated for EK remediation. The results demonstrated that the EK process enhanced with a 5% w/w NaC, coupled with AC and FeAC PRBs, exhibited superior removal efficiency compared to EK tests without PRBs. Specifically, the AC-EK test achieved a removal efficiency of 52.35%, while the FeAC-EK test demonstrated a slightly higher efficiency of 59.55%.

Using waste materials as a sustainable option for PRBs has garnered interest as an alternative approach to traditional methods. Hence, iron slag, a by-product of the steel industry, was used as an adsorbent in the EK process to capture PFOA in soil. Due to its high iron oxide content, iron slag was selected as a potential PRB material. The study's findings reveal that incorporating NaC in the Slag PRB-EK process yielded greater PFOA removal efficiency of 94.09% after three weeks. Notably, the iron slag PRB captured more than 87% of the initial PFOA. These findings highlight the potential of using iron slag waste as a sustainable approach for PFOA treatment in the EK remediation process. These results can inform the development of more efficient and cost-effective EK-PRB systems for field-scale applications, helping to address the pressing issue of PFAS contaminated soils.

CHAPTER ONE

INTRODUCTION

CHAPTER 1: INTRODUCTION

1.1 Soil contamination

The exponential rise in the world's population has resulted in the acceleration of urbanisation and the expansion of industrial production to meet the growing demand (Mahinroosta & Senevirathna, 2020b). Pollution of the environment is one of the most substantial problems humanity faces in the modern era. High levels of industrial activity, increased agricultural productivity, mining activity, construction activities, waste disposal, and misuse of products containing hazardous chemicals are just a few causes of soil pollution (Sunil et al., 2018; Yang et al., 2020). As industrialisation gained momentum in the late 19th and early 20th centuries, environmental pollution increased dramatically. Agriculture's use of pesticides and fertilisers also contributed to soil contamination. Beginning in the middle of the 20th century, the detrimental effects of soil pollution were acknowledged, and efforts were made to regulate and control pollution. The Stockholm Convention on Persistent Organic Pollutants was the first major international agreement to address soil pollution. It was signed in 2001. Today, soil pollution remains a major environmental concern, and ongoing efforts are being made to mitigate its effects and prevent further contamination. Therefore, soil contamination has a considerable detrimental impact on terrestrial ecology and public health. Per and polyfluorinated substances (PFAS) are anthropogenic contaminations of concern that have been used widely since the 1950s (Barth et al., 2021). Perfluorooctane sulfonate (PFOS) and Perfluorooctanoic acid (PFOA) are the most frequently detected PFAS compounds in the environment due to their wide range of use. These substances are commonly used in industrial materials, waterproof surfaces, packing materials, aqueous film-forming foams, surfactants, cosmetics, oil production, and pesticide additives (van Asselt et al., 2011). PFAS are still present in many sites worldwide due to their historical

use, persistence, accumulative and non-biodegradable nature, because of the high strength carbon-fluorine (C-F) covalent bonds. Consequently, due to their unique chemical characteristics, they are both thermally and chemically stable (Ziwen Du et al.).

PFAS pose a substantial risk to public health and the environment. To address this concern, many governments have implemented bans on the manufacturing and usage of PFAS. The Stockholm Convention has established guidelines for PFOS/PFOA concentration in solid waste, with countries such as Sweden and Australia capping it at 50 mg/kg for lined landfills and 20 mg/kg for unlined landfills (Epa Au, 2019). Several countries and organisations, including the United States, Canada, and the European Union, have imposed restrictions on producing and using specific PFAS chemicals. In the United States, for instance, the Environmental Protection Agency (EPA) has phased out the use of certain long-chain PFAS chemicals. Furthermore, various nations and regions have set maximum contaminant levels (MCLs) for PFAS in drinking water, which differ depending on the specific PFAS chemical and the country or region. Companies utilising PFAS must monitor and report their environmental releases (Sima & Jaffé, 2021). In 2020, the European Union (EU) prohibited using PFAS in firefighting foam and limited their use in food packaging, cosmetics, and other consumer goods. The EU is also establishing limits for PFAS in drinking water and conducting a comprehensive risk assessment of the chemicals (ECHA, 2022). In 2021, the Canadian government proposed regulatory measures to control the use, import, and sale of PFAS-containing products in a draught risk management approach for PFAS. The proposal includes the prohibition of PFAS in firefighting foam, reducing PFAS in consumer products, and establishing PFAS drinking water guidelines (Environment, 2021). The Australian government established a PFAS National Environmental Management Plan in 2020, which provides direction for managing and reducing PFAS contamination in soil, water, and air. The plan includes

measures to restrict the use of PFAS in products such as food packaging and firefighting foam (NEMP, 2020).

Contamination of water and soil around the world by PFAS is a serious issue. Significant PFOA contamination levels are found at industrial production sites and firefighting training grounds due to using AFFFs. A greater level of PFAS contamination typically characterises these sites and are therefore categorised as primary contamination sites. PFAS have long hydrophobic chains and hydrophilic functional head groups as part of their physicochemical characteristics. The hydrophilic head of PFAS allows for its dissolution in soil pore water and transport through the soil medium. This phenomenon puts the further contamination of surface water and groundwater at risk, posing a considerable threat to drinking water quality. Some plants may absorb PFAS from soil and water, which can lead to food chain contamination.

In effect, soil pollution is irreversible unless effectively decontaminated. It is challenging to restore the soil to its original state, depending on its physicochemical properties, intended future use and the remediation method employed (Virkutyte et al., 2002). Efficient waste management and sound environmental practices are needed to prevent potential environmental contamination. Scientists and engineers have developed several types of remediation technologies to mitigate the risk imposed by soil contamination. The source-pathway-receptor concept is central to the remediation of the soil. Environmental contaminations have a source (organic and inorganic pollutants discharged into the soil) and the receptor (human health, drinking water or food chain), and the pathway the receptor is exposed to (direct skin contact, food chain, drinking contaminated water). Evaluating the risk to the receptor helps to identify whether the contaminations are unacceptable so that the risk needs to be reduced. To reduce the risk, selecting a site-specific remediation method is crucial (Lee et al., 2020). Multiple remediation methods

could be used concurrently to maximize the removal rate and improve soil treatment efficiency. Numerous ex-situ and in-situ methods have been developed over time. In-situ soil remediation includes benefits such as minimal soil disruption and can be cost-effective. It also reduces the risk of exposure to potentially hazardous materials during excavation and transportation of the contaminated soil. The effectiveness and accuracy of contaminant removal are difficult to verify since the physicochemical properties of soil and contaminations are site-specific. Ex-situ technology often helps where the land is highly contaminated, and soil excavation from the site is required to control pollutants transport (Koul & Taak, 2018).

Conventional remediation methods for mixed contamination pollution include phytoremediation, thermal treatment, and physical and chemical remediation. Enhanced remediation using surfactants, nanomaterials and other adsorbents was applied to increase the rate and efficiency of removal (Hansen et al., 2016). Choosing the most environmentally friendly, cost and time-efficient method is essential. Site assessment, the investigation of the physicochemical properties of soil, and the analysis and distribution of contaminations in the soil is the first step in the remediation procedure. After the completion of the analysis, site-specific remediation technology is selected to minimize the disturbance of soil properties. Using soil washing processes that involve chemicals can potentially lead to secondary contaminations. The processes of soil capping and encapsulation could be more effective at removing pollution from the soil. Instead, it prevents further contamination of the surrounding area and groundwater or surface water contamination by immobilising and mitigating their effects.

Since the 1950s, the EK remediation method has been used to remove metal ion species from contaminated soil. This environmentally friendly method can be applied in situ and ex-situ. Since EK remediation causes minimal soil disturbance when administered in situ,

it has become one of the most sought-after remediation techniques. EK remediation has been conventionally used to remove heavy metal ions from soil and successfully removed organic pollutants in combination with other techniques and enhancing agents. It is a cost-effective method that can be used coupled with other methods to remove a wide range of contaminants. The electrokinetic (EK) method has been widely employed for the remediation of persistent organic pollutants in soil and groundwater. Researchers have recently explored the potential of using the EK process to remove per- and polyfluoroalkyl substances (PFAS) from contaminated soil. Initial electrochemical investigations have shown promising results, confirming the electrokinetic process's feasibility. Since PFOA is an anionic compound that readily dissolves in soil pore water, it can migrate through the soil matrix in response to an applied electric field.

1.1.1 Impacts of PFAS on environmental quality and human health

Most residents in industrialised nations will have some PFAS in their bodies. The long-term consequences of PFAS on human health remain unknown. However, deleterious consequences on human health are still being studied, and epidemiological studies have indicated links between PFAS and altered immune and thyroid function, liver disease, lipid and insulin dysregulation, adverse reproductive effects, renal disease, and cancer (Pelch et al., 2019). According to Harvard public health experts, bioaccumulation of PFBA in the lungs increases the risk of hospitalisation, intensive care unit admission, or death from COVID-19 infection in individuals with PFBA in their systems (HSPH, 2020). PFOA and PFOS present in pregnant women's serum are associated with a low birth weight of an infant. Adults with elevated PFOA and PFOS levels in their blood are linked to altered thyroid hormones and increased cholesterol levels (Longpré et al., 2020). Animal studies showed that a high level of PFOA and PFOS in blood serum caused cancer, delayed growth, endocrine disruption, and neonatal mortality. The Centre for

Disease Control (CDC) has reported that PFOA exposure is linked to cancer effects (Teaf et al., 2019). PFOA and PFOS presence in drinking water is associated with toxicological and epidemiological evidence of adverse health effects (Cordner et al., 2019). Hence the remediation and elimination of PFAS from the environment are highly important for protecting public health.

Environmental protection agencies have thus banned PFAS-containing products and established exposure limits for PFAS. PFAS-containing cosmetics, non-stick cookware, and other household items in several nations are now prohibited. More regulations, standards and compliance are still underway in many countries. PFOA and PFOS are included in the list of persistent organic pollutants (POPs) regulated by the Stockholm Convention. This global treaty is designed to safeguard human health and the environment by addressing the threats posed by persistent organic pollutants. Moreover, in 2012, the Organisation For Economic Co-operation and Development (OECD) and the United Nations Environment Programme (UNEP) Global PFAS group were established to reduce and eliminate PFAS emissions where possible.

1.1.2 Techniques for the remediation of PFAS-contaminated soil

PFAS is persistent, mobile, bioaccumulative and non-biodegradable in the soil and water, posing a potential risk to public health and wildlife. Several methods can be used to remove PFAS from soil. Recent technologies and remediation strategies for eliminating PFAS are summarised in several review articles (Ahmed et al., 2020; Mahinroosta & Senevirathna, 2020b; Sima & Jaffé, 2021). Excavation and landfilling methods typically entail digging up the contaminated soil and transporting it to a landfill or incineration facility. This method does not solve anything; it simply removes contaminated soil from a specific location, but there is no guarantee that PFAS was not leached into the surrounding environment. Excavation and transportation to treatment facilities are

difficult and expensive processes. Hence, in situ, soil washing method was investigated and compared to an excavated soil washing technique. A 76% removal efficiency was found for the in situ method (Høisæter et al., 2021). In a pilot scale study, 6 tons of AFFF-contaminated soil was used for the feasibility of stabilisation and solidification treatment, resulting in an average of 92% removal rate for PFOA and PFOS. The soil-washing process requires a large amount of water and solvents and generates a large amount of wastewater that must be treated. To remove PFASs from the soil, the soil washing plant utilised physical and chemical processes, including fractionation of soil particles by size and partitioning of PFASs into the aqueous phase. Subsequently, the contaminated water underwent treatment with granular activated carbon and ion exchange resins. This comprehensive approach yielded impressive average removal efficiencies of 97.1% for PFOA and 94.9% for PFOS (Grimison et al., 2023).

Numerous studies are currently being conducted on the removal, degradation, and adsorption of PFAS from soil. To reduce PFAS mobility and leaching in contaminated sites, methods such as sorbent amendment, stabilisation, and solidification have been used, and destructive techniques such as thermal treatment, encapsulation, and capping have been investigated (Bolan et al., 2021b; Sleep & Juhasz, 2021; Söregård et al., 2020b). Thermal heating is a destructive method that emits toxic gases and is a costly technique that necessitates heating contaminated soil at high temperatures, resulting in industrial waste. Thermal treatments, ultrasonic techniques, and the corona discharge method have all been used to remediate PFAS-contaminated soil (Bolan et al., 2021a; Lei et al., 2020; Söregård et al., 2020a). Mechanochemical treatment reduced PFOA and PFOS levels in dry sand by 99% and 98% in AFFF-contaminated soil (Turner et al., 2021). However, the limitation of S/S treatment is the long-term assessment (Söregård et al., 2021). As a result, a technology for removing PFAS chemicals from contaminated

soil that is less harmful to the environment and more cost-effective is required. Because of their chemical properties and behaviour in soil, it is difficult to select a universal approach that effectively addresses PFAS soil pollution. Mixed remediation technologies with advanced enhancements such as surfactant and reactive filter media are introduced To increase pollutants' efficiency and removal rate. Surfactants, nanomaterials, and other adsorbents were used in enhanced remediation to increase the removal efficiency (Hansen et al., 2016). In effect, soil pollution is irreversible unless effectively decontaminated. It is challenging to restore the soil to its original state, depending on the soil's physicochemical properties and the remediation method employed (Virikutyte et al., 2002). More than a remediation method could be used concurrently to maximize the removal rate and improve the efficiency of soil treatment.

1.1.3 Electrokinetic process for the removal of PFAS

Electrokinetic (EK) soil remediation removes contaminants from soil using an electric field. It involves applying a low-intensity DC across a soil matrix, which drives charged particles towards the electrodes. Charged particles migrate by electroosmosis and electromigration phenomenon under an electric field. The contaminants are then extracted from the soil and collected at the electrodes. EK soil remediation is a promising technology for contaminants such as heavy metals, radioactive elements, and organic compounds. It is especially effective for contaminants with a strong affinity for soil. Therefore, EK treatment has been investigated for its feasibility in removing PFAS from contaminated soil. Studies for removing PFOA from contaminated soil using EK remediation demonstrated promising results as PFOA migrated from cathode to anode by electromigration and transported by electroosmosis from anode to cathode (Söregård et al., 2019). A novel EK method with a single and two-compartment set-up was conducted to remove PFAS from soil resulting in 75% removal on GAC for single cell set-up and

89% in the two compartments set-up (Niarchos et al., 2022). In another study (Hou et al., 2022), under low voltage 24V and direct current 467-690mA, approximately 51.7% and 33% of PFOA and PFOS were degraded, respectively. Research indicated that PFOA and PFOS removal occurred through degradation. Using an Rh/Ni cathode, the feasibility of electrochemical reductive decomposition of PFOA was investigated (Zhu et al., 2022). Electrochemical treatment of PFAS using boron-doped diamond (BDD) anode and titanium sub-oxide ceramic anodes, ceramic microporous Magneli phase Ti_4O_7 electrode can achieve almost 99% of PFAS removal (Sharma et al., 2022). Combining these techniques with other enhancement methods can boost the overall EK effectiveness. In another electrochemical study using BDD anode to remove PFOA and PFOS from landfill leachate, overall removal efficiencies achieved 80% and 78%, respectively (Pierpaoli et al., 2021).

EK soil remediation has several benefits over conventional soil remediation techniques. This non-invasive technique does not require excavation or transportation of contaminated soil. It can also be applied to difficult-to-treat soil types, including clayey and silty soils. In addition, EK remediation is a relatively inexpensive technique that can be combined with other soil remediation methods to increase their efficacy. However, there are also some limitations to EK soil remediation. Treatment times can range from weeks to months, depending on the soil type and contaminant concentration. In addition, a continuous power supply is required, which can be costly. In addition, the high pH generated near the cathode during EK treatment can result in alkaline soil conditions, inhibiting plant growth and microbial activity. However, enhancing the EK technique with another remediation method can overcome the limitations.

1.2 Research hypothesis

Electrokinetic remediation (EK) has been tested in the laboratory for its potential application in removing organic contaminants from soil (Alcántara et al., 2008, 2010; Colacicco et al., 2010). The EK technique has many advantages as it can be used in situ and ex-situ. Compared to disruptive remediation techniques, in-situ applications can be cost-effective, have a lower environmental impact, and be safer for human health. EK remediation, coupled with surfactants, has been studied to remove organic pollutants and has demonstrated successful removal efficiency (Abdel-Shafy & Mansour, 2016) (Alcántara et al., 2010).

Present efforts to address the presence of per- and polyfluoroalkyl substances (PFAS) in contaminated soil primarily focus on disruptive remediation technologies such as thermal treatments and encapsulation. However, exploring environmentally friendly and minimally disruptive green technologies is crucial to effectively remove PFOA from contaminated soil. Several studies have investigated using the EK technique for PFAS removal. The EK process involves the migration of PFOA from the cathode to the anode through electromigration and from the anode to the cathode through electroosmosis, driven by direct electric current. Consequently, PFOA tends to accumulate in the middle of the reactor cell (Hou et al., 2022). To the best of our knowledge, no experimental investigations have been conducted to assess the efficacy of surfactant-enhanced electrokinetic techniques or their combination with various PRBs for PFOA removal.

The main research significance of this project is to investigate the viability of an enhanced EK soil remediation process for the effective removal of PFOA from contaminated soil. Therefore, choosing environmentally friendly and cost-effective enhancing agents to remove PFOA using the EK process effectively is essential. Our initial studies examined

the transportation of PFOA under an electric field to validate the research findings. Different enhancing agents will be further investigated to enhance PFOA from cathode to anode. Anionic surfactants, non-ionic surfactants and biosurfactants will be examined to validate that removal efficiency increase when chelating agents are introduced. In order to eliminate the secondary pollution in the soil, it is hypothesized that biosurfactants will have higher removal efficiency and environmentally friendly effects.

A permeable reactive barrier will be introduced to improve the removal efficiency upon selecting the most effective surfactant for removing PFOA in the EK process. Initial studies evaluated the performance of activated carbon and iron-coated activated carbon as PRBs to enhance the EK process in combination with surfactant. Activated carbon has shown significant adsorption capacity towards PFOA in environmental investigations. It is hypothesized that iron-coated activated carbon will have greater adsorption efficiency due to its high surface area. Based on the preliminary studies of PFOA removal in the EK cell, the PRBs will be placed in the middle of the cell where most of the contaminants are accumulated. Then the evaluation of slag as PRB will be examined. Slag is an industrial waste that is generated during the metal process. Slag is considered to have high iron oxide content. Therefore, the hypothesis is that iron slag will have a high adsorption affinity towards PFOA. Surfactant-enhanced EK process coupled with iron slag PRB will be investigated. Using industry waste as recycling material can be beneficial for environmental sustainability.

Consequently, it will be cost-efficient. Lastly, the cation exchange membrane will be assessed as the enhancement of the EK process. A comprehensive review of improved electrokinetic remediation for removing PFOA from the soil is given in the technical chapters.

1.3 Research significance

The main research significance of this study is to investigate environmentally sustainable surfactants to enhance the EK process for removing PFOA from contaminated soil. Conventional surfactants were tested to enhance HOC and POP removal, and biosurfactant was examined for efficacy. Notably, the utilisation of sodium cholate biosurfactant to enhance the EK process for removing PFOA from contaminated soil remains unexplored in the existing literature.

Subsequently, upon selection of the biosurfactant, the EK process was further enhanced by incorporating PRB to increase the overall removal of PFOA from contaminated soil. Consequently, a comprehensive investigation was conducted to assess different types of PRBs in the EK process. Although the coupling of PRB with the EK process has been utilized to remove other contaminants from soil and groundwater, its specific application for PFOA removal has not been subject to thorough investigation. Therefore, this study endeavours to identify a suitable and cost-effective PRB for efficiently removing PFOA.

Utilizing the EK process in conjunction with PRB for the laboratory-scale removal of PFOA from soil holds profound importance in advancing the project towards larger-scale implementation. This initiating approach can pave the way for treating stockpiled soil and remediating contaminated sites within affected communities. Furthermore, the in-situ EK treatment of soil contaminated with PFAS represents an innovative and promising strategy for on-site soil remediation by reducing the risk of dig and dump and other invasive techniques.

1.4 Research objectives

This project aims to examine the viability and efficacy of the EK technique for removing PFOA from contaminated soil matrix improved with various types of surfactants as

enhancing agents and coupled with PRBs. This project's research objectives are as follows:

1. Assess the feasibility of utilizing the electrokinetic (EK) process as a standalone technique for removing PFOA from contaminated kaolin soil, which serves as a representative soil model.
2. Investigate the performance of the EK remediation process when combined with various surfactants, including anionic surfactant sodium dodecyl sulphate (SDS), biosurfactant sodium cholate (NaC), and non-ionic surfactant (TW80), under constant currents of 10mA and 20mA for durations of 7, 14, and 21 days.
3. Examine the effectiveness of the EK soil remediation process in conjunction with permeable reactive barriers (PRBs) composed of activated carbon (AC) and iron-modified activated carbon (FeAC), enhanced with the most efficient surfactant identified.
4. Assess the feasibility of employing surfactant enhanced EK techniques combined with a PRB composed of slag and activated carbon (Slag/AC) for 14 and 21 days. Investigate the influence of the slag-to-AC ratio in EK tests on the overall removal rate and evaluate the effects of recycled Slag/AC PRBs within the EK process.

1.5 Thesis structure

The thesis is structured into seven chapters, which are outlined as follows:

Chapter 1 serves as the introduction chapter, providing an overview of the research study. It outlines the research topic of removing PFOA. The chapter presents the chosen PFOA removal technique, outlines the research hypothesis, and defines the study's objectives. Additionally, it provides a comprehensive description of the primary tasks required to fulfil the study's objectives and outlines the scope of the research.

Chapter 2, titled "Literature Review," critically examines the existing body of knowledge on soil remediation technologies for contaminated soil, specifically addressing PFAS contamination. The chapter presents a comprehensive overview of the scientific literature on electrokinetic remediation, encompassing its wide range of applications, limitations, and significant findings reported in previous studies. The comprehensive discussion encompasses the various factors that influence the effectiveness of electrokinetic technology in soil remediation. Then, the chapter presents the enhancement techniques and their incorporation with the electrokinetic process. Based on this evaluation, the chapter provides a clear direction for future research directions in the domain of electrokinetic remediation for addressing PFOA-contaminated soil.

Chapter 3, titled "Materials and Methods," presents a detailed description of the materials and methods employed in the current study. The chapter outlines the specific materials used, including soil samples and chemicals, providing relevant details such as their sources and characteristics. It also elucidates the experimental setup, apparatus, and instruments utilized in the research. The methods section comprehensively explains the step-by-step procedures followed in the study, encompassing sample preparation, experimental design, and the implementation of the electrokinetic remediation process. It includes information on measured parameters, data collection methods, and data analysis techniques.

Chapter 4, entitled "Investigation of the effect of surfactant on the electrokinetic treatment of PFOA contaminated soil", focuses on a study where three types of surfactants—specifically, the anionic surfactant sodium dodecyl sulfate (SDS), the non-ionic surfactant Tween 80, and the biosurfactant sodium cholate (NaC)—are employed in the electrokinetic technique for the removal of PFOA from contaminated soil. This chapter

investigates the impact of these surfactants under constant currents of 10 mA and 20 mA over experimental periods of 7 and 14 days. Furthermore, the investigation also examines the influence of the initial PFOA concentration on the effectiveness of the surfactant-enhanced electrokinetic (EK) process. Through this study, the chapter aims to shed light on the efficacy and efficiency of the surfactant-enhanced EK process for PFOA removal, providing valuable insights into the potential of surfactants in improving the remediation of PFOA-contaminated soil.

Chapter 5, titled "PFOA remediation from kaolinite soil by electrokinetic process coupled with AC/FEAC- permeable reactive barrier", the focus is on the application of activated carbon (AC) and iron-impregnated activated carbon (FeAC) in the EK remediation as effective adsorbents for the removal of PFOA from contaminated soil. The chapter extensively examines various aspects related to the utilization of these adsorbents, including sorption mechanisms, the characterization of PRB, regeneration techniques, and the potential for their reuse within the EK process.

Chapter 6, titled " Iron slag permeable reactive barrier for PFOA removal by electrokinetic process", focuses on applying a slag PRB in conjunction with the biosurfactant EK process for the remediation of PFOA from contaminated kaolinite soil. The chapter investigates the performance of the slag/AC PRB within the EK process and provides a comprehensive assessment of the removal mechanisms involved. This chapter provides a detailed assessment of PRB characterization, including the physical and chemical properties of the slag/AC PRB. It also delves into regeneration techniques, exploring methods to restore and enhance the adsorption capacity of the PRB. Additionally, the chapter explores the potential for reusing the PRB in subsequent EK remediation processes, contributing to the understanding of sustainable and cost-effective remediation strategies. This comprehensive assessment contributes valuable insights into

the performance, removal mechanisms, and potential optimization of the biosurfactant-enhanced EK process coupled with the slag/AC PRB for removing PFOA from contaminated soil.

Chapter 7, titled "Conclusions and Future Research Directions", comprehensively summarises the significant findings and offers recommendations for future research on the EK process for removing PFOA from the soil. This chapter begins by summarizing the key findings obtained throughout the study, highlighting the important outcomes and discoveries related to the EK technique and its effectiveness in PFOA removal. The findings may include the performance of different surfactants, integrating permeable reactive barriers (PRBs), and applying specific PRB materials. The chapter then presents recommendations for future research directions building upon the findings. These recommendations aim to address the existing knowledge gaps and further advance the understanding and optimization of the EK process for PFOA removal from kaolinite soil.

CHAPTER TWO

LITERATURE REVIEW

CHAPTER 2 : LITERATURE REVIEW

2.1 Conventional approaches to soil remediation

Numerous physical, biological and chemical remediation procedures have been utilised to date (Dermont et al., 2008). However, these strategies have their confinements, for example, the necessity of an enormous amount of labour, disturbance of local soil properties and it also affects the naturally occurring flora of the treated area (Angelstam, 1998). At times issues identified with optional or secondary soil contamination also come before the scientists (Stokes et al., 2014). These sorts of issues make scientists discover an eco-friendly and practical method of countering the issue of overwhelming soil contamination, such as biological remediation methods, including bioremediation and phytoremediation. Different conventional soil remediation techniques are available for various contaminations that can be applied in situ and ex situ. Soil flushing and chemical oxidation are common chemical remediation methods, while physical remediation methods include encapsulation, landfilling and thermal treatments. However, conventional methods have their advantages and disadvantages. Most conventional remediation techniques are costly and time-consuming. Choosing the appropriate method is highly based on the contaminated site, such as the soil properties and properties of the pollutants present. Remediation of contaminated sites to their original state is challenging.

2.1.1 Bioremediation

By incorporating living microorganisms like bacteria and microbes, bioremediation is a biological procedure for eliminating heavy metal ions and organic pollutants from soil (Chen et al., 2015). The approach reduces the toxicity of pollutants by converting them to fewer toxic substances using a variety of ecologically friendly microorganisms. Microbes can be developed to produce contaminant- and site-specific species to minimise

the pollutants (Zegzouti et al., 2020). Bacterial species have been reported to degrade PFAS under aerobic or anaerobic conditions; however, aerobic biotransformation was more frequently reported (Zhang et al., 2022). Long-chain PFAS, like PFOA and PFOS, are non-biodegradable and stable. Researchers discovered a biodegradation pattern for PFOA and PFOS by *Acidimicrobium* sp. A6, where A6 can defluorinated PFOA/PFOS while reducing iron, using ammonium or hydrogen as the electron donor (anaerobic oxidation of ammonium under iron-reducing conditions) (Huang & Jaffé, 2019). In a recent study, researchers found that the aerobic *Gordonia* sp. Strain NB4-1Y could degrade 6:2 FTAB and 6:2 FTSA over 7 days under sulphur-limited conditions at 85% and 88% efficiencies, respectively (Shaw et al., 2019). Renewable artificial plants for in-situ microbial environmental remediation (RAPIMER) exhibited high adsorption capacity for removing PFAS and subsequent fungal detoxification (Li et al., 2022). Combining bioremediation technology with other conventional remediation techniques can increase the effectiveness of soil contamination remediation. But because biological processes are so specific, bioremediation can only be employed for substances that degrade in a certain way. The key to a successful remediation procedure is providing the right microorganisms with the appropriate habitat for proliferation and nourishment.

2.1.2 Phytoremediation

In the phytoremediation process, plants are used to accumulate, reduce, and stabilize heavy metals and organic pollutants such as insecticides, and polycyclic aromatic hydrocarbons (Abdel-Shafy & Mansour), from the soil (Mishra & Tripathi, 2008). As opposed to destructive engineering techniques, it is a remediation strategy that is both affordable and environmentally beneficial (Sigurdur, 2011). However, phytoremediation requires contamination- and site-specific plants and is a lengthy process. This technique conquers all the restrictions of physical and chemical strategies utilised to expel

substantial metals and organic pollutants from soil (Reddy & Cameselle, 2009). For instance, it is cost-effective, eco-friendly, and less labour-intensive. It has no adverse effect on the flora and fauna of the local area (Rai, 2008). Phytostabilization is a phytoremediation technique where the contaminants are stabilized by reducing their mobility, preventing them from further spreading and leaching into the groundwater (Salt et al., 1995). Phytodegradation is when the roots of plants release specific enzymes to degrade organic contaminations mitigating its toxic effect. Phytovolatilization involves uptake, translocating, and volatilizing contaminants by plant roots, converting them to a gaseous state and eventually releasing them into the atmosphere (Limmer & Burken, 2016). Phytoextraction involves the accumulation of heavy metal ions by plants and turning them into harvestable biomass. Some plants can accumulate multi-metal ions, whereas some can only hyper-accumulate one specific metal ion (Ponz et al., 2018).

Currently, there is ongoing phytoremediation of PFAS-contaminated Loring Airforce Base in the USA, where researchers are studying the feasibility of hemp to remediate the contaminated soil (Nason et al., 2021). Furthermore, plant uptake highly depends on the PFAS chain, functional group and plant species. Phytoremediation studies conducted by (Gobelius et al., 2017) on various plant roots and tissues for uptake of PFOA and PFOS from contaminated fire training facility sites showed promising results.

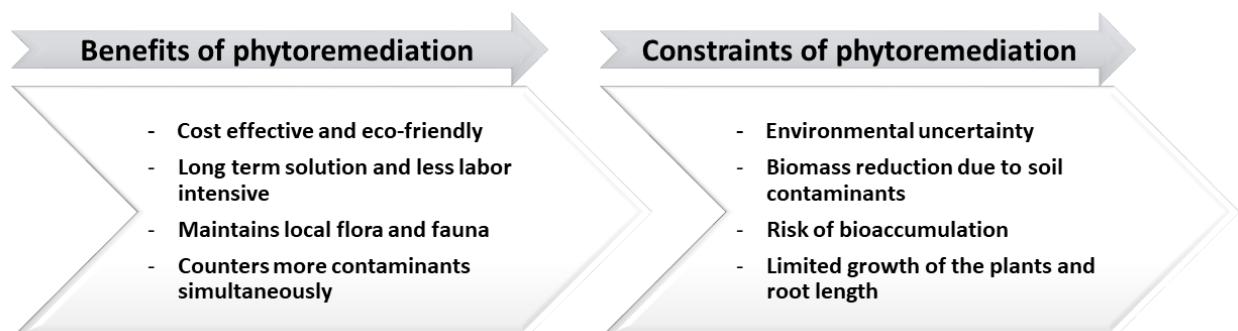


Figure 2.1: Advantages and disadvantages of phytoremediation.

Table 2.1: Microbes used in remediation for various soil contaminants.

Soil contaminants	Sources	Microbes used in the remediation	References
Cadmium (Cd)	Phosphate fertilizers, plating, sewage sludge, batteries, plastics, pigments	Bacillus species, Azotobacter species, Arthrobacter species	(Yadav et al., 2017)
Chromium (Cr)	Volcanic dust and gases, tobacco smoke, rocks, cement dust, paints, Fungicides	Bacillus species	(Giri, 2012)
Manganese (Mn)	Sewage sludge, mining, gasoline additives, volcano, fossil fuel burning	Pediastrum duplex	(Mathew, 2017)
PFOA/PFOS	Incubation	Acidimicrobium sp. Strain A6	(Huang & Jaffé, 2019)
6:2 FTSA/6:2 FTAB	AFFF contaminated	Gordonia sp. Strain NB4-1Y	(Shaw et al., 2019)
PFPeA/PFBA/TFA PFAAs	Landfill soil Waste-activated sludge during anaerobic digestion	Mixed culture Mixed culture	(Sun et al., 2020) (Li et al., 2021)
PFOS	Wastewater treatment sludge	Enterobacter species Pseudomonas aeruginosa strain HJ4	(Nie et al., 2002) (Kwon et al., 2014)
6:2 FTOH 5:3 Acid/PFHxA		Gloeophyllum trabeum Psychrobacter species	(Merino et al., 2018) (Ma et al., 2010)
Copper (Cu)	Mining, pesticides, fungicides, forest fires, volcanic eruptions, leather processing, plating	Pseudomonas species	(Lal, 2019)
		Enterobacter species Sulfobacillus thermotolerans	(Lu et al., 2006) (Liu et al.)
Iron (Fe)	Mining, sewage and sludge, fertilizers, herbicides, electronic waste, steel and alloy manufacturing, metal extraction	Fusarium species Acidithiobacillus ferrooxidans	(Viet et al., 2016) (Bradl, 2005)
		Zetaproteobacteria Pseudomonas aeruginosa	(Singer et al., 2011) (Braud et al., 2009)

Silver (Ag)	Photo processing industry, mining, cloud seeding,	sewage, smelting,	Thiobacillus species	(Lakshmanan et al., 2019)
			Leptospirillum ferrooxidans	(Johnson et al., 2008)
Pyrene and phenanthrene	Wood burning, cigarettes, asphalt, insecticides,	coal tar, plastics, dyes	Bacillus polymyxa Bacillus species,	(Saifuddin et al., 2009) (Ramesha et al., 2017)

2.1.3 Thermal treatment

Thermal soil treatment involves heating the soil, evaporating contaminants, and capturing them for safe disposal or further treatment. When chemical oxidation and bioremediation are ineffective, thermal remediation can decontaminate pollutants. Steam, electric resistance heating, and desorption are all examples of thermal techniques that can be used (Millán et al., 2020; O'Brien et al., 2018). The primary mechanism for successful decontamination is through direct steam injection, and the extraction of contaminants can be collected at the extraction wells. Steam injection can destroy some organic compounds, decreasing the viscosity of contamination and accelerating volatilization. It is an effective method for the remediation of volatile and semi-volatile hydrocarbons from high and semi-permeable soils. Since the method is based on injecting steam directly into the soil, it is limited to low permeable soils and boiling point of water. This method is mostly used to decompose hydrocarbons, but the high energy consumption and soil damage resulting from high temperatures are the limitations associated with thermal treatment (Vidonish et al., 2016). Hence post thermal treatment, the ability of the contaminated site to return to its original state is very limited. Thermal destruction methods have gained much attention for removing PFAS from contaminated soils. Thermal treatment of PFAS-contaminated soil is one of the prevalent methods used in the industry to treat

contaminated sites. The process involves heating the soil to high temperatures (400-1000⁰C), which results in mineralisation, but the degradation process and pathways are still unknown. Thermal decomposition of PFAS is conducted under pyrolytic conditions (absence of oxygen), and it can result in the formation of organofluorine, including volatile organofluorine, at temperatures >500 ⁰C (Wang et al., 2022). Studies demonstrated that heating PFAS-contaminated soil by 350⁰C and 400⁰C reduced the concentration by 99.91% and 99.998%, respectively (Crownover et al., 2019). Another study for destructive thermal decomposition was carried out at temperatures 250⁰C-700⁰C and indicated the reduction of PFAS by 99.4% (Jacobs, 2019).

Electric resistance heating uses electric conductivity. This method is based on directly passing electricity through soil by stacking multiple electrodes making the contaminants mobile and readily available for extraction. For a successful rate of decontamination presence of water is required. This method works well for the removal of volatile hydrocarbons. Desorption or in-situ thermal conduction heating uses thermal conductivity. Since this method is based on conduction heating, the presence of water is not required. The contaminants are destroyed and evaporated as the heat passes through the soil. If necessary, the vacuum system carries the contaminations to the surface for safe disposal or further treatment. A study by (Taube et al., 2008) has shown the successful removal of mercury from the soil by thermal treatment at 470⁰C with a removal rate of 99%. Another study (Falciglia et al., 2011) has demonstrated the effect of thermal desorption of artificially polluted diesel soil using thermal treatments. The results have shown that time, temperature and texture of soil influence the efficiency of the treatments. Gasification of PFAS-containing biosolids has been investigated and reduced PFAS below the detection limit (Kumar et al., 2023). The high melting point of PFAS makes

them resistant to thermal treatment. The required high energy consumption is expensive and requires a high initial investment in infrastructure, especially when the contaminated site is big.

2.1.4 Soil washing

Soil washing is a technology used for the removal of contaminants from soil. This remediation technique can be in situ soil flushing. On-site soil washing involves chemical washing or solvent extraction of soil using an appropriate chemical solution to remove the contaminants, washing the soil with clean water to remove the remaining chemical, and lastly, wastewater treatment by a portable purification system (Liu et al., 2018). Soil washing can also be ex-situ, where the contaminated soil is excavated and treated. The first step of soil washing involves the removal of coarse impurities such as rubbish, wood, and metals, which can be achieved by manual sorting or sieving. Then the solvent-extraction process takes place (Silva et al., 2005). Appropriate surfactants, acids or organic solvents are added to improve the contaminants removal efficiency.

In situ, soil flushing has been a widely used remediation technology for removing contaminants as it reduces the need for extraction, transportation, and handling of hazardous substances. This technique involves the separation of contaminants from soils by dissolving and suspending the contaminants in the wash solution. Wash solutions are usually water or other aqueous chemical solvents that assists in the separation process. This method applies to contaminated sites with highly soluble pollutants and selected organic contaminants. Furthermore, it is ineffective to decontaminate several hazardous contaminants using this method alone (Dermont et al., 2008) (Mahinroosta & Senevirathna, 2020b). Washing PFAS-contaminated soil with water or other solvents is an effective remediation technique. Depending on the type of PFAS being targeted and

the soil matrix, the washing solution can be either an aqueous or organic solvent. It has been demonstrated that PFAS soil washing is effective at removing PFAS from soil, but its efficacy may vary depending on the type and concentration of PFAS present, as well as the soil's properties. In addition, the process may require a substantial amount of water and generate a significant amount of contaminated waste that can be expensive to dispose of properly (Grimison et al., 2023). A potential advantage of PFAS soil washing is that it can be performed on-site, thereby reducing the costs and risks associated with transporting contaminated soil to off-site treatment facilities. However, care must be taken to ensure that the washing process does not create additional environmental risks, such as spreading contamination to nearby soil or water sources.

Soil washing has been used to treat PFAS-contaminated sites and the recovered water, utilizing water as a flushing agent with and without solvents. The implementation of this technology has been delayed due to various concerns, including the high consumption of reagents, the lack of an effective strategy for treating washing effluent, and the significant loss of soil nutrients after washing (Mahinroosta & Senevirathna, 2020a). However, soil-washing remediation methods are more efficient when enhanced or coupled with other techniques, such as surfactants or secondary remediation processes (Meng et al., 2019). In situ, soil flushing of PFOS-impacted soils was studied using 5 beds of 50% ethanol as solvent, which resulted in the elimination of PFOS by 98% (Senevirathna et al., 2021). In situ, the soil washing method was tested, and the contaminated water from soil washing was treated with AC to prevent further leaching. It was then compared with an ex-situ soil washing; results indicated that excavated samples removal efficiency of PFOS was 60-70% and the in-situ removal rate 73% (Høisæter et al., 2021).

2.1.5 Immobilization

Solidification/stabilization is widely studied and effective for mixed waste-contaminated soil. Vitrification is an effective in-situ or ex-situ physical remediation technique which can be used for mixed waste-contaminated soils. The primary mechanism of this method is turning wastes into glass-like crystalline particles by passing an electric current through electrodes at high temperatures. Once it is cooled, the solid product is chemically stable. The high temperatures of this process destroy the organic compounds by pyrolysis and combustion; heavy metals are usually fused in the solidified product and can be disposed of (Celary & Sobik-Szołtysek, 2014). Vitrification can cause physical disturbance and irreversible change to soil microorganisms by elevated temperatures up to 2000⁰C (Ballesteros et al., 2017).

The immobilization technique has been a significant part of the remediation of PFAS-contaminated sites. This method uses various sorbents to immobilize and stabilize PFAS compounds in the soil, preventing further leaching of PFAS into the groundwater. Different sorption materials have been used in bench-scale laboratories and field scales. Common materials used for studies include granular activated carbon (GAC), powdered activated carbon (PAC), biochar (BC), resins and minerals. Firefighting site-impacted groundwater studies found that longer-chain PFAS, such as PFOA and PFOS adsorbed on GAC, surfaced better than the short-chain PFAS. The presence of other organic compounds impacted PFAS adsorption (Liu et al., 2019; Rodowa et al., 2020).

Solidification and stabilization treatment was carried out by (Sörengård et al., 2021) in the long-term (6 years) pilot-scale of soil contaminated with PFAS containing aqueous film-forming foam using GAC as an adsorbent. Results showed 97% removal efficiency. Biochar is considered a sustainable green adsorbent to reduce PFAS substances. PFAS adsorption onto biochar reduced the concentration of PFAS in leachate by 98-100%,

where eight different types of adsorbents were tested (Sørmo et al., 2021). In this study, researchers observed that the presence of organic matter affected the adsorption of PFAS onto biochar surfaces as the organic substances were adsorbed, leaving little room for PFAS adsorption.

Stabilization and solidification studies in Australian AFFF-impacted sites were studied using two different sorbents RemBind® (Mixture of activated carbon and aluminosilicate clay, aluminium oxyhydroxide) GAC. Both sorbents retained >99% of PFAS. However, long-chain PFAS were difficult to desorb and highly pH-dependent (Kabiri et al., 2021).

2.1.6 Mechanical treatment

Mechanochemical (MC) destruction based on high-energy ball milling is a promising remediation technology for soils polluted with persistent organic compounds, which can quickly mineralize organic pollutants and generate amorphous carbon (Sui et al., 2018). MC treatment of petroleum-contaminated soils resulted in amorphous carbon, carbonate, and iron oxides. The end material can be recycled for further use in wastewater treatment (Wang et al., 2022). MC treatment has been successfully implemented to immobilize heavy metal-contaminated soils reducing their leachability (Montinaro et al., 2007). Mechanochemical remediation of PFOS and PFOA-amended sand via planetary ball mining was studied by (Turner et al., 2021), demonstrating milling experiments conducted in the Canadian firefighting training area reduced PFOS contamination by 96%.

2.1.7 Encapsulation

Encapsulation does not extract contaminants but decontaminates by mitigating pollutants and preventing surrounding sites and groundwater from further pollution (Liu et al., 2018). Encapsulation of the contaminated site does not allow it to be restored to its

original state, so the treated soil cannot be used for any cultivation (Shtripling et al., 2016). This method uses cement to mix with soil to stop the spread. Other materials that can be used are those that do not react with contaminations and do not allow them to spread more. The most used method is permeable or semi-permeable barriers for the site. Some examples of encapsulation are slurry walls, thin walls, injection wells, and artificial ground freezing. The main mechanism of the reactive barrier is it shelters the contaminants so when the toxic chemical reaches the walls; they are stabilized, degraded or converted into less toxic forms; therefore, even if it passes through the barrier, it's not toxic for the environment (Herlem et al., 2019). Encapsulation of PFAS-contaminated soil to inhibit further leachability (Barth et al., 2021).

2.1.8 Electron beam technology

A high beam electron energy irradiation has been applied in food fresh-keeping to remediate heavy metal-contaminated water and soils. HEEB irradiation reduces toxic compounds in the soil (Zhang et al., 2015). However, the additional chemical agents to increase the reduction efficiency can cause secondary pollution.

Electron beam technology has been used to reduce PFAS in soil. The high-energy electron beam is passed through the soil and degrades the PFAS. The process of irradiating a material with accelerated electrons results in an advanced oxidation-reduction process that oxidizes and reduces reactive species without needing additional reagents. Furthermore, this process does not generate secondary contamination.

2.2 Physical-chemical remediation methods

Physico-chemical remediation is the remediation process where chemical processes are combined with physical treatments. For example, several research studies showed that the electrokinetic process enhanced with chemical oxidation, chelating agents, surfactants

or reactive filter media demonstrated a better contaminant removal efficiency than the standalone electrokinetic process. In effect, applying chelating agents and surfactants increased the mobility of contaminants under an electric field. Reactive filter media (RFM), alternatively, act as adsorbing materials for enhancing the efficiency of contaminants removal from soils. Surfactants and reactive filter media are significant when dealing with persistent contaminants. Previous studies demonstrated the successful removal of polycyclic aromatic hydrocarbon (PAH) and hydrophobic organic compounds (HOC) from the soil in lab-scale experiments using an electrokinetic process coupled with different types of surfactants (Abdel-Shafy & Mansour, 2016).

2.2.1 Solvent extraction

Solvent extraction is a chemical extraction method for removing pollutants from soil matrices. This method mainly removes hydrophobic, persistent organic contaminants and industrial wastes. It is difficult to select environmentally non-disruptive approaches to remove persistent organic pollutants from soil effectively. Low-toxicity extraction solvents must be used to remove hydrophobic organic contaminants that minimize secondary pollution and are less harmful to the soil environment. This method is best suited in combination with other remediation technologies, especially with the electrokinetic process when persistent compounds are broken down into simpler or more mobile ones to increase their mobility and efficiency of removal under an electric field.

2.2.2 Supercritical fluid extraction

Supercritical fluid extraction is a novel in-situ method for removing hazardous contaminants from soil. This method is cost-effective and non-destructive since it uses carbon dioxide solvents. When the solvent temperature exceeds its vapour-liquid critical point, the solvent reaches an equilibrium phase, and contaminant transfer occurs. The supercritical fluid extraction method is a relatively clean and efficient alternative

extraction method and can be used in combination with electrokinetic remediation for better removal efficiency of contaminants.

2.3 Electrokinetic remediation method (EK)

Anthropogenic water and soil contamination have increased due to various human activities, including urban development, long-term wastewater irrigation, and mining. Pollutants frequently encompass heavy metal ions and hydrophobic organic compounds (HOC) or persistent organic pollutants (POPs) that exhibit perseverance in the environment, specifically in plants, posing a great risk to human health through transmission within the food chain. Electrokinetic remediation, an in-situ technique, has emerged as an effective method for the remediation of heavy metals from the soil, thereby mitigating the risks associated with contaminated soil and groundwater. A significant research focus is the environmentally sustainable and efficient removal of heavy metals, HOCs, and POPs from the soil. Electrokinetic remediation, utilizing low-intensity direct electric current, offers a practical approach for addressing these challenges, particularly in low-permeability soils and scenarios involving mixed contaminations. Applying a low-density direct current through strategically positioned electrodes in the contaminated soil facilitates the movement of contaminants before precipitation near the anode or cathode area (Virikutyte et al., 2002), allowing the contaminants in the soil matrix to be mobilised. The contaminants are pumped out after being transported to the cathode or anode electrode compartments. While the EK method has been extensively studied and proven effective for removing heavy metals, its application for removing organic contaminants, particularly PFAS compounds, remains relatively limited. The focus of research in the EK method has primarily been on heavy metal remediation, and further investigation is

required to explore its potential and effectiveness in removing organic contaminants like PFAS compounds.

2.3.1 Fundamentals of electrokinetic remediation

Transport mechanism

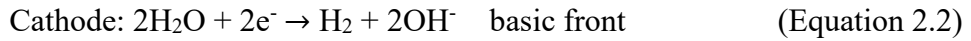
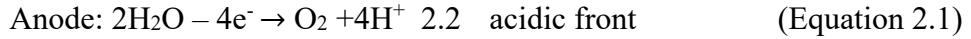
The electrokinetic remediation method uses a low-intensity direct current to remove contaminants from low-permeability contaminated soils. This technique employs several mechanisms, including electroosmosis, electromigration, and electrophoresis, to transport contaminants to the electrode chamber. As the concentration of contaminants in the soil-water system increases, so does their transportation, resulting in their accumulation in the electrode chamber. The contaminants that have been collected are then safely disposed of, effectively decontaminating the soil.

Electroosmosis: In the context of soil remediation processes, it is observed that the soil surface area typically carries a negative charge. Upon applying an electric current, the cations in the pore water near the soil surface exhibit movement towards the cathode. This movement is facilitated through the pore water, dragging the water molecules along. Consequently, water transfer from the anode to the cathode region occurs, commonly called electroosmosis (**Figure 2.2**).

Electromigration: electromigration refers to the transport mechanism in which ions in soil pore water migrate towards the oppositely charged electrode (**Figure 2.2**). This mechanism is the common transportation in EK remediation, especially when target contaminants are heavy metals or charged organic contaminants.

Electrophoresis is the movement of colloids in soil solution towards electrodes of opposite charge, like electromigration. This type of transportation is insignificant when dealing with tightly packed soil matrix.

Electrolysis: Electrolysis refers to the chemical reaction that takes place at the anode and cathode when an electric current is applied.



Water decomposition occurs at the electrodes. According to equation 2.1, oxidation of water at the anode generates H^+ ions and releases oxygen gas, and this causes an acid front and moves towards the cathode. Reduction occurs at the cathode (equation 2.2), generating OH^- ions and hydrogen gas, resulting in a basic front at the cathode and hydroxyl ions moving towards the anode. The electrolysis process changes pH across the soil during the EK process. The area near the anode exhibits a lower pH of around 3, and the region near the cathode has a higher pH of around 12. Hydroxyl ions and hydrogen ions move towards the anode and cathode by electromigration, hydrogen ions being smaller, tend to travel faster, leading to rapid acid front migration. Rapid soil acidification leads to contamination desorption from the soil. High pH values result in soil alkalization, which may cause contamination precipitation, consequently slowing down the transport of contaminants.

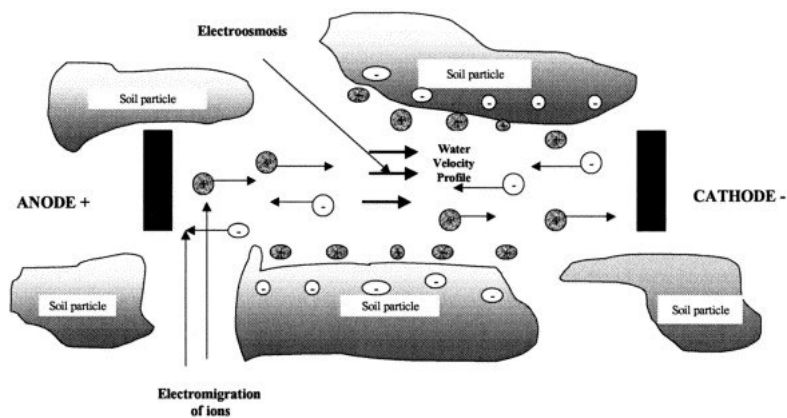


Figure 2.2: electroosmosis and electromigration of ions (adapted from Virkutyte (2002)).

2.4 Influence of factors on the electrokinetic process.

The applicability and performance of electrokinetic remediation techniques depend on the soil's physicochemical properties, contaminant species, electrode type, applied current density and experimental time.

2.4.1 Soil properties

Physicochemical properties of the soil, such as soil type, chemical compounds present in the soil, pH, and electric conductivity buffering and sorption capacity, highly affect the electrokinetic treatment. The buffering capacity and sorption capacity of the soil greatly impacts contamination transportation within the interstitial fluid of the soil. The high sorption ability of the soil can hinder the transportation of the contaminants requiring enhancing techniques for better transportation. The high acid/base buffering capacity increases the contaminants' solubility before being transported within the interstitial soil fluid. The pH gradient of the soil and the pore water of the soil has an impact on the sorption and solubility of the contaminant ions.

The electrical conductivity of soil refers to its capacity to conduct electric current and is typically measured in milli Siemens per meter (mS/m). This property is influenced by the chemical characteristics of the soil as well as its moisture content. The electric conductivity of soil plays a significant role in electrokinetic processes as it directly affects the flow of direct electric current through the soil matrix. Higher conductivity enables better current flow, while lower conductivity restricts the movement of electric charges. Therefore, understanding and considering the electric conductivity of soil is crucial for optimizing and assessing the effectiveness of electrokinetic remediation techniques.

2.4.2 Influence of the electrode type

Electrodes are crucial to the EK process to conduct the applied electric field. Inert to anodic dissolution, electrodes are used for the EK remediation process. Many types of electrodes can be used, including graphite, platinum, titanium, stainless steel, gold and silver (Virkutyte et al., 2002). Stainless steel electrodes are also used in the EK process; however, when subject to corrosion, they can release Cr, leading to secondary contamination (Wen et al., 2017). Inert electrodes such as platinum and graphite are preferred because metallic electrodes can be oxidised at the anode (Qiao et al., 2018). However, graphite electrodes are commonly used due to their low cost, especially in lab-scale pilot studies.

Electrode corrosion can occur, resulting in electrode voltage loss and energy loss. As a result, removal efficiency and electrode resistance can be affected, leading to greater energy consumption (Wen et al., 2021). When a large overpotential is applied, even inert graphite electrodes can corrode (Liu et al., 2011). For EK technology, the ideal electrode should be durable and strong enough to withstand increased pressure and facilitate transportation. It should withstand corrosion and crystallisation to increase service life and lower operating costs.

2.4.3 Impact of contamination type

The efficacy and effectiveness of the EK process are dependent on the contamination type. Successful remediation of mixed pollution is challenging, and decontamination using the conventional technique could be more effective. No universal technology for removing heavy metals and organic contaminants from the soil exists. Because heavy metals and organic contaminations have varied chemical properties and behaviours in soil, therefore they require different methods or combined soil remediation techniques for an effective removal rate (Alshawabkeh, 2009).

Hydrophobic organic contaminants such as polycyclic aromatic hydrocarbons (PAH) are composed of non-polar two or more benzene rings which are not soluble in water; therefore, it persists in soil (López-Vizcaíno et al., 2012; Shih et al., 2020). PAHs are primarily produced in the environment due to incomplete combustion of fossil fuels. Anthropogenic sources of PAHs readily enter the environment as gases from the combustion of fuel, wood, coal, petrol and oil. PAHs carry carcinogenic, mutagenic, and teratogenic properties if they enter the human body. Due to their hydrophobic and non-ionic chemical properties, hydrocarbons are immobile under an electric field (Bamforth & Singleton, 2005). The electrokinetic method successfully remediates of PAH from the soil when coupled with other remediation methods or enhancement agents. Table 2 concludes the efficiency and removal rate of various soil contaminants using EK treatment in previous studies.

PFOA is highly persistent in soil due to a strong carbon-fluorine bond, and it is not biodegradable but has high bioaccumulative properties. PFOA is partially soluble in water due to the carboxylic acid functional group. Electrokinetic remediation processes show promising results in removing hydrocarbons from the soil in combination with enhancing agents. Due to the solubility in the soil pore water and the anionic nature of PFOA, electrokinetic remediation can be used to remove PFOA from the soil. However, enhancing agents like adsorbents, reactive filter media and surfactants must be used simultaneously to increase efficiency. The use of electrokinetic remediation to remove PFOA from soil needs to be further investigated. Adsorption efficiencies of PFOA from wastewater have been investigated in published research, but transportation, adsorption and removal efficiencies from soil need further study.

Table 2.2: Performance studies for various soil contaminants using electrokinetic treatment.

EK treatment	Enhancement	Removal rate	Reference
Target pollutant			
Chromium	Citric acid pre-acidification enhancement	77.66%	(Meng et al., 2018)
Chromium, Copper and Nickel	EDTA-enhanced EK in combination with cation exchange membranes	Reduction from 80% to 20%	(Song et al., 2020)
Organochlorine pesticide	Triton-X advanced oxidation Surfactant enhanced.	88.05% (1,2,4-TCB) 56.36% (4,4-DDE)	(Suanon et al., 2020)
Organochlorine pesticide D.D.T. and chlordan	TX-100; S.D.B.S., ethanol as solubilizing agents	TX-100 on chlordan and DDDs 80%; on DDT 70.4%; SDBS inefficient.	(Meng et al., 2019)
Cadmium and Lead	Acid enhanced EK	removal and can be used as a reliable predictive tool.	(Rezaee et al., 2019)
Phenanthrene	SDS; Brij 30; Hydrogen peroxide	SDS 9.97%; Brij 6.31%	(Park et al., 2002)

		Hydrogen Peroxide	
		54.7%	
		At 10mA(7 Days)	
		84.2%	
Phenanthrene	Hydroxypropyl- β -cyclodextrin	56% removal rate with 6.85mM HPCD	(Ko et al., 2000)
Phenanthrene	Brij30; APG, SDS Surfactant enhanced EK	APG-75.1% removal rate after 4 weeks; Brij30 56.5% after 4 weeks.	(Park et al., 2007)
Mixed contamination	Co-solvent (n-butylamine) extraction coupled with EK	Phenanthrene migrated towards the cathode proportional to the concentration of co-solvent;	
Heavy metals and organic pollutants		Nickel ions were immobilized rather than removed.	(Maturi et al., 2008)
PFAS	Ion-exchange membrane	26%-56%	(Söregård et al., 2019)

[EDTA-Ethylenediaminetetraacetic acid; EK-electrokinetic remediation; TX-100- **Polyethylene glycol tert-octylphenyl ether**; **TCB-trichlorobenzene**; **DDE**-Dichlorodiphenyldichloroethylene; **SDBS**-Sodium Dodecyl Benzene Sulphonate; **DDT**-Dichlorodiphenyltrichloroethane; **DDD**-Dichlorodiphenyldichloroethane; **SDS**-Sodium dodecyl sulfate; **Brij-30**-Polyethylene Glycol Dodecyl Ether; **Pb**-lead; **Cd**-Cadmium; **HPCD**- 2-hydroxypropyl-beta-cyclodextrin; **APG**-alkyl polyglucoside; **PFAS**- polyfluoroalkyl substances]

2.5 Electrokinetic enhancement

Organic and inorganic contaminants are effectively eliminated in the electrokinetic (EK) process through the occurrence of water electrolysis, electroosmosis, electromigration, and electrophoresis phenomena (Acar & Alshawabkeh, 1993). These transportation mechanisms are responsible for the electrokinetic removal of organic and inorganic contaminations from the soil. During the EK process, the movement of the pollutants in the soil is simultaneously achieved by phenomena such as sorption/desorption, precipitation and desorption. Electric current, experimental time, voltage gradient and electrolytes influence the removal efficiency of the EK process. To enhance the EK remediation efficiency, enhancing agents are added to improve these mechanisms for better removal of contaminants from the soil matrix. When selecting enhancing agents, it's important to consider that OH^- released into the soil can cause precipitation of heavy metal ions and strong adsorption of contaminations on the soil surface. In the case of organic pollutants, the absence of a charge can hinder transportation. Therefore, the enhancing agents must be selected to overcome the limitations without causing secondary contaminations.

2.5.1 Surfactants aided electrokinetic remediation

Surfactants are agents that assist in remediation processes by enhancing the efficiency of contaminant removal. Typically, surfactants speed up the process by binding them to the contaminants, making them more easily transportable for extraction. Surfactants are more important when dealing with organic compounds because they tend to be highly persistent in soil (Luthy et al., 1997). The low solubility and bioavailability of hydrophobic organic compounds limit the removal of PAHs, HOCs and PFOS by conventional remediation processes. Hence, surfactants are used to improve the removal efficiency of such organic contaminants. The presence of surfactants in the environment can reduce water's surface

and interfacial tension, thereby enhancing organic contaminants' solubility. Surfactants usually consist of a hydrophobic chain on one end and a hydrophilic chain (water-soluble group) on the opposite side of the molecule. The interaction of the water-soluble group with an interstitial fluid of soil ensures its solubility. The interaction of the hydrophobic group with organic pollutants assures the solubilization of organic contaminants. The molecule then forms a structure called a micelle. The minimum concentration at which it occurs is called the critical micelle concentration (CMC) (Alcántara et al., 2008).

Surfactants increase the water solubility and biodegradability of persistent hydrophobic compounds by reducing the surface and interfacial tension. Surfactants contain water-soluble and insoluble groups, and the interaction with hydrophobic organic compounds creates a spherical-shaped molecule; as a result, organic contaminant solubility is significantly enhanced above CMC. Surfactants are classified into anionic, cationic and non-ionic according to their chemical properties, but the commonly used surfactants are anionic and non-ionic. Surface active agents can change the solution's surface properties, increasing the solubility of hydrophobic contaminants in environmental applications. Research studies on the adsorption capacity of PFOS using cationic and anionic surfactants established that anionic surfactant demonstrated low sorption capacity. Still, it increased the solubility of PFOS in natural sediments (Pan et al., 2009). The result suggests that surfactants can assist in electrokinetic remediation for removing PFOS from the soil.

2.5.2 Permeable reactive barrier

Permeable reactive barrier (PRB)-assisted remediation technology is a passive remediation system specially designed to remove heavy metals and organic compounds from soil. PRB enhances soil remediation technologies by trapping or degrading them (Li et al., 2011). Due to the environmental issues posed by remediation processes, selecting

enhancing agents that are safe for the environment and living organisms is crucial. There are different types of PRB have been proposed and evaluated for their excellent use in the removal of heavy metals and organic contaminants from soils. Surfaces with large pores, such as activated carbon or ion exchange resins, have higher adsorption capacity than those with smaller pores. Several materials are used as PRB in the EK process, such as activated carbon, nano zero-valent iron (nZVI), zeolite, surface-modified AC, compost, and carbonised food waste (Andrade & dos Santos, 2020; Ghobadi, Altaee, Zhou, McLean, Ganbat, et al., 2020b; Han et al., 2010). EK and PRB have successfully removed heavy metal ions and hydrophobic organic pollutants from the soil through adsorption and degradation. Studies have shown that the PRB-enhanced EK system significantly improved the removal efficiency. Lab scale EK study conducted by (Chen et al., 2022) utilised slag PRB to remove copper from contaminated soil. It concluded that experimental results indicated better removal efficiency when coupled with PRB. Fe/C PRB enhanced EK resulted in better removal efficiency for removing persistent organic pollutants from contaminated soil (Sun et al., 2017).

2.5.3 Activated carbon

Activated carbon is an excellent adsorbent for heavy metals and organic matters removal (Gong et al., 2007). Granular activated carbon impregnated with iron oxide has high adsorption efficiency for removing heavy metals and organic contaminants (Meng et al., 2019). It has been studied extensively to remove hazardous contaminants from wastewater (H.-C. Kim et al., 2010; Suresh Kumar et al., 2017a). Activated carbon showed an excellent adsorbent capacity for removing PFOS from aqueous solution with removal rates as high as 99%, but the regeneration of granular activated carbon was not possible (Z. Du et al., 2014). Activated carbon is well known for its use as reactive filter media to increase the removal efficiency of contaminants in combination with the

electrokinetic process. Hence, it is possible to use activated carbon as reactive filter media to remove PFOS from the soil.

2.5.4 Chitosan

Chitosan is a polysaccharide obtained from crustaceans. It is an emerging cost-effective adsorption material that has been widely used in wastewater treatment and soil-enhanced soil remediation techniques (Bautista-Baños et al., 2016). Studies have demonstrated high adsorption capacity for removing heavy metals and organic compounds. Chitosan is an effective adsorbent for treating heavy metals due to the presence of amino and hydroxyl groups (Ren et al., 2008; Vunain et al., 2016). Chitosan demonstrated a great adsorption capacity for removing PFOS from wastewater (Z. Du et al., 2014). The surface area properties of chitosan make it possible to use it as adsorption media to remove PFOS from the soil in combination with the electrokinetic process. However, the regeneration properties of chitosan need to be further investigated. Since it has high adsorption efficiency for PFOS, it can be combined with the electrokinetic process or other remediation methods.

2.5.5 Biochar

Biochar is an adsorbent widely used to remove heavy metals and organic compounds from water and soil (Qin et al., 2020). The negative charge and biochar's high surface area make it a suitable adsorbent to reduce the mobility of heavy metals in soil (Khalid et al., 2017). Biochar is a solid pyrolysis product generated during biomass heating at 300 to 500 °C without oxygen. This carbon-rich, porous, purpose-produced charcoal consists of stable aromatic organic matter with about 70 to 80% carbon concentrations. Nutrient availability in biochar is affected by the type of biomass, processing conditions, and the type of bonds associated with the elements (Anawar et al., 2015). High surface area and negative charge of biochar play an important role in removing hazardous materials.

Biochar is easier to regenerate than compost due to its high permeability and low cation exchange capacity. These attributes have the potential to enhance the soil's ability to retain water, regulate pH levels, increase surface sorption capacity, and augment cation exchange capacity (CEC), and base saturation. These attributes are influenced by the pyrolysis temperature and the inherent properties of the feedstock (Anawar et al., 2015). Changes in the characteristics of the soil, mainly the increase of pH, can make the heavy metals immobilised in the soils and consequently lead to their precipitation (Khalid et al., 2017). Biochar comes at different pH's, and slightly alkaline pH biochar will help to capture soluble metal ions transporting from towards the cathode. Activated biochar successfully reduced low TOC soil leachate PFAS concentrations (by 98-100%), and with high TOC reductions was lower (23-100%), which can be due to the pore-clogging at higher TOC (Sørmo et al., 2021). As a result, it is hypothesised that biochar can be utilised with EK as an enhancement agent.

2.5.6 Carbon nanotubes

Carbon nanotubes are effective adsorbents for heavy metal removal and organic contaminants due to their high chemical stability, large surface area, excellent mechanical and electrical properties, high adsorption capacity and well-developed mesopores (Herlem et al., 2019; Matos et al., 2017). Carbon nanotubes demonstrated promising results in immobilising and adsorbing heavy metals in wastewater Matos et al. (2017)s. Moreover, carbon nanotubes showed high efficiency in removing PFOS from wastewater. There is also a potential for applying carbon nanotubes as reactive filter media with the electrokinetic process to remove PFOS from the soil. However, carbon nanotubes are more costly than biomaterials or activated carbon.

2.5.7 Nanoscale zero-valent iron

Increasing the removal efficiency of heavy metals and persistent organic pollutants from soil using environmentally friendly enhancing agents has become a research significance. Nanoscale zero-valent iron adsorbents demonstrated great potential in immobilizing heavy metals and degrading persistent organic compounds (Jiang et al., 2018). Nanoscale zero-valent iron (nZVI) has low toxicity, great surface area and activity and is cost-efficient. Reduction, oxidation, adsorption, and co-precipitation are the primary mechanisms used by nZVI to remove contaminants. Direct and catalytic reduction at the surface of nZVI or corrosion products are two pollutant reduction mechanisms that nZVI mediates (Jiang et al., 2018). Surface-modified nZVI PRB utilized EK to remove trichloroethylene from contaminated soil and had a removal rate of 96.7% under optimal conditions (Song et al., 2022).

Table 2.3 lists a few examples of removing heavy metal and persistent organic pollutants from contaminated soils by nZVI. It is also observed that coupling nZVI with surfactants or other remediation techniques enhances contaminant removal efficiency. nZVI is a promising, cost-effective alternative to remediate heterogeneous contaminated soils. The high removal efficiency of PAH from soil using nZVI is a promising result that could also be applied to remove PFOS from the soil as a future study. There are no published research studies on removing PFOS from contaminated soils using nZVI; however, nZVI has a large surface area, making it suitable for removing PFOS from the soil when coupled with ionic surfactants.

Table 2.3 Soil remediation through the application of nzvi for the Removal of heavy metals and organic pollutants

Target contaminant	Treatment	Performance	Reference
Pb polluted soil	0.2g/L nZVI and 0.2M citric acid	The removal efficiency of Pb – 83%	(Wang et al., 2014)
Cr polluted soil	nZVI/Biochar	100% and 91.4%	(Su et al., 2016)
Polycyclic Aromatic Hydrocarbon (PAH)	nZVI	100% Anthracene and BPE. 90% PHE.	(Pardo et al., 2016)
Phenanthrene	nZVI/SDS.	80% degradation of PHE.	(Peluffo et al., 2016)

[EDTA -Ethylenediaminetetraacetic acid; EK- Electrokinetic; TX-100-t-Octylphenoxyethoxyethanol; Polyethylene glycol tert-octylphenyl ether; SDBS - Sodium dodecylbenzenesulfonate; DDT-dichloro-diphenyl-trichloroethane; DDD – 1,1-dichloro-2,2-bis(p-chlorophenyl)-ethane; EK –Electrokinetic Remediation; Pb –Lead; Cd – Cadmium; SDS-Sodium dodecyl sulfate; Brij-30 – Polyoxyethylene(4)lauryl ether; HPCD- hydroxypropyl-beta-cyclodextrin; APG- Alkyl polyglycoside]

CHAPTER THREE
MATERIALS AND METHODS

CHAPTER 3 : MATERIALS AND METHOD

3.1 Materials

PFOA with purity > 99% was purchased from Sigma-Aldrich, Australia, to spike the soil artificially. In this study, the utilization of commercially sourced Kaolin clay procured from Keane Ceramics Pty Ltd. (Australia) serves as a representative model soil for electrokinetic soil remediation. The selection of kaolin clay is based on its physicochemical characteristics' attributes, including a low organic content and reduced cation exchange capacity, which collectively contribute to a low buffering capacity. The physicochemical properties of kaolin soil are shown in **Table 3.1**. It helps to understand the transfer of organic pollutants under a low direct electric field without interferences of organic or inorganic impurities. Methanol HPLC grade for the extraction of PFOA from soil post-experiment and the mobile phase used was purchased from Sigma-Aldrich, Australia. Ionic surfactant sodium dodecyl sulphate (SDS) in the form of a fine powder, Tween80 non-ionic surfactant in viscous liquid form, sodium cholate (NaC) biosurfactant obtained as finely powdered form were all procured from Sigma-Aldrich, Australia

Powdered Activated carbon was purchased from Sigma-Aldrich, Australia, with a 100-mesh particle size. The same AC was used for modification, and iron sulphate was used and obtained from Sigma-Aldrich, Australia, to modify the AC surface potassium permanganate. A PRB slag was obtained from the environmental engineering laboratory and mixed with powdered activated carbon for all the experiments. Another PRB was used in the last chapter, and the cation exchange membrane was purchased from Fujifilm, Australia.

The School of Electrical Engineering in the Faculty of Engineering and Information Technology (FEIT) at the University of Technology Sydney (UTS) supplied the DC

bench scale power supply (EA-PS 3016-10B) and current meter (Keithley 175 Autoranging multimeter) for this study. Electrical wires for the connection of power supplies and electrodes were purchased from Jay Cars Australia Pty. Graphite electrodes were used for all EK experiments and obtained from Graphite Australia Pty Ltd. Cellulose filter papers were used in all tests to prevent soil particles from penetrating electrode chambers (pore size 5-13 μm , LLG labware).

Table 3.1: Physical properties of Kaolin soil

Physico-chemical characteristics	Values
Particles size	46.81
Clay	51.17
Silt	2.02
Permeability (m/sec)	4×10^{-10}
Density (g/cm ³)	1.45
Porosity (Kg/m ³)	633
Organic matter	0.02
CEC (cmol/kg)	2.65
pH	6.28
Electrical conductivity (mS/cm)	0.26

3.2 Methods

3.2.1 Soil Preparation

The selection of PFOA as the target contaminant in this study is derived from its status as one of the predominant PFAS compounds identified in environmental matrices. PFOA-spiked kaolinite soil was prepared by carefully combining 1 kg of kaolin with a 1L PFOA solution of the desired concentration, ensuring thorough mixing. The stock solution of 1000 ppm PFOA was prepared in MilliQ water by mixing 1g of PFOA powder in 1L MQ water. Then it was diluted to 100 ppm (in 1L MilliQ water) for the surfactant enhanced EK studies. The stock solution was diluted to a 10-ppm target concentration for the rest of the experiments. After spiking the kaolinite with PFOA, it was left to equilibrate for at

least 72 hours to achieve desired homogeneity and uniform concentration. The soil in a saturated state was layered and uniformly compacted within the reactor.

3.2.2 Surfactants

Laboratory-scale electrokinetic tests were conducted to assess the removal of PFOA using various surfactants, including anionic surfactant sodium dodecyl sulphate (SDS), biosurfactant sodium cholate and non-ionic surfactant Tween80. Surfactants are used to increase the removal rate of contaminants in the EK process under the imposed electric field. In the surfactant enhanced EK experiments, the effect of surfactants was investigated for the removal of PFOA under a constant current of 20 mA. In each experimental setup, a concentration of 5% w/w surfactants was employed within the cathode chamber, TW80, on the other hand, was used in the cathode chamber and in the anode chamber to evaluate the effectiveness of the surfactants. The most effective surfactant was then used in the PRB system to enhance the EK process.

3.2.3 Permeable reactive barrier (PRB)

FeAC has a high adsorption capacity due to the AC surface and iron coating. FeAC demonstrated great adsorption capacity in water treatments. FeAC was prepared using two different methods and will be investigated in bench-scale electrokinetic tests as RFM. The first method used H_2SO_4 and HNO_3 (1:1 v/v) to oxidise the granular activated carbon, 30g of dry GAC was mixed in a solution and left at room temperature for 24 hours and thoroughly washed until pH was neutral and oven dried at 105°C for 12 hours. Then it was mixed with $\text{FeCl}_3 \cdot 6\text{H}_2\text{O}$ solution (1:10 w/v), left for 24 hours at room temperature, washed until the solution was clear, and dried for 12 hours at 105°C . The surface of FeGAC was analysed using FTIR, SEM and XRF to check the iron coating. The second method used 0.4M KMnO_4 as an oxidising agent, dry 30g GAC mixed with 0.4M KMnO_4

solution left for 24 hours at room temperature and washed with distilled water until colourless. Then it was dried in the oven overnight at 105⁰C.

Other PRBs, such as slag, were mixed with AC with different ratios to evaluate the effectiveness of the PRB in the EK system. CEM PRB was sandwiched between AC and used for EK experiments to obtain improved removal efficiency.

3.2.4 Electrokinetic cell set-up

A schematic diagram illustrating the setup of the electrokinetic cell is depicted in **Figure 3.1**. **Figure 3.1.a** shows a schematic of a non-PRB EK test, while **Figure 3.1.b** shows a schematic of PRB-improved EK tests. The reactor is built of plexiglass and has the following dimensions: 23 cm³ x 8 cm³ x 11 cm³. As seen in Figure 3.1, the reactor is divided into three sections, two compartments at either side of the reactor containing electrolyte solutions and electrodes. The spiked soil is compacted in the middle section. Filter paper is placed between the soil and the plexiglass plate, separating the soil sections from the electrolyte chambers to stop soil leaching. Two graphite electrodes (15cm × 1cm) are used at both ends and connected to a DC bench power supply to apply the electric field. Distilled water is used as an anolyte. Since PFOA tends to accumulate in the centre of a soil section, PRB was loaded. PRB was placed between two filter sheets to keep it from penetrating the soil. Distilled water was periodically added using peristaltic pump to replenish the water loss. Surfactants (5% w/w) were added to the catholyte chambers. Beakers are placed at both ends to collect wastewater and overflow from cathode and anode compartments.

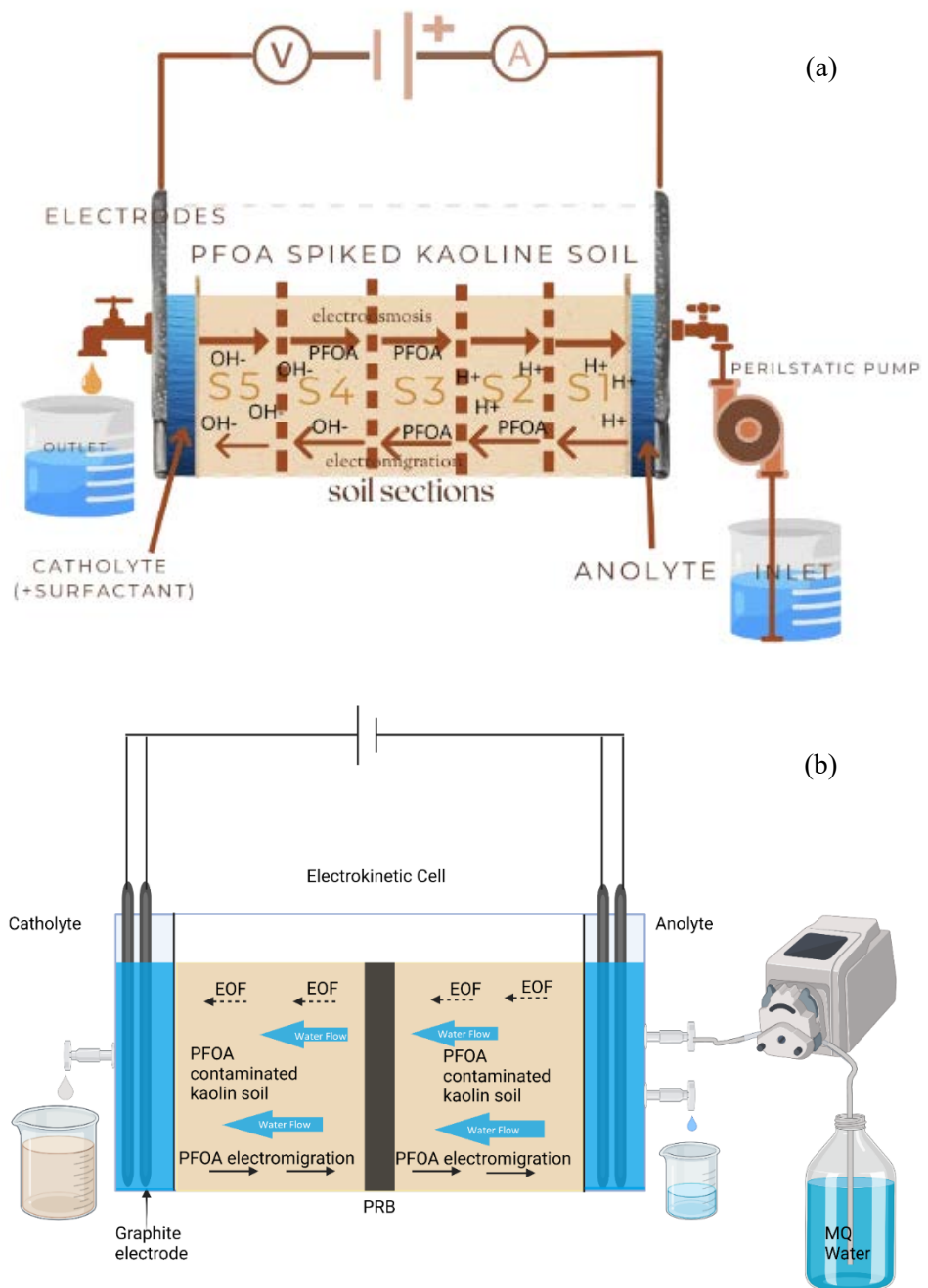


Figure 3.1: Diagram of lab scale EK reactor cell (a) surfactant enhanced EK test design
(b) surfactant, and PRB enhanced EK test design

3.2.5 Extraction procedure for PFOA

After completing the EK experiment, the soil was sliced into 5 equal sections in non-PRB tests and 6 equal sections in PRB-enhanced EK experiments. Each soil section was mixed thoroughly to reach homogenous consistency. After mixing well, soil samples were taken

and placed in centrifuge tubes and centrifuged at 9000 rpm for ten minutes to separate the soil pore water. Soil pore water was then transferred into clean test tubes to analyse PFOA. The remaining soil was then transferred into glass dishes and dried at 105⁰C for 16 hours in the oven. Dried soil samples were pulverised using mortar and pestle. PFOA was extracted using a triple methyl alcohol extraction method. In each extraction cycle, 5 mL of methyl alcohol was added to 5 g of dried soil. The mixture was subjected to agitation on a flat shaker at 180 rpm and 22°C for 60 minutes. Subsequently, sonication was carried out at 30°C for 30 minutes, followed by centrifugation at 9000 rpm for 10 minutes. After three consecutive extractions, the resulting supernatants were collected and combined. The combined supernatant was then appropriately diluted and subjected to syringe filtration for subsequent analysis using liquid chromatography-mass spectrometry (LC-MS).

3.2.6 PFOA removal

The assessment of removal effectiveness subsequent to the EK treatment involved the calculation of PFOA removal for each soil section (Ghobadi, Altaee, Zhou, McLean, & Yadav, 2020b; Ortiz-Soto et al., 2019):

$$Removal\ Efficiency_i = \frac{m_{i,initial} - m_{i,final}}{m_{i,initial}} \times 100\% \quad (\text{Equation 3.1})$$

In the context of this study, " $m_{i,initial}$ " represents the initial concentration (mg/kg) of PFOA in section i prior to treatment, while " $m_{i,final}$ " denotes the remaining PFOA concentration (mg/kg) in section i after undergoing the EK experiment.

The total PFOA removal efficiency of the EK process was calculated by the following equation (3.2) (Ghobadi, Altaee, Zhou, McLean, & Yadav, 2020a; Ortiz-Soto et al., 2019)

$$Total\ PFOA\ removal = \frac{m_{final} - m_{initial}}{m_{initial}} \times 100\% \quad (\text{Equation 3.2})$$

m_{initial} is the initial PFOA concentration (mg/kg) before the experiment, and m_{final} is the residual PFOA concentration (mg/kg) in the soil after the EK experiment.

3.2.7 Specific energy consumption (SEC)

One of the most important factors is power consumption to evaluate the overall cost of EK remediation. Energy consumption is an important factor in the EK process as electric current is responsible for the transportation of the contaminants, and dissolution of the compound under an electric field (Villen-Guzman et al., 2015). Power consumption is also important for the evaluation of the cost.

In this study, the specific energy consumption was calculated by the following equation (3.3)

$$E_u = \frac{10^{-3}}{V_s} \int V I dt \quad (\text{Equation 3.3})$$

In this context, "Eu" stands for the specific energy consumption (kWh kg⁻¹), "I" represents the electric current (A), "V" denotes the applied voltage (V), "t" indicates the experimental time (h), and "Vs" signifies the total volume of treated soil (kg).

3.2.8 Analytical approach

Initial and post-experimental soil sections were evaluated for pH, EC and PFOA content. The pH value and EC ($\mu\text{S}/\text{cm}$) of soil sections, soil pore fluid, PRBs, anolyte solution, catholyte solution and catholyte overflow were all measured using a pH/EC multimeter (Thermo Scientific EUTECH PC450). To measure the pH, dry soil and distilled water were mixed to make slurry at a ratio of 1:5 (w/v), shaken well on a flat shaker for at least 15 min and taking an average of 5 readings of each sample (Altaee et al., 2008). Soil electric conductivity was measured before and after each experiment as well as anolyte

and catholyte solutions and PRBs where applicable. For both pH and EC, an average of 5 readings were taken.

The soil moisture content during the EK process is an important factor as it defines the dissolution rate of contamination and their transportation under an electric field by electroosmosis and electromigration (Yan et al., 2018). The soil's moisture content is measured before to the electrokinetic experiment, and the kaolinite soil sample is measured before and after drying at 95°C for 24 hours. The moisture content is calculated as follows:

$$\text{Moisture content} = \frac{\text{Weight of kaolinite after drying}}{\text{Weight of kaolinite before drying}} \times 100 \quad (\text{Equation 3.4})$$

Liquid chromatography – Mass spectroscopy (LC/MS) (Shimadzu LCMS 8060) is used to analyse PFOA before and after each experiment. For the analysis standard calibration solution is made and run with each experiment. PFOA calibration standards were made at 40, 20, 10, 5 and 2.5 µg/L concentrations. C18 reverse-phase 5µm 100 × 2.1 mm column was used. Mobile phases were Methanol HPLC grade and Methanol and MilliQ Water (50:50). The supernatants collected after each extraction were mixed and diluted using a volumetric flask and then transferred to vials with syringe filters. The recovery of the extracted analyte was evaluated to assess the extraction process's effectiveness. Data analysis was performed to calculate key parameters, including mass balance, removal efficiency, and total PFOA removal rate. These calculations were used to quantify the proportion of PFOA that was successfully recovered, the extent of contaminant removal, and the overall rate of PFOA removal achieved through the extraction method.

Characteristic analysis of PRB is important in this study to define the change observed during the EK process. PRBs in this study adsorb the PFOA and facilitate the

transportation of the contaminants. The specific surface area of the permeable reactive barriers (PRBs) was determined through the utilization of Brunauer-Emmett-Teller (BET) nitrogen adsorption-desorption isotherms, along with the Barrett-Joyner-Halenda (BJH) method. These measurements were conducted using a Micromeritics 3-Flex™ surface characterization analyzer at a temperature of 77K. The objective of this analysis was to investigate the changes in the PRBs' surface area following the electrokinetic (EK) process. For the examination of the PRBs' surface and elemental composition before and after the EK process, as well as the modified PRB before and after the modification process, scanning electron microscopy (SEM) coupled with Energy-dispersive X-ray spectroscopy (EDS) was employed. The zeta potential values of the PRBs were assessed both before and after the EK treatment using a Nano-ZS-seizer (Model ZN3600) from Malvern Panalytical. Additionally, a Fourier transform infrared spectrometer (FTIR) was used to identify the functional groups present in the soil and PRBs.

CHAPTER FOUR

**INVESTIGATION OF THE EFFECT OF
SURFACTANT ON ELECTROKINETIC
TREATMENT OF PFOA CONTAMINATED SOIL**

CHAPTER 4 : INVESTIGATION OF THE EFFECT OF SURFACTANT ON ELECTROKINETIC TREATMENT OF PFOA CONTAMINATED SOIL

This chapter has been derived from the publication listed below:

Ganbat, N., et al. (2022). "Investigation of the effect of surfactant on the electrokinetic treatment of PFOA contaminated soil." Environmental Technology & Innovation, 28, 102938.

4.1 Background

PFOA belongs to a group of chemicals called PFAS. PFOA-contaminated environmental pollution is one of public health's most critical and emerging problems. Since the 1950s, PFAS have been widely employed in many applications due to their unique physicochemical properties (Teaf et al., 2019). These substances are used in industrial resources, waterproof surfaces, packaging materials, fire hydrant foams, surfactants, cosmetics and pesticide additives (van Asselt et al., 2011). The strong carbon-fluorine (C-F) bonds of PFOA make them chemically stable, very persistent in soil, and highly resistant to biodegradability. At the end of the chain, the hydrophilic functional group enables PFOA mobility in an aqueous medium (Deng et al., 2015). PFOA and PFOS are the most common PFAS compounds detected in the environment (Hassan et al., 2020). PFOA and PFOS manufacturing and using products containing them have been phased out. Their emissions have been reduced in many countries due to their toxic and persistent nature, which accumulates in the soil and plants posing a significant risk to public health through the food chain and drinking water (US EPA, NSW EPA, EU).

Conventional soil remediation methods such as mechanochemical treatment, ball stabilization and solidification, thermal treatment, electrochemical tests, and encapsulation have been applied to remove and mitigate PFOA and PFOS from polluted soils in situ and ex-situ (Bolan et al., 2021b; Mahinroosta & Senevirathna, 2020b;

Senevirathna et al., 2021). Some of the remediation technologies mentioned above, such as thermal treatments, are not cost-efficient due to their high energy demands (Crownover et al., 2019; Jacobs, 2019). Stabilization and solidification treatments involve the adsorption of PFAS compounds onto adsorbent surfaces; however, it does not degrade the contaminants. Also, the presence of other organic contaminations in soil reduces the adsorption efficiency of PFAS. Encapsulation treatments mitigate the PFAS compounds transported across the soil; long-term leaching is still unknown. Excavation and landfilling raise exposure to risk while handling contaminated soils. Electrochemical studies demonstrated the feasibility of PFAS removal from contaminated soils. Their study evaluated the transport, mobilization, and desorption of PFAS under a low constant electric field. The EK experiments achieved limited PFAS removal from the contaminated soil, and most PFAS accumulated in the middle section of the soil. To date, limited studies have been carried out on the surfactant-enhanced EK treatment of PFAS-contaminated soils. (Hou et al., 2022) investigated electrochemical destruction and mobilization of PFOA and PFOS in saturated soil. They reported a high degradation rate of 92.1% and 92.2% in the cathode region and a lower rate of 55.1% and -37.1% in the anode region (Hou et al., 2022). The study also found that PFOA and PFOS were accumulated in the soil's middle section. Wang et al. studied the electrochemical degradation of PFOA by Ti/SnO₂-Sb anode via peroxymonosulfate (PMS) activation. It was hypothesized that PFOA was converted into a shorter chain and that the k_{PFOA} value rose with the increase in current density (Wang et al., 2020). In another lab-scale study, electro-dialytic remediation was applied to remove PFAS from contaminated soil. The investigation revealed that the primary mode of transport for PFOA and PFOS was electromigration directed towards the anode. Based on these findings, the study proposes that in situ remediation trials hold significant promise for removing PFOA and PFOS

contaminants. This highlights the potential for future application and development of in situ remediation approaches as effective strategies for mitigating PFOA and PFOS contamination.

EK remediation is a widely recognized in-situ technique employed to extract heavy metal ions from soil matrices (Ghobadi, Altaee, Zhou, McLean, Ganbat, et al., 2020b). This method harnesses a low-intensity direct electric current to facilitate the remediation process, rendering it suitable for implementation in soils characterized by low permeability and mixed contaminant compositions. Electric current assists in the transport of contaminants in the soil before precipitation near the cathode zone. A low-density direct current is applied through anode and cathode electrodes strategically placed in the contaminated soil. This approach enables the mobilization of contaminants in the soil matrix. The contaminants transported toward the cathode or anode electrode compartments are pumped out (Cameselle & Gouveia, 2018). Electromigration is the primary transport mechanism for negatively charged molecules in the EK process. However, several studies demonstrated the co-transport mechanism by electroosmosis for negatively charged molecules such as oxyfluorfen and phenol (Kuppusamy et al., 2017; Meng et al., 2019)

Conventionally, removing organic compounds by the EK process is more challenging than metal ions due to their low water miscibility, adsorption onto the soil, or neutral charge. Therefore, researchers used the surfactant-enhanced EK process to remove soil organic contaminants. (Yuan et al., 2006) evaluated the removal of hexachlorobenzene from contaminated clayey soil using TW80 and β -cyclodextrin enhanced EK system. Results revealed a lower removal rate of hexachlorobenzene in the EK process with the TW80 enhancement agent. This study recommended sodium dodecyl sulphate (SDS) as a washing solution for soil remediation due to its biodegradability and low adsorption on

the soil surface (Giannis et al., 2007). Researchers found that soil treatment by simultaneous use of SDS (catholyte) and TW80 (anolyte) resulted in improving the removal efficiency of polycyclic aromatic hydrocarbon (PAH) from the soil (Boulakradeche et al., 2015). SDS enhanced-EK remediation for removing kerosene from contaminated soils increased the removal of the contaminant from 40% in non-enhanced EK to 55% (Fardin et al., 2021). Using Tween80 and an enhancement agent in the EK achieved 45% kerosene from the soil. Sodium cholate, a non-toxic biosurfactant, possesses a structurally significant hydrophobic moiety characterized by a large, rigid, and planar structure originating from a steroid nucleus, which incorporates two or three hydroxyl groups (Sugioka et al., 2003). Sodium cholate (NaC) was chosen as a representative biosurfactant considering its exceptional solubilization capabilities, notable biodegradability, and biocompatibility. According to a reported investigation, exposure to NaC demonstrated no discernible impact on cell morphology, thereby corroborating its classification as an environmentally benign surfactant (Dong et al., 2009). According to the research (Zeng et al., 2013), sodium cholate (NaC) exhibited a remarkable solubilization rate of 2,4,6-trichlorophenol (2,4,6-TCP). It demonstrated exceptional environmental compatibility, positioning it as an excellent surfactant for surfactant-enhanced soil remediation processes. Previous EK investigations have indicated that PFAS compounds are predominantly transported through soil via electroosmosis and electromigration mechanisms, accumulating in midsections. However, electromigration towards the anode was identified as the primary transport mechanism for PFOA. Among the approaches employed to augment the removal of organic compounds in soil, surfactant-enhanced EK processes have emerged as a noteworthy method (Söregård et al., 2019). Three types of surfactants, nonionic (TW80), anionic (SDS), and biosurfactant (sodium cholate), were evaluated in this study for PFOA

removal from kaolinite soils. The negatively charged SDS surfactant was introduced to the cathode zone to electromigrate towards the anode with the PFOA molecules. Sodium cholate is another anionic biosurfactant introduced to the cathode to enhance PFOA removal towards the anode zone. TW80 was introduced to the anode and is expected to react with PFOA in the soil and transport towards the cathode electrode.

This study investigates the feasibility of the surfactant-enhanced EK process for PFOA removal. Kaolinite was used as a model soil to eliminate soil impurities (organic and inorganic matter) effect on the PFOA removal by the EK process. Surfactants are introduced to increase the mobility and solubility of PFOA, hence increasing the removal efficiency.

To date, no investigation has explored the influence of surfactants on enhancing the EK process for the removal of PFOA from soil matrices. In this study, three distinct scenarios were examined for the treatment of PFOA: i) a conventional EK process, ii) an enhanced EK process utilizing an anionic surfactant, and iii) an enhanced EK process employing a nonionic surfactant. The impact of anionic and nonionic surfactants on the EK performance was evaluated by introducing anionic surfactants sodium dodecyl sulfate (SDS) and sodium cholate into the catholyte, while nonionic Tween80 was added separately to the anolyte and catholyte. The objective was to assess the efficiency of the EK system in removing PFOA from kaolin soils contaminated with the target compound. Notably, Tween80, recognized for its low toxicity, cost-effectiveness, low polarity, and high solubility capacity, has commonly been employed as a flushing solution and an enhancing agent in electrokinetic treatments for the removal of hydrophobic organic compounds (HOCs) (Cheng et al., 2017). The performance of the surfactant-enhanced electrokinetic (EK) process was evaluated in relation to the extension of the testing duration from one week to two weeks in this study.

4.2 Materials and methods

4.2.1 Materials and preparation of the soil

Chapter 3 (Materials and Methods) section furnishes an elaborate account of the materials, soil preparation techniques, and the equipment employed in conducting the electrokinetic (EK) experiments. *Table 3.1* provides a comprehensive overview of the characteristics associated with the kaolin soil employed in the electrokinetic (EK) tests. The experimental design is shown in **Figure 4.1**, ionic surfactants were added to the cathode chamber, and non-ionic surfactants were added to either cathode or anode chamber. Anionic surfactant sodium dodecyl sulphate, anionic biosurfactant sodium cholate and nonionic tween80 surfactants were used to enhance the bench-scale electrokinetic tests. The performance of these three different types of surfactants has been evaluated at different parameters.

Surfactants are employed to improve the removal efficiency of contaminants in the EK process when subjected to an applied electric field. In this experiment, the effect of anionic surfactant was investigated for PFOA removal in EK experiments under constant voltage and constant current. 5% w/w SDS was used as an enhancement agent for each experiment.

Nonionic TW80 surfactant was added to the anolyte solution. Anionic surfactants, SDS and NaC were introduced into the catholyte solution as an enhancing agent to enhance the EK process. A concentration of 5% w/w was utilized for each experimental setup.

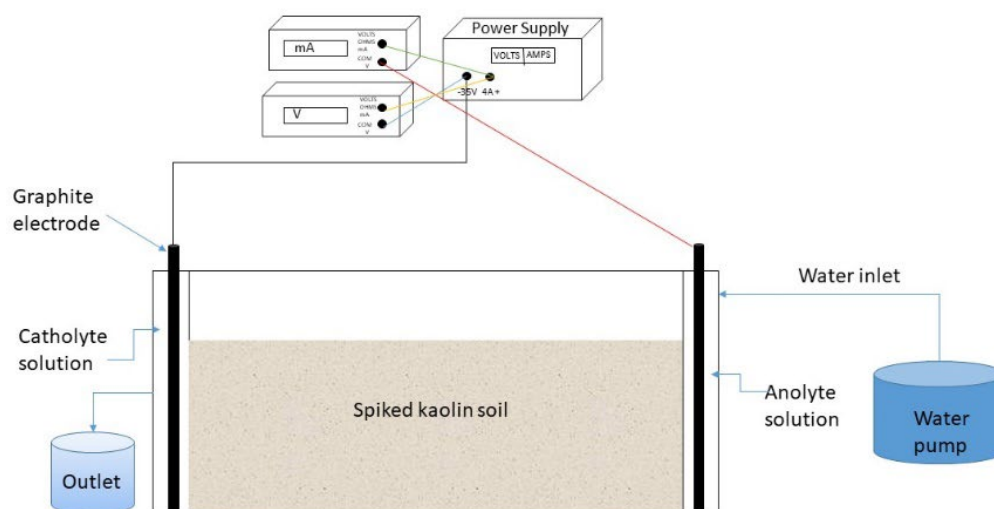


Figure 4.1:Electrokinetic cell set up scheme.

4.3 Analytical procedure

Each experiment was carried out for seven days, during which the current and voltage were diligently measured by a multimeter (Keithley 175) at hourly intervals. Upon completion of the experiments, samples from both the anode and cathode chambers were carefully collected and stored in polypropylene tubes. The soil section was divided into five equal parts, ensuring thorough mixing, and subsequently transferred to individual polypropylene tubes while any excess soil was safely stored. Following the sample collection, each soil section underwent centrifugation and was dried overnight at 100 °C. The dried soil samples were analysed for parameters such as pH and conductivity and were further extracted to determine the concentrations of PFOA.

4.3.1 Extraction of PFOA from soil

After the EK tests were completed, PFOA quantification was performed for each soil section using a triple methyl alcohol extraction method. In each extraction cycle, 5 mL of methyl alcohol was added to 5 g of dried soil, followed by agitation on a flat shaker at 180 rpm and 22°C for 60 minutes. Subsequently, sonication was carried out at 30°C for 30 minutes, followed by centrifugation at 9000 rpm for 10 minutes. The supernatants

obtained from three consecutive extractions were combined, diluted, and subjected to filtration for subsequent analysis using liquid chromatography-mass spectrometry (LC-MS). Furthermore, Fourier-transform infrared spectroscopy (FTIR) was employed to analyse the chemical bonds associated with PFOA.

4.3.2 Soil pH measurement

Soil pH was measured before and after the experiment for pore fluid pH of each soil section, anolyte, and catholyte solution using a pH meter (model HACH HQ40d multi metre). pH is measured by 1:5 (w/v) dried soil and distilled water, shaken well on a flat shaker for at least 15 min and taking the average of 5 readings of each sample.

4.3.3 Soil conductivity measurement

Soil conductivity is measured before and after each experiment and anolyte and catholyte solutions using a conductivity meter (model HACH HQ40d multi metre). Same as the pH measurements 1:5(w/v), dry soil to distilled water, then shake on a flat shaker for at least 15 min, taking the average of 5 readings of each sample.

4.3.4 LC-MS analysis

A triple quadrupole ultra-high-performance liquid chromatography-tandem mass spectrometer (UHPLC-MS/MS; LC/MS 8060, Shimadzu) equipped with a binary pump and Shim-pack column (1.6 μm , 2.0 mm \times 50 mm) was used analyze PFOA before and after each experiment. A standard calibration solution is made and run with each experiment for the analysis. PFOA calibration standards were made at 40, 20, 10, 5 and 2.5 $\mu\text{g/L}$ concentrations. C18 reverse-phase 5 μm 100 \times 2.1 mm column was used. Mobile phase Methanol and Milli-Q Water.

4.4 Experimental set-up

In this study, eleven EK experiments with different surfactants and constant current gradient were conducted at room temperature for seven and fourteen days. The EK experiments are detailed in *Table 4.1*. The electrolyte solution was distilled water, while the flushing solutions utilized were SDS (5% w/w), Tween 80 (5% w/w) and sodium cholate (5% w/w). As indicated in Table 2, 10 mA and 20 mA constant current gradients were used for the experiments. Approximately 100mg/kg PFOA kaolin mixture was used for all experiments. Anionic surfactants SDS and sodium cholate were loaded into the cathode chambers, whereas the nonionic Tween80 surfactant was loaded into the anode chamber; besides, the fluid level was kept constant in the inlet reservoir to ensure a constant steady hydraulic gradient throughout the soil. Initially, the experiments were carried out over a period of seven days, during which the electric current applied across the soil gradient decreased, and the electroosmotic flow subsided at constant currents of 10 mA and 20 mA.

As shown in *Table 4.1*, surfactants with 5% m/m were used at 10mA and 20mA constant current for one week, and the experiments with the highest efficiency were tested for two weeks. Experiments E1 and E2 were carried out without surfactants to explore the effect of EK remediation to remove PFOA from kaolin. Later, it was used to compare the efficiencies of surfactant-enhanced EK. Experiment E3 SDS-EK, experiment E6 NaC-EK and experiment E8 tween80-EK were carried out under 10 mA constant current for one week. Experiment E4 SDS-EK, experiment E5 NaC-EK and experiment E9 Tw80-EK were carried out under 20 mA constant current gradient for one week. At the end of each experiment, the concentration of PFOA was analysed in each soil section and catholyte and anolyte solutions. SDS-EK and NaC-EK under 20 mA constant current

were tested further for two weeks to investigate the removal efficiency of PFOA under increased time.

At the end of each experiment, aqueous solutions from the anode and cathode chambers were collected. Then the soil compartment was divided into five equal sections, and each section was mixed and homogenized, then dried overnight in a 105 °C oven. Dried samples were pulverized, and samples were taken from different parts. PFOA was measured for each soil section using tripe methyl alcohol extraction. Samples were taken in duplicate from each section for analytical analysis. Subsequently, supernatants collected from each extraction were mixed, diluted and filtered for LC-MS analysis. In addition, a separate set of samples was collected to determine the pH and conductivity of each soil section.

Table 4.1: Experimental design

Exp No.	Target Contamination	Concentration of target contamination (mg/kg)	Surfactant and dosing point	Current (mA)	Surfactant Concentration (% w/w)	Duration (says)
E1	PFOA	100	NA	10	-	7
E2	PFOA	100	NA	20	-	7
E3	PFOA	100	SDS/cathode	10	5	7
E4	PFOA	100	SDS/cathode	20	5	7
E5	PFOA	100	NaC/cathode	10	5	7
E6	PFOA	100	NaC/cathode	20	5	7
E7	PFOA	100	TW80/anode	10	5	7
E8	PFOA	100	TW80/anode	10	5	7
E9	PFOA	100	SDS/cathode	20	5	14
E10	PFOA	100	NaC/cathode	20	5	14

4.5 Results and Discussion

4.5.1 Change in current and voltage

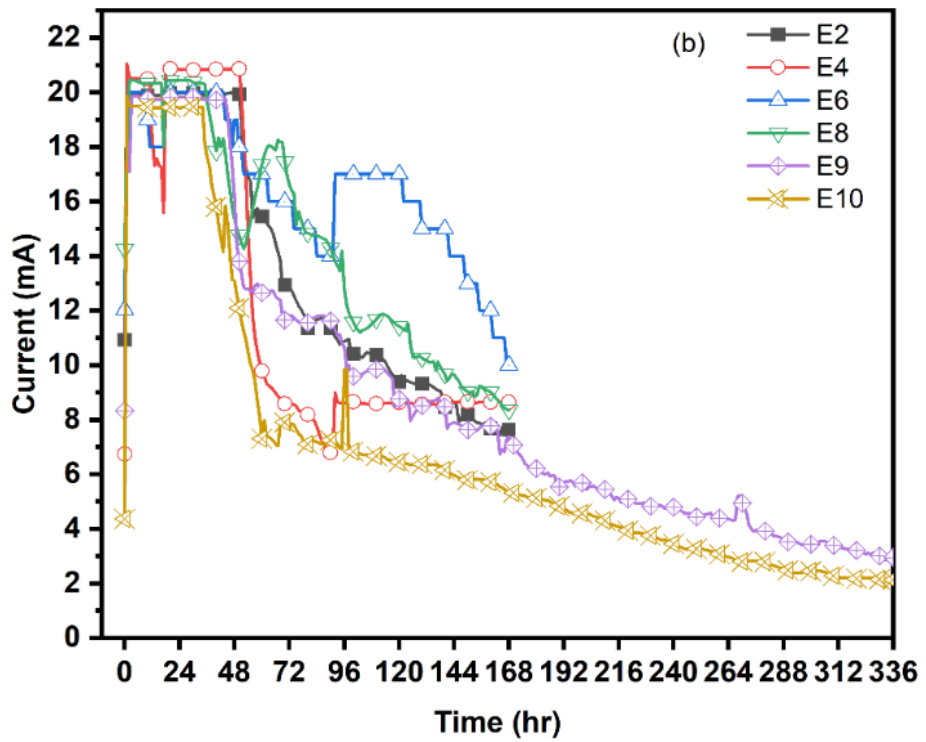
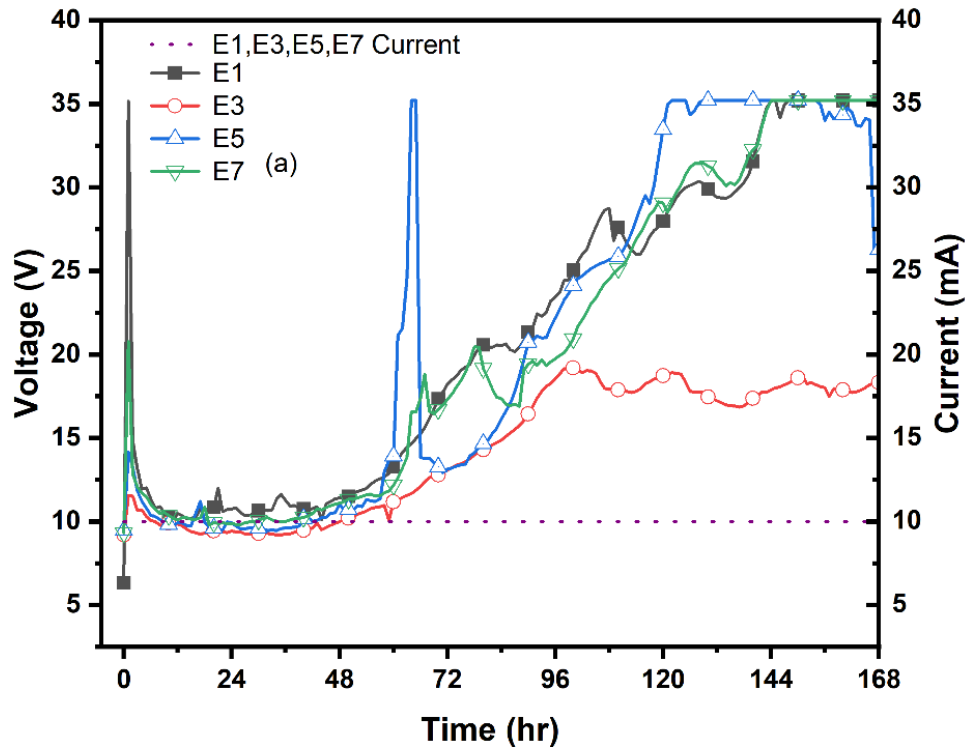
The EK treatments were performed at a fixed current of 10 mA and 20 mA continuously for 168 hours in all experimental trials. However, two additional tests involving the application of SDS and NaC surfactants were conducted for an extended period of 336 hours under a constant current of 20 mA. The variations in electric current and voltage over time for experiments E1 to E10 are depicted in Figure 4.2. The current density varied significantly throughout all experiments conducted, and the change in current in all tests carried out at 20 mA followed a persistent trend. The current density increased to a maximum value in the beginning due to the increasing number of ions in the pore solution due to the salt's dissolution. Thus, as the ions electromigrated towards the electrodes, the current reduced and stabilized gradually over time due to increased soil resistance and decreased electrical conductivity and degree of saturation. Similar current change trends were reported by (Fardin et al., 2021; Ghobadi, Altaee, Zhou, McLean, & Yadav, 2020a). The EK experiments, denoted as E1-E8, were conducted continuously for 168 hours under a constant current of 10 mA and 20 mA, while experiments E9-E10 were carried out for 336 hours at a constant current of 20 mA. During these experiments, a notable variation in electric potential was observed across the EK cell. The changes in voltage over time for the EK experiments performed at 10 mA for 168 hours are visually presented in **Figure 4.2a**. Due to the consistent and stable operating conditions, the electric current remained constant throughout the EK treatment, while the voltage gradually increased over time. As depicted in **Figure 4.2a**, experiments E1 and E7 reached a maximum voltage of 35V after 144 hours, experiment E5 reached the same maximum voltage after 127 hours, and experiment E3 reached a maximum voltage of 19V after 96 hours, maintaining relative stability with slight fluctuations until the

conclusion of the experiment. The progressive rise in voltage observed in experiments E1, E3, E5, and E7 can be attributed to the increasing soil resistance over time, resulting from the precipitation of dissolved ions. The outcomes indicated that in the experiments conducted at 10 mA, the voltage reached 35 V after approximately 140 hours, whereas in the 20 mA experiments, this threshold was reached after around 48 hours (**Figure 4.2c**). The rapid increase in voltage in the 20 mA experiments is attributable to the accelerated electrolysis reaction, leading to swifter transport and the convergence of acid and alkaline fronts within the soil. The electric current remained stable initially during the EK experiments, then reached a near-steady value of 34 V from 48 hours until the conclusion of the experiments. As mentioned previously, the elevation in voltage reflects the soil's resistivity to the electric current due to the interaction of acid and alkaline fronts within the soil and the subsequent precipitation of ions. Consistent with prior studies, a decrease in electric current corresponds to a gradual increase in voltage across the electrokinetic cell (Fardin et al., 2021; Ghobadi, Altaee, Zhou, McLean, Ganbat, et al., 2020a)

The variations in electric current observed in the EK experiments conducted at 20mA are illustrated in **Figure 4.2b**. Initially, the electric current remained stable at 20 mA for a significant duration, primarily due to the electrolysis reaction taking place at the anode and the subsequent increase in dissolved ions within the pore solution (as indicated by **Equations 4.2 and 4.3**). The electric current passing through the soil cell is closely associated with the presence of free ions, making it a crucial factor influencing the transportation of contaminants through the soil. **Figure 4.2b** displays that experiments E2 and E4 reached a maximum electric current of 20 mA, sustained for 51 hours. Subsequently, the current gradually declined in experiment E2, reaching 7.63 mA after 168 hours, while in experiment E4, it dropped sharply to 7 mA after 87 hours before recovering to 8.7 mA until the experiment's conclusion. In experiment E6, the current

initially remained constant at 20 mA for 44 hours, then decreased to 14 mA after 94 hours, increased briefly to 18 mA, and gradually decreased again to 10 mA by the end of the study. Experiment E8 witnessed a decline in electric current from 20 mA after 34 hours, ultimately stabilizing at 8.7 mA. Similarly, in experiment E2, the current remained steady at 20 mA for 50 hours before gradually decreasing to 8 mA. The decrease in current observed in experiments E2, E4, E6, and E8 can be attributed to the higher soil resistance encountered, which correlates with an increase in electric potential (as shown in **Figure 4.2c**).

Figures 4.2b and 4.2c present the profiles of electric current and potential observed in experiments E9 and E10, which were extended to a duration of 336 hours. Despite doubling the experimental timeframe, the current and voltage change patterns closely resembled those observed in the 168-hour experiments. In experiments E9 and E10, the electric current initially reached 19.22 mA and 19.46 mA, respectively, before experiencing a rapid decline after 45 and 39 hours. Subsequently, the electric current gradually decreased over time, ultimately reaching 3 mA by the conclusion of experiment E9 and 2 mA by the conclusion of experiment E10. Generally, the electric current recorded at the end of experiments E9 and E10 was lower than that observed in the one-week experiment conducted at a constant current of 20 mA (as depicted in **Figure 4.2b**)



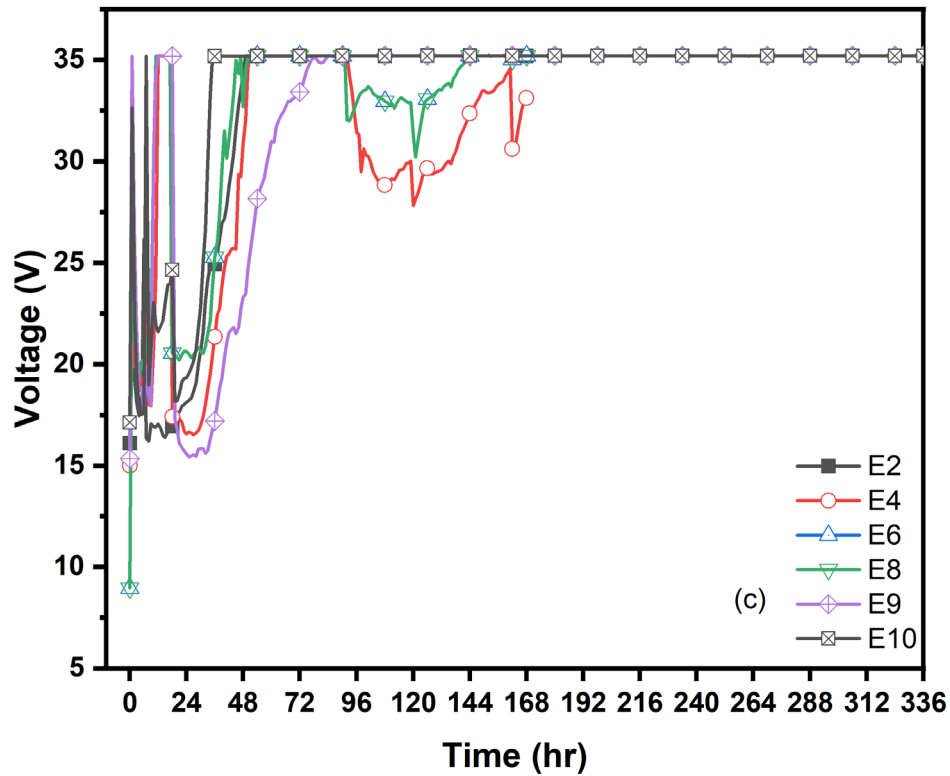


Figure 4.2: (a) Change in electric current and voltage over time in EK tests E1-E3-E5 and E7 (b) Change in electric current in E2, E4, E6, E8 and E9-E10 (c) Voltage during EK test in E2, E4, E6, E8 and E9-E10

4.5.2 Change in pH of the soil

The pH distribution across the soil, spanning from the anode to the cathode (sections 1 to 5), subsequent to the remediation experiments, is depicted in **Figure 4.3.a**. All EK tests were conducted without pH control. After the EK treatment, soil pH in sections close to the anode compartment decreased to lower than the initial soil pH and gradually increased in the soil sections toward the cathode zone. Soil pH gradually decreased from the anode side as the cations generated at the anode were transported towards the cathode. The decrease in pH affected in low pH across soil sections as it resulted from the production of H^+ ions through electrolysis reaction at the anode ($2H_2O - 4e^- \rightarrow O_2 + 4H^+$). An increase in soil pH in the sections near the cathode was beneficial for the removal of PFOA, which was due to the advancement of hydroxide ions (OH^-) generated through

water electrolysis at the cathode ($2H_2O - 2e^- \rightarrow H_2 + 2OH^-$) and affected the pH distribution near the cathode soil sections. In contrast, the soil pH in section S4 closely resembled the initial soil pH, as indicated in **Figure 4.3a**. The effective mobility of hydrogen ions was found to be approximately 1.8 times higher than that of hydroxyl ions, as established by (Acar & Alshawabkeh, 1993). As evident from **Figure 4.3a**, the observed lower soil pH in sections S1 to S4 can be attributed to the preferential migration of hydrogen ions compared to hydroxide ions in response to the applied electric field. However, in section S4, the soil pH gradually approached its initial value, whilst a notable increase in pH was observed in section S5, resulting from the advancement of the alkaline front originating from the cathode. It is worth noting that the sorption of PFOA in soils tends to increase as the pH decreases, as discussed in subsequent sections (Oliver et al., 2019).

Figure 4.3a provides a comprehensive view of the pH variations observed during the EK processes conducted at a constant current of 10 mA for 7 days. Among the EK experiments, experiment E3 displayed somewhat higher soil pH compared to other EK experiments. Across the first three sections (S1-S3), the change in pH was relatively insignificant. However, a notable increase in soil pH was observed in sections S4 to S5 in experiment E1. E1, E5 and E7 were performed under the same experimental conditions; experiments E5 and E7 showed a steady increase in pH from sections S1 to S5. This gradual increase in soil pH from sections S1 to S5 indicates the progressive influence of the EK treatment. **Figure 4.3a** also presents the soil pH profiles of the EK experiments conducted at a constant current of 20 mA for 7 days. In all experiments, the soil pH in sections S1 to S4 was lower than the initial soil pH (pH 4.4), with experiment E8 showing a slightly higher pH compared to the other experiments. This lower pH can be attributed to the progression of the acid front in the soil from the anode towards the cathode

electrode. However, in section S5 of all experiments, the soil pH exceeded the initial pH due to the advancement of the alkaline front originating from the cathode region. The highest pH value was recorded in section S5 of experiment E4 (pH 6.8) when an SDS surfactant agent was utilized. Furthermore, Figure 4.3a presents the soil pH data from the EK experiments conducted for 2 weeks (experiments E9 and E10). In all soil sections, the soil pH in experiment E9 was slightly higher compared to experiment E10. Gradual increases in soil pH were observed in sections S1 to S4, surpassing the initial soil pH in section S5. Section S5 of experiment E10 exhibited the lowest pH (pH 4.6) among all experiments. This can be attributed to the extended duration of the EK process, allowing the acid front to propagate further through the soil specimen.

4.5.3 Change in the soil's electric conductivity

Following a seven-day EK treatment, the kaolinite soil's electric conductivity (EC) demonstrated a decrease in sections S1 to S4, followed by a slight increase in sections S4 and S5 (**Figure 4.3b**). Conversely, in the fourteen-day EK experiments, the EC of all soil sections exhibited a general decrease (**Figure 4.3b**). The initial increase in soil EC can be attributed to the higher concentration of soluble soil ions in the anode section (S1), facilitated by the acidic conditions that promote the dissolution of ionic species (Ghobadi, Altaee, Zhou, McLean, Ganbat, et al., 2020a). The high value of EC is correlated to the presence of free protons. The EC decreased when the concentration of ionic species in soil pore fluid probably decreased due to meeting the acid and alkaline front in the soil section S5. **Figure 4.3b** presents the EC of experiments E9 and E10 conducted for two weeks; both experiments showed a trend of a gradual decrease in soil EC from S1 to S5, with experiment E9 having the lowest EC values. Overall, the EC of experiments E9 and E10 was lower than that of experiments E1 to E8 due to the longer treatment time and the higher electric current than experiments conducted at 10 mA, i.e. E1 E3, E5, and E7. It

should be mentioned that the enhancement agent could influence the soil EC due to the interaction between the OH^- and H^+ ions generated at the cathode and anode with the surfactant agent, causing a fluctuation in the soil EC. Accordingly, the soil EC in section S1 was higher in Experiments E1 and E2 performed without enhancement agents.

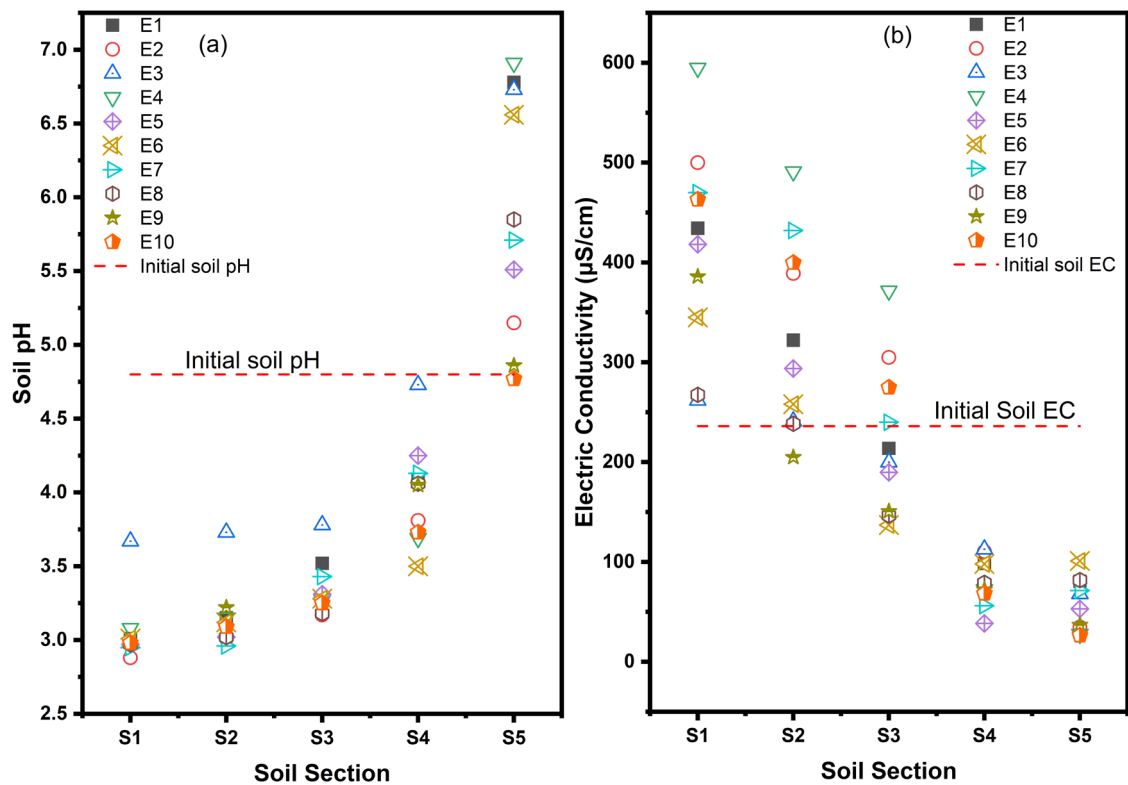


Figure 4.3: (a) pH across soil sections after all EK tests (b) electric conductivity across soil sections after all EK tests

4.5.4 Performance of EK and different types of surfactants

Figure 4.4 presents the residual concentration profiles of PFOA across different soil sections subsequent to the end of the EK tests. The data depicted in Figure 4.4 confirm the transportation dynamics of PFOA from both the anode and cathode zones, resulting in its substantial accumulation within the central section of the soil (S3). These findings agree with the previous studies that concluded PFAS compounds' transport by electroosmosis and electromigration, thereby accumulating in the soil's mid-section

(Niarchos et al., 2022). PFOA's transportation behaviour was comparable in soil sections S1, S2, S4, and S5. Investigations pertaining to PFAS sorption in soil have indicated an inverse relationship between soil pH and the sorption capacity of PFOA, wherein lower soil pH levels are associated with higher sorption rates of PFOA (Oliver et al., 2019). PFOA, characterized by its negatively charged carboxylic functional group (**Figure 4.5c**), is a water-soluble contaminant that exhibits favourable availability within the soil pores for electrokinetic transport. Its migration behaviour is determined by the combined effects of electromigration towards the anode and electroosmosis towards the cathode, leading to a distinct spatial distribution pattern within the soil matrix following EK treatment. Additionally, the sorption characteristics of PFOA are influenced by the soil's pH conditions from the progression of alkaline and acid fronts during the EK process. The soil charge, which is positively charged when the pH is below the point of zero charge (pH_{zpc}) and negatively charged when the pH surpasses pH_{zpc} , plays a significant role in PFOA sorption. Consequently, regions near the anode, where the soil exhibits a positive charge due to pH values below pH_{zpc} (**Figure 4.3a**), promote enhanced adsorption of the negatively charged PFOA species. In contrast, PFOA adsorption on the soil decreases near the cathode due to the high soil pH or when $pH > pH_{zpc}$. Thus, PFOA removal was higher at the cathode zone due to i) the electrostatic repulsion between PFOA and the soil surface and ii) the electromigration of PFOA towards the anode. Another study also noted the negative relationship of PFOA with pH, where an increase in pH resulted in decreasing sorption of PFOA in soil (Groffen et al., 2019). The accumulation of PFOA in the low pH region near the anode could be due to PFOA electromigration and electrostatic interaction with the positively charged soil surface. These findings would explain the PFOA concentration in sections S1 and S2 and a slight drop in sections S4 and S5. As soil pH increased in the latter sections, a tangible decline in the PFOA

concentration was observed near the cathode zone. Considerable PFOA concentration in section S3 is attributed to PFOA transport from the cathode and anode by electromigration and electroosmosis mechanisms and accumulation in the middle section. Due to the charge difference, the negatively charged PFOA electromigrated from the cathode to the anode zone, whilst the electroosmosis flow carried water-soluble PFOA from the anode towards the cathode. This phenomenon was also observed in earlier studies (Hou et al., 2022; Söregård et al., 2019). As shown in **Figure 4.4a-4.4i**, the accumulation of PFOA in the anode region indicates that electromigration is the main mechanism for PFOA transport in the soil sections near the cathode and is consistent with the pH distribution across soil sections. At the same time, electroosmosis was responsible for PFOA transport across the soil specimen and accumulations in the catholyte chamber. As displayed in **Figure 4.4a-4.4b**, the catholyte chamber contains more PFOA concentration than the anolyte chamber. Generally, the soil near the anode acquires a positive charge during the EK process, favouring PFOA adsorption. The effect of soil charge on the PFOA removal is due to the electrostatic interaction between negatively charged PFOA compounds and positively charged soil surface. Notably, there is significant PFOA removal from the soil section 4 despite the soil pH being lower than pH_{zpc} (Fig 4.4 and 4.5a). The results agree with the literature (Niarchos et al., 2022; Söregård et al., 2019), suggesting that electromigration is preferable for PFOA near the cathode.

The profile of the PFOA distribution in the soil in the unenhanced EK experiments, E1 and E2 (**Figure 4.4a**), was similar to the enhanced EK experiments, E3 to E8 (**Figure 4.4.b-g**). Increasing the EK duration to two weeks promoted PFOA transport from the cathode to the anode zone. As seen in **Figure 4.4h-4.4i**, the accumulated PFOA in soil sections is below the initial PFOA concentration. In contrast, in one-week-long experiments, the accumulated PFOA concentration in the anode region is higher than the

initial value. However, the lower PFOA concentration close to the anode zone was probably due to soil compaction over time, reducing the electroosmosis flow and PFOA transport from the anode zone.

Interestingly, increasing the electric current from 10 mA to 20 mA increased PFOA concentration in section S3 in experiments E4 and E6 (**Figure 4.4c and 4.4e**). These results may be explained by the fact that higher electromigration and opposing electroosmotic flow met at a higher rate, leading to more PFOA accumulation in the middle section. However, the lowest concentration of PFOA across the soil sections was observed in experiment E10, followed by experiment E9, due to a longer treatment time under 20 mA electric current.

As shown in **Figure 4.5**, PFOA removal in the unenhanced EK experiment E1 was 14.49%. An extra 31% PFOA removal was achieved when the electric current of the unenhanced EK process increased from 10 mA to 20 mA in experiment E2 (~19% total PFOA removal). The PFOA contaminant was removed from soil sections S1, S2, S4 and S5 and accumulated in section S3 (**Figure 4.5a**). In the conducted experiments, the removal efficiency of PFOA varied among different soil sections. The highest rates of removal, ranging from 85% to 95%, were observed in section S5, except for experiments E4 and E6, which exhibited a slightly lower removal efficiency of 72%. Notably, the majority of the PFOA was concentrated in section S3 for experiments E1 to E8. In contrast, experiments E9 and E10 demonstrated a PFOA removal of 63.51% and 14.92% from section S3, indicating a more effective PFOA removal efficiency in the extended two-week EK experiments. Furthermore, in the enhanced EK processes carried out at 10mA, experiments E3, E5, and E7 exhibited PFOA removal rates of 13.84%, 17.67%, and 7.65%, respectively (**Figure 4.5b**). The experiment with the highest PFOA removal was E5, which utilized a sodium cholate enhancement agent. In experiments E4 and E6,

conducted with anionic surfactants (SDS or NaC), increasing the electric current from 10 mA to 20 mA led to higher PFOA removal from the soil. However, the PFOA removal decreased in experiment E8, which used a nonionic surfactant (TW80). The increase in electric current facilitated the electrolysis reaction in the soil and enhanced PFOA transport. Nevertheless, the lower PFOA removal in experiment E8 could be attributed to the application of the surfactant in the anode compartment, which resulted in a negligible impact on PFOA removal. The incorporation of TW80 in the anode compartment to enhance PFOA removal was hindered by the gradual compaction of the kaolinite soil over time, reducing electroosmosis flow from the anode to the cathode zone. In all EK tests conducted, the electroosmotic flow exhibited high rates during the initial 72 hours, with a peak volume of 250-300mL within 24 hours. However, after this period, the electroosmotic flow rapidly decreased as the pH in the soil sections declined due to the progression of the acid front throughout the EK system. This behaviour was particularly observed in soils with low pH buffering capacity, leading to a sharp reduction in the electroosmotic flow and subsequent removal of contaminants (Cameselle & Gouveia, 2018; Saichek & Reddy, 2003). Furthermore, utilising TW80 nonionic surfactant in the electrokinetic (EK) process resulted in a reduced electroosmotic flow. This can be attributed to the low dielectric conductivity of TW80, which hinders the dissolution of ions and subsequently affects the relative movement of ions. It is important to note that the dielectric conductivity directly influences the electroosmotic flow, as established by previous research (Cheng et al., 2017). The TW80 nonionic surfactant possesses characteristics such as a low dielectric constant, high viscosity, and low critical micelle concentration (CMC). These properties collectively contribute to the diminished electroosmotic flow and subsequently impact the removal efficiency of PFOA in the electrokinetic tests. Previous studies reported that TW80 efficiency is highly hindered by

sorption onto the soil, and its efficiency highly depends on the soil properties (Fardin et al., 2021).

The highest PFOA removal in one-week EK experiments was 32.6% in experiment E6 with sodium cholate enhancement agent, followed by 15.73% PFOA removal in experiment E4 with SDS enhancement agent. SDS was selected as a conventional enhancing agent to improve the transportation of PFOA to the anode. The movement of the negatively-charged SDS under an electric field is contrary to the direction of electrokinetic flow. However, the experimental results revealed less removal achieved in the SDS-EK, which can be caused by the reaction of SDS at the cathode producing salt and hindering the transportation towards the anode. Therefore, the SDS-enhanced EK system did not significantly improve the removal efficiencies. PFOA removal in experiment E6 was twice that in experiment E4. In experiments E9 and E10, the duration of the EK process was extended to 2 weeks to investigate its impact on the EK performance. PFOA removal in experiment E9 was three times higher than in experiment E4, and in experiment E10, it was 2.3 times higher than in experiment E6. PFOA removal was 45.97% and 75.67% in experiments E9 and E10, respectively (**Figure 4.5b**). In general, results revealed that sodium cholate experiments achieved higher PFOA removal from the kaolinite soil under 10 mA and 20 mA electric current for both one- and two-week experiments. TW80 enhanced EK experiments E7 and E8 achieved the lowest PFOA removal rate, 12.90% and 7.65%, respectively (**Figure 4.5b**). The performance of sodium cholate-enhanced EK experiments is better than the SDS and TW80 enhanced and unenhanced EK experiments (**Figure 4.5b**). The increased PFOA removal efficiency of sodium cholate-enhanced EK tests could be due to the greater PFOA dissolution into surfactant micelles and the transport of PFOA-containing micelles under the induced electric potential. An earlier study observed that NaC had superior solubilization of 2,4,6-

trichlorophenol compared to SDS and cyclodextrin, achieving a higher removal rate (Zeng et al., 2013). The study also concluded that sodium cholate is a bile salt with a lower micelle aggregation number than most typical aliphatic surfactants and a lower critical micelle concentration (CMC) than other surfactants, such as the SDS. The strong interaction between PFOA and NaC biosurfactant assisted in the transportation of PFOA to the anode.

The results underline the surfactant-enhanced EK process to improve PFOA removal from kaolinite soil, much higher than reported in previous studies using contaminated soils. In real soil, the expected PFOA removal could be lower than in the experiments with kaolinite soil due to the higher cation exchange capacity and presence of organic matter that influences PFOA transport in the soil. Unlike heavy metal contaminants, PFOA showed irregular transportation in the EK process due to electromigration toward the anode and electroosmosis transport towards the cathode. PFOA's relatively high water solubility, about 9.5 g/L, promotes the electroosmosis transport mechanism toward the cathode. Besides, low soil pH near the anode would encourage PFOA adsorption, requiring a longer processing time for removal. It is evident that increasing the EK duration from 1 to 2 weeks resulted in 2.3 times higher PFOA removal in the NaC-enhanced EK process.

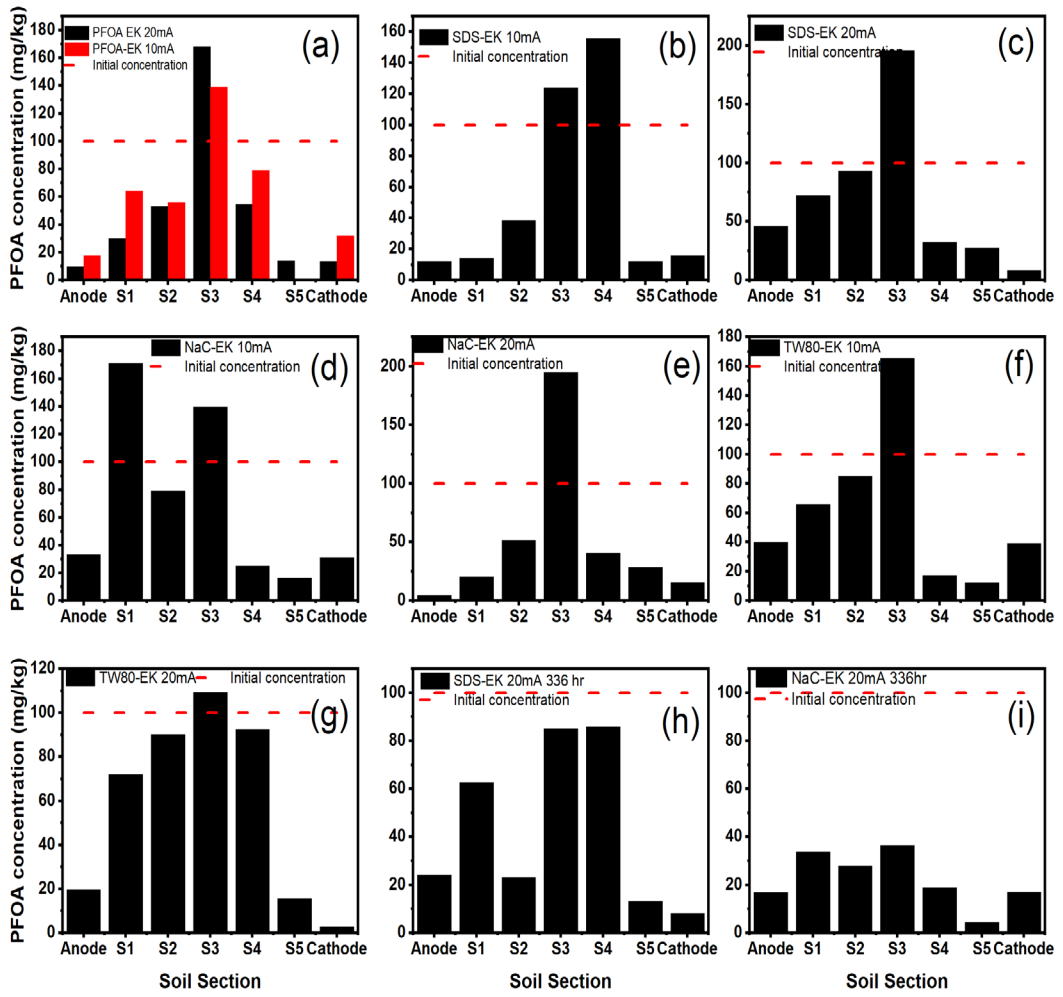


Figure 4.4: residual PFOA concentration (mg/kg) in the soil sections after EK tests (a) E1-E2; (b) E3; (c) E4; (d) E5; (e) E6; (f) E7; (g) E8; (h) E9; (i) E10.

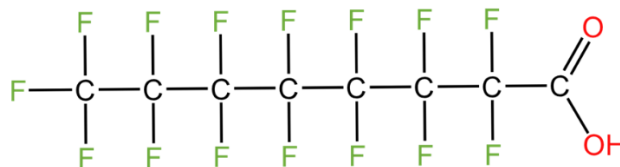
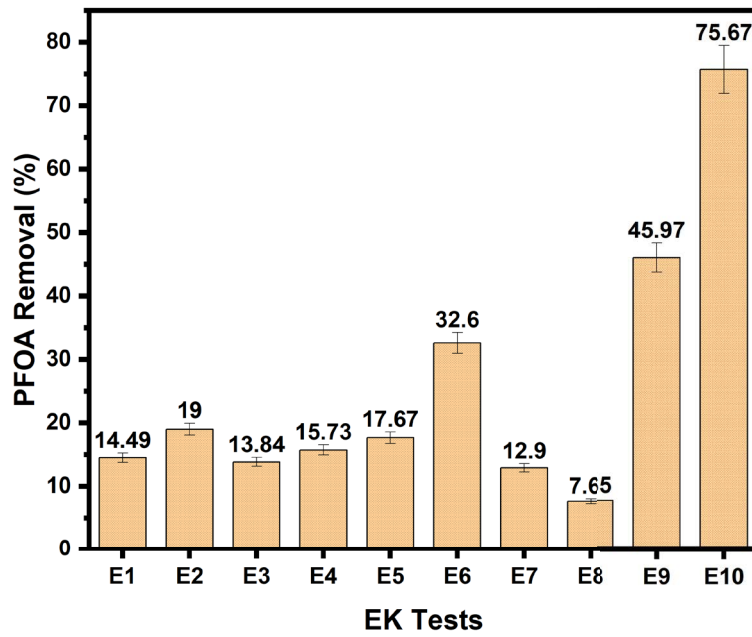
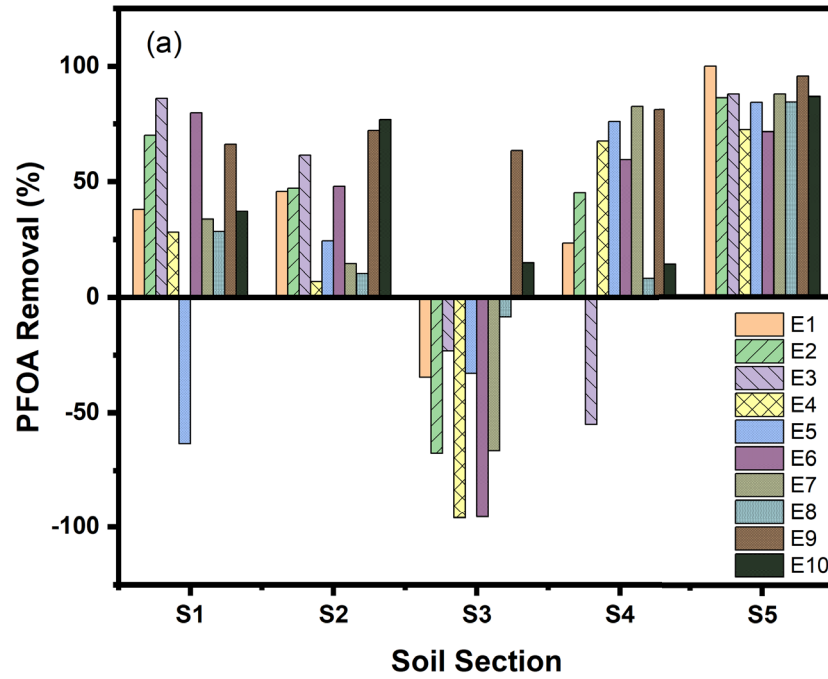


Figure 4.5: (a) removal rate (%) in soil sections after EK tests; (b) overall removal rate of PFOA after EK tests (c) PFOA's chemical structure

4.5.5 Impact of PFOA concentration

Surfactant-enhanced EK experiments were performed to investigate the relationship between the concentration of PFOA in the soil and its removal efficiency. The objective was to assess how PFOA concentration variations influenced the EK process's effectiveness when surfactants were introduced. By conducting these experiments, valuable insights were gained regarding the impact of PFOA concentration on the overall removal efficiency in surfactant-enhanced EK systems. In comparison to Tween80, NaC and SDS surfactant enhanced EK tests demonstrated a higher removal rate. To further investigate the relationship between PFOA concentrations and its removal, additional NaC and SDS surfactant-enhanced EK experiments were conducted for two weeks, using a fixed PFOA concentration of 10 mg/kg in kaolinite soil. This experimental setup allowed for an evaluation of how different initial PFOA concentrations influenced the efficiency of PFOA removal during the surfactant-enhanced EK process.

Figure 4.6a provides a comprehensive overview of the voltage and current variations observed during the 336 hour duration of the NaC and SDS-enhanced EK experiments. Initially, a decrease in voltage was observed, followed by a subsequent increase to a stable value of 35.21 V after 48 hours, which was maintained for the remainder of the experiment. Notably, there was a significant voltage fluctuation during the first 48 hours of the NaC-enhanced experiment before reaching a stable state. In **Figure 4.6b**, the change in electric current over time is depicted for both the SDS-enhanced and NaC-enhanced EK tests. In the SDS-enhanced test, the current remained constant at 20mA for the first 48 hours, while in the NaC-enhanced test, it remained constant for 72 hours. Subsequently, the electric current gradually decreased for 336 hours, reaching final values of 2 mA and 3 mA for the SDS and NaC-enhanced tests, respectively.

The pH variations in different soil sections of the EK tests enhanced with 5% w/w NaC and SDS are depicted in **Figure 4.6c**. It can be observed that the pH values gradually increased towards section S5 in both experiments. Notably, the NaC-enhanced EK experiment exhibited slightly higher pH values in sections S4 and S5 compared to the SDS-enhanced test. Specifically, in the NaC-enhanced EK test, the pH in section S4 reached the initial pH value, whereas the SDS-enhanced test displayed a lower pH value in the same section. However, both experiments demonstrated a consistent trend of gradual pH increase towards section S5. This trend aligns with the pH changes observed in other EK tests conducted in the study.

Figure 4.6d provides an overview of the PFOA concentration in each soil section for the EK tests enhanced with 5% NaC and SDS, using a PFOA concentration of 10 mg/kg. At the conclusion of the experiments, the PFOA removal efficiencies were determined to be 37.42% and 26.59% in the NaC and SDS-enhanced EK tests, respectively. The figure also presents the percentage of PFOA removal from each soil section at the end of the EK experiments. Notably, the highest PFOA removal rates in both experiments were observed in section S5, ranging from 85% to 55%. In the NaC-enhanced EK test, section S1 achieved a PFOA removal rate of 73%. A significant PFOA accumulation was also observed in soil section S3 for both tests. It is worth mentioning that the overall PFOA removal rate in the EK experiments with a PFOA concentration of 10 mg/kg was lower compared to the experiments with a concentration of 100 mg/kg. Specifically, the removal rate decreased by half in NaC and SDS-enhanced EK tests. This decrease in removal efficiency can be attributed to the lower concentration of PFOA ions in the soil pore fluid, resulting in reduced availability for migration and transport compared to the EK tests conducted with a PFOA concentration of 100 mg/kg.

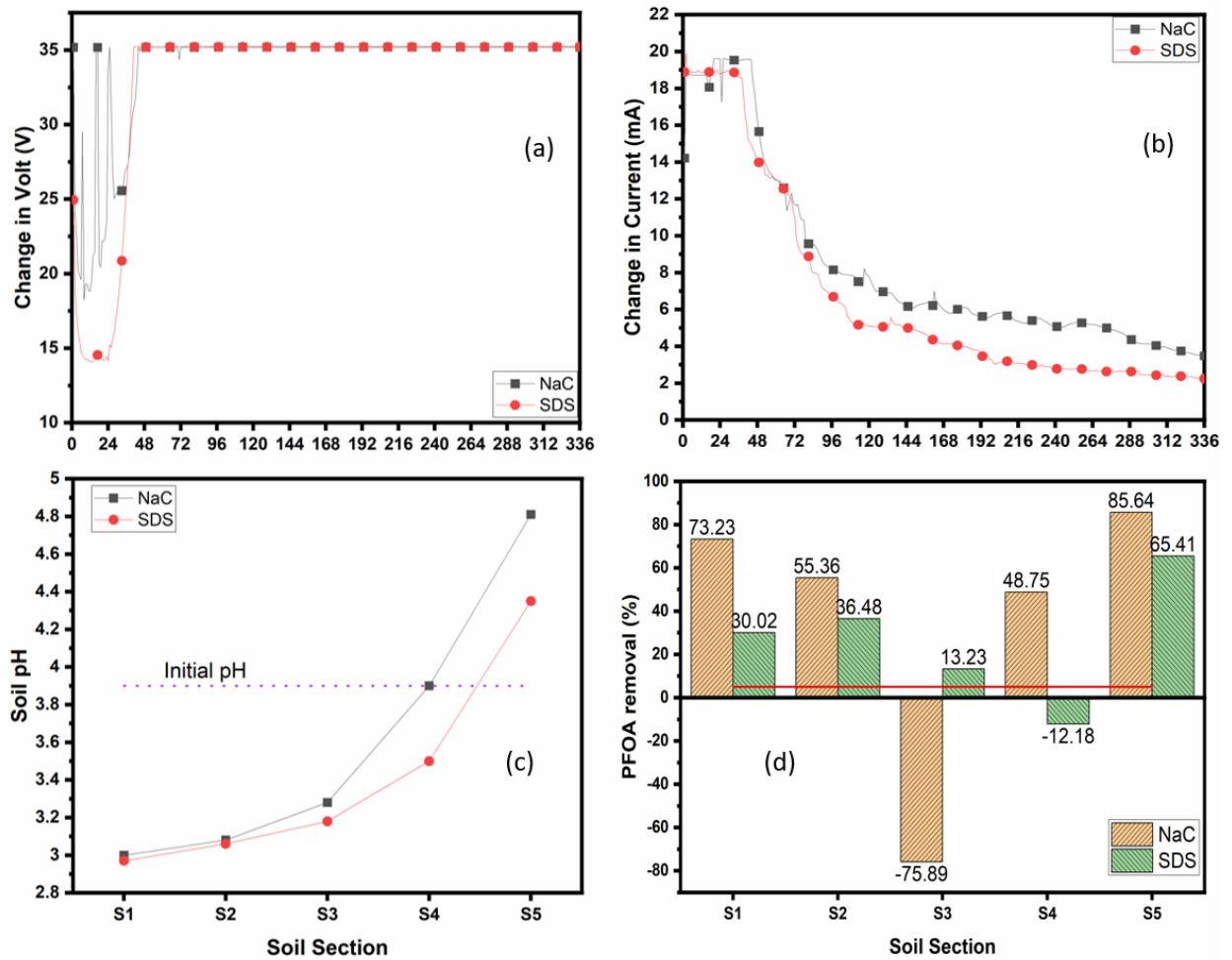


Table 4.2: Total removal rate and the mass balance of EK tests

Figure 4.6: (a) change in voltage over time (b) change in current (c) pH through soil sections (d) PFOA removal rate through soil sections.

Experiment Name	Initial [PFOA] (mg)	Residual [PFOA] (mg)	Mass Balance (%)	Removal Rate (%)
<i>PFOA-EK 10mA</i>	103.19	88.23	87.93	14.49
<i>PFOA-EK 20mA</i>	100.34	81.28	84.72	19.00
<i>SDS-EK 10 mA</i>	100.39	86.49	100.67	13.84
<i>SDS-EK 20mA</i>	99.94	84.21	106.70	15.73
<i>NaC-EK 10mA</i>	104.89	88.06	107.01	16.04
<i>NaC-EK 20mA</i>	99.54	67.03	97.50	32.66
<i>T80-EK 10mA</i>	99.51	86.67	93.51	12.90
<i>T80-EK 20mA</i>	100.62	92.91	96.59	7.65

<i>SDS-EK 20mA 2WK</i>	<i>100.00</i>	54.02	94.22	45.98
<i>NaC-EK 20mA 2WK</i>	<i>99.90</i>	24.30	92.16	75.68

4.5.6 Energy Consumption and mass balance

The energy consumption associated with EK studies is an important factor in determining the overall cost of the treatment (Ghobadi et al., 2020b). The specific energy consumption (SEC) for all experiments was determined by applying **Equation 3.3**, as outlined in **Chapter 3** of the study.

The outcomes of the EK tests demonstrate that a substantial increase in electric current led to a considerable rise in power consumption (**Figure 4.7**). Generally, the specific power consumption increased with the electric current increase of the EK process. In the unenhanced EK processes, the power consumption increased from 0.0255 kWh/kg in experiment E1 to 0.050 kWh/g in experiment E2 due to increasing the electric current from 10mA in experiment E1 to 20mA in experiment E2. A similar observation was recorded in surfactant-enhanced EK processes; SEC was 0.017 kWh/kg and 0.044 kWh/kg in experiments E3 and E4, respectively. The SEC is proportional to the electric potential and current of the EK experiment; the higher the electric potential and current, the higher the SEC is (**Equation 3.3**). Accordingly, the SEC in experiment E6 was higher than in experiments E4 and E8 due to the higher electric potential in experiment E6 (Fig 2b and 2c). SEC in experiment E6 was 0.061 kWh/kg, 0.04 kWh/kg and 0.057 kWh/kg in experiments E4 and E8, respectively. Equation 4 also shows that the SEC increases with increasing the duration of the EK process in experiments E9 and E10. At the end of the EK process, the SEC was 0.0699 kWh/kg in experiment E10 and 0.052 kWh/kg in experiment E9. For EK processes conducted at 20 mA, Experiment E10 recorded the highest SEC, followed by experiment E6> experiments E8> experiment E9> experiment

E2> experiment E4. It is worth noting that although experiment E6's duration was longer than experiments E6 and E8, the SEC in experiment E9 was lower than in experiments E6 and E8. The higher average electric potential and current in experiments E6 and E8 was probably the reason for the higher SEC in these experiments compared to experiment E9.

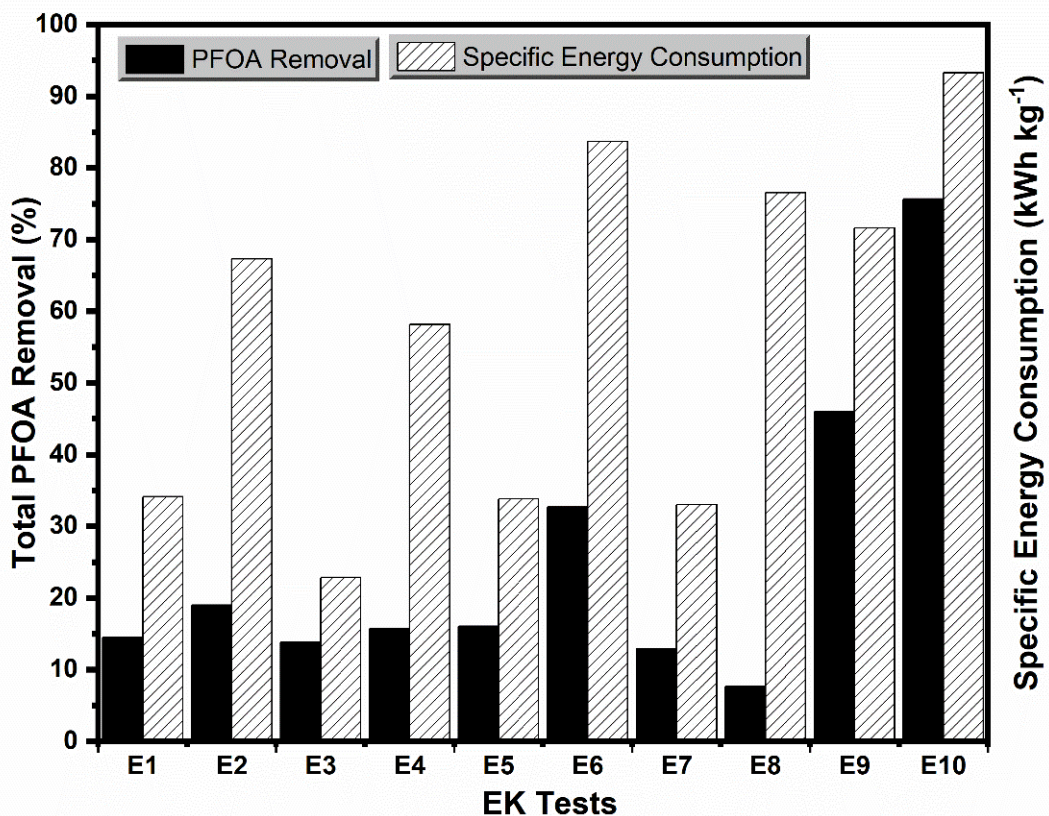


Figure 4.7: Total PFOA removal and specific energy consumption.

Table 4.2 provides an overview of the mass balance and total PFOA removal rate in both EK experiments. The mass balance of each experiment was evaluated by summing the residual PFOA in the soil and in the electrolyte solutions and soil pore water, which were then divided by the initial quantity of PFOA in the soil. This calculation allows for an assessment of the overall PFOA removal efficiency and the effectiveness of the EK treatment in each experimental condition (Ghobadi et al., 2021). According to the data

presented in **Table 4.2**, the mass balance of unenhanced EK studies fluctuated between 84.72-87.93%. In contrast, surfactant-enhanced EK studies exhibited higher mass balance, ranging from 92.16 to 106.7%. Increasing the treatment time influenced the removal efficiency of PFOA significantly. Notably, experiments conducted under identical experimental conditions but with different processing times showed a remarkable twofold enhancement in PFOA removal efficiency. This emphasizes the importance of optimizing the processing time to achieve more effective remediation outcomes (**Table 4.2**). Notably, TW80-enhanced EK exhibited the lowest PFOA removal rate, while NaC-enhanced EK experiments demonstrated the highest PFOA removal rate of 32.66% among all EK experiments conducted for one week. Extending the EK treatment time to two weeks at 20 mA, NaC-enhanced EK experiments reached a substantial rate of 75.68% PFOA removal, followed by an SDS-enhanced EK experiment demonstrated a respectable result of 45.98%.

4.6 Conclusions

This laboratory-scale study aimed to investigate the remediation potential of PFOA-contaminated kaolin soil using an EK treatment approach. Initially, the effectiveness of conventional EK treatment without the use of enhancement agents was examined as a baseline for comparison with surfactant-enhanced EK experiments. It was hypothesized that the EK process alone would yield limited success in removing PFOA from the contaminated soil due to its persistent nature in the environment. Thus, the introduction of various surfactants was explored as a means to enhance PFOA removal from the kaolinite soil matrix. Both anionic (sodium cholate, SDS) and nonionic (TW80) surfactants were considered in the EK process. The results revealed that TW80-enhanced EK experiments conducted at 10 mA and 20 mA treatment settings achieved the lowest PFOA removal rate. Following closely behind were the SDS-enhanced EK experiments,

indicating these surfactants' potential to assist in removing PFOA from the contaminated soil matrix. Experiment E6, which involved NaC-enhanced EK conducted at a constant current of 20 mA, displayed a remarkable removal efficiency of 35% within one week, surpassing all other one-week experiments. To further evaluate the performance of the EK system over time, the PFOA removal efficiency was measured over two weeks. The results revealed a substantial improvement in PFOA removal, with the NaC and SDS-enhanced EK tests achieving removal efficiencies of 75.68% and 45%, respectively. Notably, the NaC and SDS-enhanced EK experiments exhibited nearly double the removal efficiency compared to the one-week experiments. The extension of the experimental duration from one to two weeks significantly enhanced the removal efficiency. These findings underscore the promising potential of surfactant-enhanced EK experiments in enhancing the removal of PFOA from contaminated soil. However, it should be noted that the efficacy of PFOA removal was notably influenced by the choice of surfactant, with NaC biosurfactant demonstrating the highest removal efficiency. Future research endeavours should encompass the removal of various PFAS compounds from kaolinite soil utilizing surfactant-enhanced EK processes, exploration of PFAS removal using surfactant-enhanced EK in real soil conditions, and the implementation of pilot-scale studies to assess the surfactant-enhanced EK process for PFAS treatment while considering surfactant biodegradability in soil matrices.

This study investigated the remediation of PFOA-contaminated kaolin with EK coupled with surfactant-enhanced treatment. PFOA removal was initially evaluated by traditional EK treatment without enhancement. Non-enhanced EK tests were then compared with enhanced treatments. After EK treatment, the initial concentrations were all slightly decreased. TW80 EK under 10 mA and 20 mA treatment conditions resulted in the lowest removal rate, followed by SDS-enhanced EK tests. NaC-enhanced EK treatments

increased removal efficiency by up to 35% at 20mA for one week. The removal efficiency of PFOA highly increased with the application of sodium cholate surfactant up to 75.68%. SDS-enhanced EK reached up to 45% over two weeks of EK treatment at 20 mA constant current. The application of surfactant enhanced EK removal of PFOA increased with an increase in electric current and treatment duration time. The transportation of PFOA in the EK cell was observed from the cathode to the anode. Duration of EK treatment had no significant effect on pH change across the soil sections.

CHAPTER FIVE

PFOA REMEDIATION FROM KAOLINITE SOIL BY ELECTROKINETIC PROCESS COUPLED WITH AC/FEAC- PERMEABLE REACTIVE BARRIER

CHAPTER 5 : PFOA REMEDIATION FROM KAOLINITE SOIL BY ELECTROKINETIC PROCESS COUPLED WITH AC/FEAC- PERMEABLE REACTIVE BARRIER

This chapter has been derived from the following article submitted for publication (under review)

(Journal of Chemical Technology and Biotechnology): JCTB-23-0224, PFOA remediation from kaolinite soil by electrokinetic process coupled with AC/FeAC-permeable reactive barrier. by Ganbat, Namuun; Altaee, Ali; Hamdi, Faris M.; Zhou, Junliang; Tapas, Marie Joshua; Hawari, Alaa; Samal, Akshaya K.; Khabbaz, Hadi

5.1 Background

Ineffective waste management, intensive industrial activity, urbanisation, commercial plantations and mining, all contribute to soil contamination with hazardous substances. In recent years, PFOA-contaminated land has become an emerging environmental issue. The contamination of soil has a significant effect on the environment, living organisms, and ecosystems. Unavoidably, PFOA contamination is a public health concern. PFOA is one of the most prevalent PFAS compounds detected in the environment. A strong C-F covalent bond endows PFOA compounds with unique and potent physicochemical properties. The PFOA compound's hydrophobic chain and hydrophilic head account for their water and oil-repellent properties. Due to its physicochemical properties, PFOA is widely used in non-stick cookware, surface sprays, and firefighting foams. Since PFOA is non-biodegradable, persistent, and accumulates in the environment, the soil becomes an enormous sink for PFOA contamination. Although PFOA-containing products have been phased out and banned in many countries, PFOA-contaminated land remains a major environmental issue. Primary sources of PFOA contamination include fire training lands such as airports, military sites, and PFOA production sites. The secondary pollution sites are mainly pathways that produce by-products containing PFOA (Epa Au, 2019). In 2009, PFAS compounds were added to the Swedish Contamination List and the Stockholm

Convention on Persistent Organic Pollutants as a pollutant of concern (European, 2020b). This convention is an agreement to protect humans and the environment from persistent organic pollutants. In accordance with this convention, chemicals are subject to restriction and elimination. Since 2012, the Australian government has been a member of the United Nations Environment Program/Organisation for Economic Co-operation and Development (OECD/UNEP) Global Perfluorinated Chemicals Group (European, 2020a). The group works to reduce and eliminate products containing PFAS. Therefore, PFOA-containing products have been phased out of production and used in several nations. (Lenka et al., 2021) .

Because PFOA soil contamination is an emerging environmental issue, several remediation studies for contaminated sites are still in the experimental stages (Mahinroosta & Senevirathna, 2020a). Thermal heating is one of the most prevalent physical remediation techniques used to clean up PFAS-contaminated sites (Altarawneh et al., 2022). Thermal heating is an energy-inefficient, costly and destructive method that involves heating the contaminated soil at high temperatures, resulting in industrial waste. Consequently, less environmentally damaging methods are preferred. Lab-scale stabilisation and solidification tests on PFOS- and PFOA-contaminated firefighting training soils demonstrated that granular activated carbon has a greater sorption capacity towards PFOA (Barth et al., 2021). Planetary ball milling has been studied as a mechanochemical remediation technique for AFFF-contaminated soils; it reduced PFOA and PFOS in dry sand by 99 and 98% (Turner et al., 2021). The electrochemical destruction of PFOA and PFOS was studied on a lab scale, and the results indicated 51.7 and 33.3% degradation, respectively. (Hou et al., 2022).

Electrokinetic remediation is a widely recognized technique employed in the remediation of heavy metal-contaminated soils. This method involves the application of a low-

intensity direct electric current through the soil, transporting contaminants between strategically placed anode and cathode electrodes at suitable distances (Virkyute et al., 2002). Electrokinetic remediation for contaminated soils aims to remove contaminants from low-permeability soils under the influence of a low-level direct current, with electroosmosis, electromigration, and electrophoresis as the primary transport mechanisms (Acar & Alshawabkeh, 1993). The transport of contaminants towards the electrode of opposite charge increases when dissolved charged particles are in the interstitial fluid. The contaminants are then collected in the chambers of one of the electrodes and disposed of appropriately. Most hydrophobic organic particles are nonionic and, unaffected by an electrical field (Cheng et al., 2017). Successful remediation of persistent organic pollutants is challenging, and their removal using the conventional technique is difficult. Various studies have recently used enhanced electrokinetic processes to increase the efficiency and productivity of the EK system. Recent studies demonstrated the effects of different surfactants as enhancing agents for removing PFOA-contaminated kaolin (Ganbat et al., 2022). The research findings demonstrated that the sodium cholate-enhanced EK system was the most effective surfactant as enhancing agent, resulting in the highest PFOA removal rate.

EK remediation in conjunction with a permeable reactive barrier (PRB) has attracted the interest of researchers due to its effective application and increased EK efficiency. PRB-assisted remediation technologies are passive remediation systems designed specifically to remove hydrophobic organic compounds and heavy metals from soil (Li et al., 2011). PRB enhances EK soil remediation technologies by capturing contaminants and decreasing their concentration in anolyte and catholyte chambers (Ghobadi, Altaee, Zhou, McLean, Ganbat, et al., 2020b). Numerous PRB types are utilised in EK systems according to their absorption mechanisms, cost-effectiveness, and lifetime. Commonly

employed PRBs include biochar, AC, nZVI, and biomaterials. The application of biological PRB-enhanced EK remediation to remove diesel-contaminated clay was investigated on a lab scale (Mena et al., 2016). The results indicated a successful increase in electroosmotic flow and a promising performance for future in-situ applications. In a laboratory setting, the utilization of compost as a PRB in an EK process proved successful in removing copper from polluted soil, achieving a removal rate exceeding 90% (Ghobadi, Altaee, Zhou, McLean, Ganbat, et al., 2020b). The removal of cadmium using array electrode EK with PRB was evaluated, and the average removal rate was 93.1% (Zhou, Liu, et al., 2020). Numerous applications of EK enhanced with PRB for eliminating inorganic and organic contaminants have been proven effective.

Activated carbon (AC) derived from coal and other carbon-rich materials have a distinctive physicochemical structure, a large surface area, and a well-developed porous structure, making it an ideal candidate for the adsorption of contaminants from water and soil. Hydrophobic interactions and electrostatic attractions are the primary adsorption mechanisms for PFAS on AC. Hydrophobic properties of PFOA permit a high adsorption capacity on AC, given that hydrophobicity is the predominant adsorption mechanism for AC. Granular activated carbon (GAC)-PRB-enhanced EK was studied to remove TCP-contaminated clay, and more than 80% of the TCP was successfully removed (Ruiz et al., 2014). GAC impregnated with iron oxide has high adsorption efficiency for removing heavy metals and organic contaminants, as it has a good binding capacity. It has been studied extensively to remove hazardous contaminants from wastewater (H. C. Kim et al., 2010; Suresh Kumar et al., 2017a). The combination of Fe/C PRB with EK is promising and efficient for removing persistent organic pollutants (Sun et al., 2017).

This study evaluated sodium cholate biosurfactant-enhanced EK, combined with AC and FeAC PRB, to remove PFOA-contaminated kaolin clay. Our previous study demonstrated

the high efficiency of sodium cholate biosurfactant for PFOA removal from the kaolinite soil (Ganbat et al., 2022). The effectiveness of AC and FeAC as PRB in the EK system and their post-regeneration performance were investigated. Although electrochemical studies for the degradation of PFAS compounds were conducted in the past, the combination of surfactant-enhanced EK and PRB for removing PFOA-contaminated soils has not been reported yet. The Ek experiments were conducted for two-week at 20 mA electric potential to compare PFOA removal by different PRBs.

5.2 Materials and methods

5.2.1 Experimental set-up and analysis

Materials, soil preparation, and electrokinetic cell set-up are outlined in more detail in **Chapter 3 (Materials and Method)**. This study additionally integrated PRB and AC (70 g) purchased from Sigma-Aldrich in Australia. Iron Sulphate and Potassium Permanganate were purchased from Sigma Aldrich in Australia to modify AC. The characteristic of the non-modified and modified PRBs provided in **Table 5.1**. Following the preparation of the saturated soil, it was methodically layered into the reactor cell and compacted in a uniform manner to ensure the homogeneous dispersion of PFOA. To evaluate the concentration of PFOA in the soil before and after the EK tests, the samples were subjected to analysis using Liquid Chromatography-Mass Spectrometry (LC-MS) techniques.

Table 5.1: Physicochemical properties of PRB

Parameter	AC	FeAC
Particle size analysis (%)		
>2mm	0	2.59
1-2 mm	71.63	-
<1mm	28.37	-
Surface area (m^2g^{-1})	950	146.57
pH	5.25	5.93
Electrical conductivity (mS cm^{-1})	4.14	5.50

5.2.2 Iron coating of AC

FeAC PRB was made using a modified version of a method that has been published (Chen et al., 2007) (Suresh Kumar et al., 2017a). The AC was washed with DI water to get rid of any surface pollutants, and it was then dried for 4 hours in an oven at 105°C . In the meantime, 0.5M KMnO_4 solution was prepared and mixed with AC for 12 hours. The oxidised AC was filtered, washed thoroughly, and dried in the oven at 105°C . 10% m/m $\text{FeCl}_3 \cdot 6\text{H}_2\text{O}$ solution and oxidised AC were added, and the slurry was mixed at 250 rpm for 12 hours to create FeAC. The mixture was filtered, washed with DI water, and dried at 105°C in the oven. The surface modification of FeAC was then analysed using a BET analyser and SEM-EDS.

5.2.3 Electrokinetic cell setup

Figure 3.1b displays the schematic setup diagram for the EK tests, consisting of a $23 \times 8 \times 11 \text{ cm}^3$ plexiglass reactor. The reactor comprises two electrode compartments at either end, a soil compartment, a PRB compartment, and an electrolyte reservoir. In the middle of the soil compartment, 2 cm PRB sandwiched between two filter papers was employed, and contaminated soil was loaded onto both sides. A layer of cellulose filter paper, held in place by a perforated plexiglass plate, was interposed between the electrode chamber

and the soil compartment to act as a barrier, ensuring that soil did not enter the electrolyte chambers. A consistent electric current was employed utilizing a DC bench power supply, and both the electric current and voltage were documented on an hourly basis using a multimeter. The electrode chambers on either side of the reactor were equipped with two (15 x 1 cm) graphite rod electrodes (Graphite Australia Pty Ltd). The biosurfactant NaC was added to the catholyte solution (Sigma-Aldrich) based on the previous study results, where NaC outperformed other conventional surfactants in enhancing PFOA removal in the EK process (Ganbat et al., 2022). Regular injections of ultra-pure water were made into the anolyte compartment to make up for water loss brought on by electroosmotic flow. Throughout the experiment, electroosmotic flow and current intensity were periodically measured

The EK experiments were performed at room temperature conditions, without pH regulation, employing a constant initial current of 20 mA. The specifics of the six EK experiments are presented in **Table 5.2**. The anolyte consisted of MQ water, while the catholyte comprised a 5% (w/w) solution of NaC biosurfactant. To ensure a continuous hydraulic gradient across the soil, the fluid level in the inflow reservoir was carefully maintained at a constant level throughout the duration of the experiments. The EK test was carried out for two weeks using PFOA-contaminated kaolin soil with an initial concentration of 10 mg/kg concentration.

To evaluate the effectiveness of the PRB-enhanced EK test, experiment T1 was conducted as a control and reference experiment to examine the removal of PFOA without a PRB with only 5% wt NaC biosurfactant introduced at the cathode. Experiment T2 examined the efficacy of AC-PRB coupled with NaC biosurfactant. Experiment T3 investigated the effects of iron-loaded AC (FeAC)-PRB coupled with a biosurfactant. In experiments T2 and T3, the PRBs were loaded in the middle of the soil compartment with a fixed electrical

current (20 mA). In contrast, experiments T4 and T5 investigated the regeneration and reuse of AC and FeAC PRB tests. AC and FeAC PRBs were recovered by methanol extraction and reused. The impacts of placing FeAC PRB close to the anode were investigated in experiment T6.

Table 5.2: Biosurfactant enhanced EK test design

Ex p No.	Target Contamination	Concentration of target contamination (mg/kg)	Surfactant and dosing point	RFM type and position	Surfactant Concentration (% w/w) Catholyte	Duration (days)
T1	PFOA	10	NaC/cathode	NA	-	14
T2	PFOA	10	NaC/cathode	AC in the middle	-	14
T3	PFOA	10	NaC/cathode	FeAC in the middle	5	14
T4	PFOA	10	NaC/cathode	Regenerated AC in the middle	5	14
T5	PFOA	10	NaC/cathode	Regenerated FeAC in the middle	5	14
T6	PFOA	10	NaC/cathode	FeAC at the anode	5	14

5.2.4 PFOA extraction

After a period of fourteen days, the power supply was disconnected, and the experimental arrangement was disassembled. Subsequently, samples were collected from both the anolyte and catholyte compartments to evaluate the concentrations of PFOA, as well as to measure pH and electrical conductivity (EC). The soil sample was extracted into six equal sections (S1-S6, from anode to cathode), duplicate samples were obtained from each section, and the soil pore water was separated using a centrifuge. The remaining soil sample was then dried in an oven at 105°C for 12 hours. The previous study's methods were applied to extract PFOA from a soil sample (Ganbat et al., 2022). Triple methyl alcohol extraction was used to extract PFOA from each sample, and the extraction

recovery for PFOA was around 92%. 5mL of methyl alcohol was added to 5 g of dry soil, shaken at 250 rpm, 25⁰C for 60 minutes, sonicated for 30 minutes at 30⁰C, and then centrifuged for 10 minutes at 9000 rpm (Zhan et al., 2020). After three extractions, the supernatants were collected, diluted, and filtered for further LC/MS analysis; PRB was also extracted the same as soil samples. **Equation 3.1** was used to determine the removal efficacy. A 1:5 (w/v) ratio of dry mass to DI water slurry was prepared to measure the pH and EC of the soil and the PRB. HACH HQ 11D model pH and electric conductivity meter was used for all the measurements. The Zeta potential of PRB was measured before and after the EK test. BET analyser was used to measure the surface area of AC before and after the iron loading procedure. SEM coupled with EDS was used to analyse the surface characteristics of AC-PRB and FeAC PRB before and after the EK test and after the reused EK experiment.

5.3 Results and discussion

5.3.1 Change in the current and voltage

Among the crucial factors influencing the electrokinetic test, the constant current stands out as a primary variable, as it governs the behavior of contaminants within the soil medium under the influence of a direct electric field. **Figure 5.1** presents the electric current and voltage variation over time for the EK tests. The applied electric current in this study was 20 mA. However, the applied current in all EK tests decreased with increased elapsed time to a final value below 5 mA. The electrolysis reaction that generates hydrogen ions at the anode and hydroxide ions at the cathode under the applied current causes the current to rise at the beginning of the EK test. This increase in current is related to the increase in additional mineral dissolution (Hahladakis et al., 2016). Generation of the acid front at the anode and solubilisation of free ions in the soil induces ions to electromigrate to the electrodes (Ghobadi, Altaee, Zhou, McLean, Ganbat, et al.,

2020b). As shown in **Figure 5.1a**, the current surged at the start of the experiment and remained constant for several hours before gradually decreasing. The pattern of change in current over time in EK testing for removing PFOA is consistent with previous studies (Ganbat et al., 2022). This phenomenon may be caused by PFOA migration and accumulation in the soil, which increases soil pore resistance and reduces the electrical current. A similar change in the electric current was observed in a bench-scale study that used FeC PRB EK to remove phenanthrene from contaminated soil and EK tests for removing copper ions from contaminated soil (Ghobadi, Altaee, Zhou, McLean, Ganbat, et al., 2020b; Ren et al., 2019).

As shown in **Figure 5.1a**, EK tests were constant at 20 mA for at least 48 hours before they began to decline progressively. In experiment T1, the electric current maintained stable at 20 mA for 44 hours, then gradually decreased to 3.48 mA at the end of the experiment. The electric current in experiment T2 was steady for 50 hours and then dropped to 2.51 mA after 336 hours. However, experiments T3 and T6 remained steady at about 20 mA for 144 and 168 hours, respectively. The prolonged constant current in the FeAC PRB experiments is accountable for the Fe ion's presence on the AC surface. Upon the completion of the EK test, experiments T4 and T5 utilizing recycled PRB witnessed a gradual reduction in the electric current, stabilizing at 1.9 mA and 1.49 mA, respectively, after maintaining a constant level for 27 hours. FeAC-EK tests had higher average electric currents than AC-EK tests; experiments T3 and T6 were 11.0 mA and 13.23 mA, respectively, whereas the AC-EK test had an average electric current of 7.21 mA. Experiment T3 with FeAC PRB exhibited a higher electric current than experiment T2 and T5 experiments with AC PRB due to i) the electric conductivity of FeAC being higher than that of the AC PRB (**Table 5.2**), ii) the propagation of acid front in the soil caused the dissolution of iron ions and migration towards the cathode zone and iii) the

formation of a complex of PFOA with Fe^{3+} result in the transportation towards the cathode. Interestingly, the electric current profile in experiment T5 was similar to that in experiments T2 and T4, indicating that most Fe coating film on the AC was lost during the EK and regeneration processes. Experiment T4 with regenerated AC exhibited the lowest average electric current of 5.14 mA, followed by experiment T5 with regenerated FeAC of 4.31 mA.

Ions precipitation and convergence of acid and alkaline fronts in the soil increases soil resistivity to electric current and hence the electric potential. **Figure 5.1b** shows an increase in the electric potential of all experiments from 30 hours to 150 hours. For example, the average electric potential in experiment T6 was 24.09 V and 26.14 V in experiment T3. In contrast, the average electric potential in experiment T4 was 33.9 V and 29.18 V in experiment T5, indicating early metal ions precipitation or acid and alkaline front convergence in the soil. Generally, the electric potential in the EK experiments increased slowly over time as a result of increasing the soil resistivity. Finally, it reached a constant value and remained constant until the end of the EK experiments (**Figure 5.1b**).

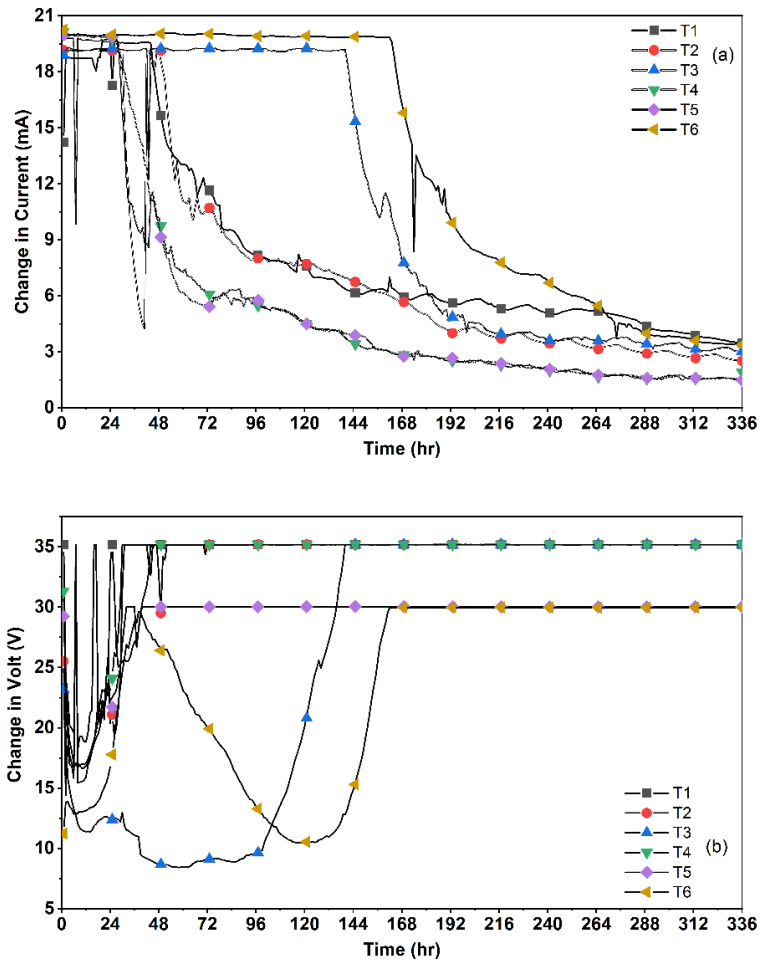


Figure 5.1: change in current of all experiments after 2 weeks.

5.3.2 Change in pH and electric conductivity of the soil

The effective ionic mobility of the hydrogen ion under an electric field is higher than that of hydroxyl ions; this enables hydrogen ions to migrate through the soil faster. As a result, acidic pH predominates in soil sections. The diffusion coefficient for H^+ and OH^- are relatively high, and their dissociation factor in water is also high and rapid; consequently, their electromigration defines the soil chemistry (Figuroa et al., 2016). As shown in **Figure 5.2a**, the soil pH was acidic, i.e. $> pH 7$, in soil sections 1 to 6 due to the fast development of the acid front from the anode to the cathode. In experiments T1, T2, and T4, the soil pH remained below the initial value of 4.7 as a result of acid migration from the anode to the cathode. Conversely, in experiments T3, T5, and T6, the soil pH was

below the initial pH of sections S1 to S3 but increased above the initial pH of sections S4 to S6 due to the movement of alkaline substances from the cathode to the anode zone. Notably, experiments T3, T5, and T6 utilizing FeAC PRB led to a slight rise in the initial soil pH due to the formation of iron hydroxide resulting from iron migration towards the cathode zone.

In experiment T1, the pH values in sections S1 through S3 were 3.00, 3.08, and 3.28, then slightly increased to pH 3.9 in section S4 before rising to pH 4.84 in section S5. Figure 5.2a shows an insignificant change in sections S1 to S3 pH of experiments T1 to T5, but soil pH increased in sections S4 to S6 closer to the cathode region. The inconsistency in soil pH of experiments T1 to T6 is due to the application of different PRB types. Experiment T6 had the highest overall soil pH, between pH 3.96 and pH 6.55. As mentioned before, experiments with FeAC PRB exhibited higher soil pH, especially in soil sections near the cathode zone, due to the creation of iron hydroxide caused by iron ions leaching from the FeAC PRB. Technically, low pH increases PFOA sorption in soils with high contents of sesquioxides (Fe and Al oxides) (Oliver et al., 2019). Nevertheless, the experimental findings imply that pH levels are not directly correlated with PFOA accumulation or removal rates in kaolinite soil.

One of the key components of EK is the soil's electric conductivity, which measures the soil pore fluid's ability to carry electric current and is determined by ion concentration in the soil water. The EC and the soil pH are inversely correlated (**Figure 5.2b**). Water hydrolysis at the anode generates H^+ ions, increasing the anode's electric conductivity. The soil EC showed a progressive reduction from the anode to the cathode region, indicating that more free ions are in the anode than in the cathode region. According to experimental data, EC values peaked in section S1 and then dropped gradually over the soil sections towards the cathode zone. As anticipated, the low EC in soil sections close

to the cathode is caused by metal ions precipitation in the alkaline environment. As shown in **Figure 5.2b**, the EC of non-PRB-EK and AC PRB were lower than that of FeAC. The presence of the iron film on the AC surface may be responsible for these findings. The soil's conductivity and ions content rose due to the micro electrolysis of Fe close to the PRB (Chen et al., 2007; Yan et al., 2013); these results are in accordance with the soil's pH. Previous studies have supported the inversely associated relationship between soil pH and EC, the low pH in sections in the anode region, and a gradually increasing inclination towards the cathode section (Andrade & dos Santos, 2020; Ghobadi et al., 2021; Guedes et al., 2019).

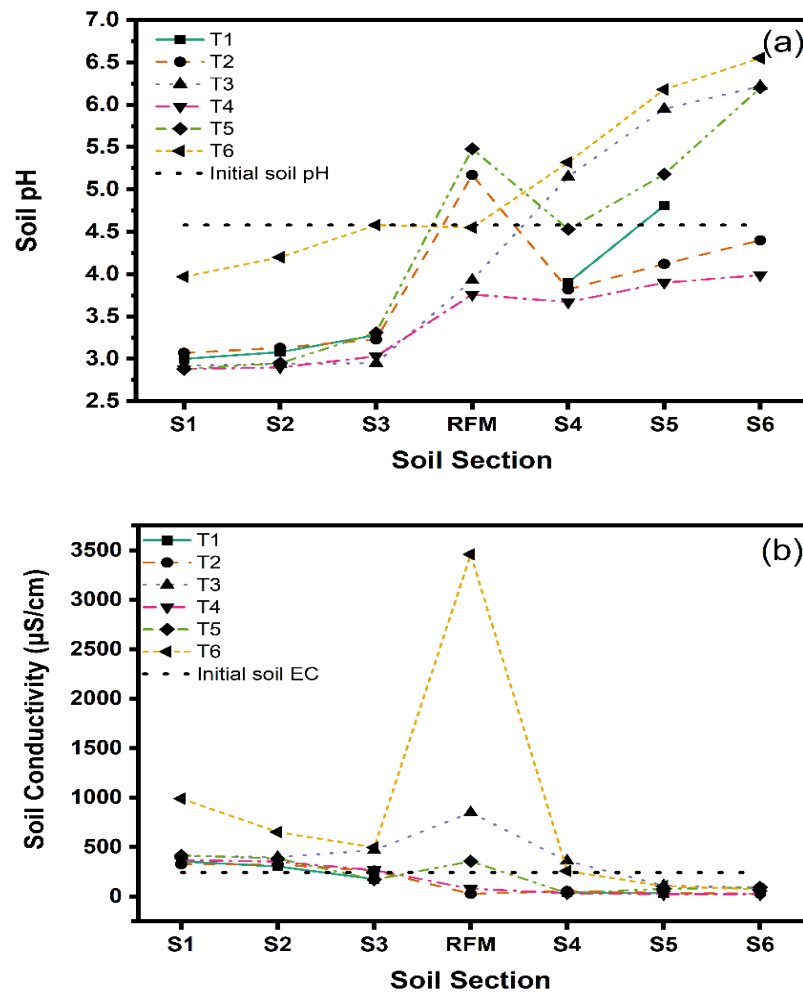


Figure 5.2:(a) pH across the soil section of different EK tests (b) electric conductivity of the soil sections for all EK tests

5.3.3 Removal of PFOA from soil

Based on the PRB used in the EK tests, the residual concentration of PFOA in soil sections exhibited a fluctuated distribution (**Figure 5.3a**). During the EK process, PFOA was mainly transported by electroosmosis and electromigration (Guedes et al., 2019). Sodium cholate (NaC) biosurfactant was added to the catholyte in all EK experiments to facilitate the transportation of PFOA. NaC endorses PFOA dissolution into surfactant micelles, improving the removal efficiency and PFOA-containing micelle transport. The environmental biocompatibility of NaC, low micelle aggregation number and low critical micelle concentration contributed to its selection as an enhancement agent (Sugioka et al., 2003). In a previous study, NaC demonstrated a superior removal rate to conventional surfactants, e.g. TW80 and SDS (Ganbat et al., 2022). As anticipated in a non-PRB enhanced EK experiment T1, PFOA accumulated in the middle section S3, as illustrated in **Figure 5.3a**. Due to electroosmotic flow going in the cathode's direction and PFOA anion electromigration towards the anode direction, PFOA accumulated in the middle of the EK cell. The findings of another lab-scale electrochemical investigation have validated a similar PFOA transportation pattern (Hou et al., 2022).

As PFOA accumulated in the middle of the EK cell, PRB was positioned there in experiment T2 to optimize the removal of PFOA during the EK process. PFOA content in soil sections exhibited a decreasing tendency towards the cathode region in experiment T2 (AC-PRB), as seen in **Figure 5.3b**. The concentration of PFOA was 1.15 mg/kg near the anode in section S1 and then slightly dropped to 0.546 mg/kg near the cathode in section S6. In the conclusion of the EK test, the PRB contained 0.253 mg/kg of PFOA. FeAC PRB was used in the middle section of experiment T3 and at the anode in experiment T6 to capture PFOA in the soil to study the impact of FeAC PRB on PFOA removal. Previous studies revealed the affinity to PFAS contaminants. As presented in

Figure 5.3c and **Figure 5.3f**, the PFOA concentrations were lowest in section S1 (circa 0.34 mg/kg), dramatically increased in sections S4 and S5, and then decreased to 0.125 mg/kg in section S6. In experiments T3 and T6, the PFOA concentration increased near the cathode in sections S4 and S5, probably, due to the PFOA adsorption on iron hydroxide that was dissolved from the FeAC PRB by the acid front from the anode to the cathode and carried by the electroosmosis flow towards the cathode. The EDS results show Fe and O in the FeAC PRB before and after the EK process, confirming the theory of PFOA adsorption on the iron oxide that migrated towards the cathode (**Figure 5.3**).

As depicted in **Figures 5.3d** and **5.3e**, reused PRB in experiments T4 and T5 exhibited a similar trend of PFOA distribution in the soil sections post the EK process. The following PFOA concentrations were found in experiment T4, 1.5413 mg/kg to 0.2458 mg/kg in sections S1 to S6. Likewise, experiment T5 showed a declining tendency towards the cathode, with PFOA concentrations of 2.038 mg/kg to 0.383 mg/kg in sections S1 to S6. Given the high concentration near the anode, electromigration likely served as the main mechanism for migrating PFOA anion in experiments T2, T4 and T5. Although experiment T5 used a regenerated FeAC, the experiment showed an AC-PRB-like pattern. Following the first cycle of the EK test and throughout the regeneration process, it is likely that some Fe was dissolved in the low pH and migrated to the cathode.

In experiment T6, the FeAC was placed near the anode to study the impact of the PRB on the PFOA removal. Sections S4 to S5 had the greatest PFOA concentrations of 4.429 mg/kg and 2.854 mg/kg, respectively, while section S1 presented the lowest concentration of 0.312 mg/kg. These results indicate that the majority of the PFOA was electromigrated towards the cathode region. The experimental data of these studies can be hypothesized that as a result of micro-electrolysis close to the FeAC PRB, PFOA formed a complex

with Fe, thereby an electron transfer to the PFOA, which resulted in the formation of the following positively charged complex that had been migrated to the cathode.



PFOA degradation in the presence of Fe^{3+} in water treatment study resulted in the formation of $[C_7F_{15}COOFe]^{2+}$ complex through electron transfer from PFOA to Fe(III) (Liu et al., 2013). However, the mass balance of this study's analysis and the negligible concentration of intermediates demonstrated that PFOA was not degraded into small-chain compounds but interacted with the Fe to generate a net-positive complex. The migration of PFOA towards the cathode is assumed to have been caused by the generation of the complex mentioned above. The formation of ferric hydroxide close to the cathode, where hydroxide ions are continuously released by electrolysis reaction, may explain the apparent development of brown precipitate in sections S5-S6. The EK process with FeAC near the anode did not significantly improve the PFOA removal, as most PFOA was found near the cathode in the soil sections S4 and S5.

According to **Table 5.2**, the EK process with the FeAC PRB in the middle had the highest PFOA removal rate of 59.55%, followed by the AC PRB with 52.35% removal and regenerated AC PRB with 40.37% removal. Placing the FeAC close to the anode in experiment T6 caused a sharp drop in PFOA removal efficiency to 21.96%, with most of the PFOA accumulated in sections S4 and S5, as seen in **Figure 5.3f**. The movement of the PFOA-Fe complex towards the cathode region could be attributed to the sharp drop in removal rate where the PRB position was altered. In the unenhanced and AC-enhanced EK process, the electromigration of PFOA towards the anode was dominant.

Although experiment T3 had a higher removal rate than experiment T2, using a regenerated FeAC in experiment T5 declined the PFOA removal efficiency from 59.55%

to 20.62% (**Table 5.2**). Experiment T4 with a regenerated AC PRB had a higher % PFOA removal of 40.37% than experiment T5 (20.61%). Apparently, upon FeAC regeneration, the PFOA removal efficiency decreased dramatically, possibly related to the surface characteristics' failure to recover. As shown in **Figure 5.3g**, the removal of PFOA in experiments T3 and T6 was relatively high in the soil sections close to the anode sections S1-S3 and lowest in S4 and S5, particularly in experiment T6. The significant difference in the removal rate of FeAC PRB tests can be attributed to their position in the EK cell. As can be evident, PFOA migrated primarily towards the anode, and positioning the PRB at the anode did not substantially increase removal efficiency as a whole. PFOA removal in experiment T2 was lowest in sections S1–S2, then increasing towards section S6. According to the experimental data, the PFOA anion electromigrated towards the anode during the AC-PRB EK process, whereas the high PFOA concentration near the cathode in the EK experiments with FeAC PRB was due to the formation of a positively-charged iron-PFOA complex that migrated towards the cathode. In a previous study, Fe-modified GAC outperformed GAC at adsorbing PFOA from an aqueous solution (Ahn et al., 2022). It was hypothesized that Fe-modified AC PRB would have a higher removal rate by adsorption mechanism. However, in this investigation, FeAC PRB enhanced the removal rate of PFOA contamination by enhancing the transportation mechanism. PFOA adsorption onto the PRB was insignificant, according to the experimental data.

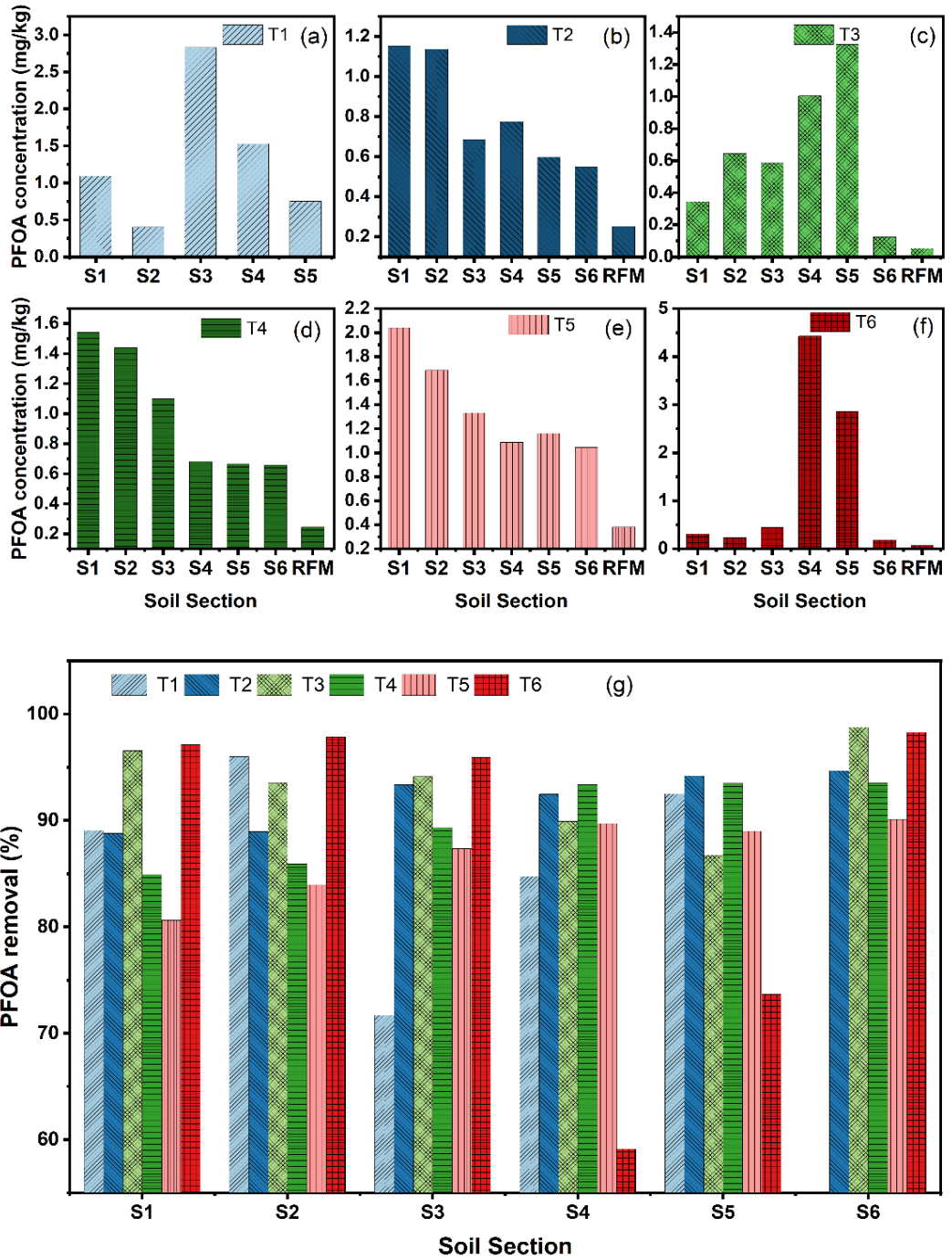


Figure 5.3:(a) PFOA distribution in soil sections after remediation (b) PFOA removal rate in soil sections post-treatment.

Table 5.3: Mass balance, residual PFOA concentration and removal efficiency

Experiments	Initial PFOA in soil (mg)	Residual PFOA in treated soil (mg)	PFOA mass in RFM (mg)	PFOA mass in electrolyte solution (mg)	PFOA mass in soil pore water (mg)	Mass balance (%)	PFOA removal (%)
T1	10.17	6.80	-	3.07	0.09	99.98	33.16±0.11
T2	10.46	4.89	0.25	5.54	0.10	108.44	52.35±0.42
T3	10.00	4.05	0.05	5.74	0.12	100.51	59.55±0.01
T4	10.21	6.08	0.24	3.75	0.11	95.15	40.37±0.21
T5	10.50	8.35	0.38	5.70	0.07	109.83	20.62±0.42
T6	10.84	8.45	0.06	2.27	0.04	100.16	21.96±0.75

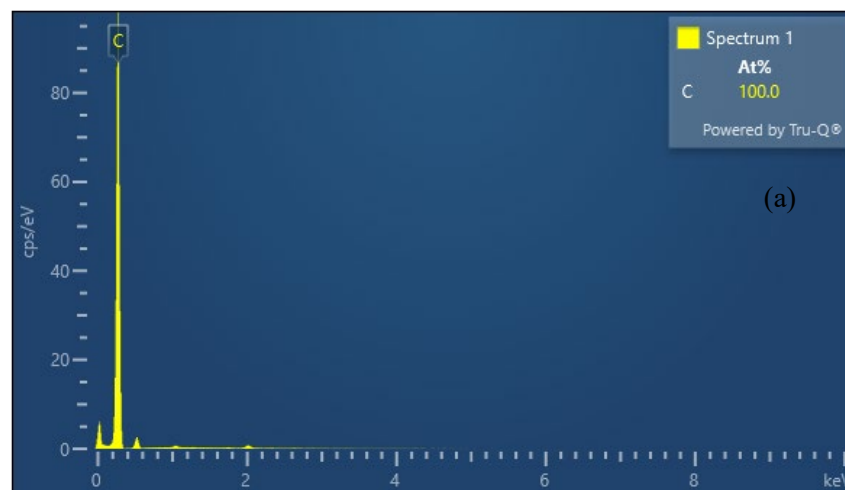
5.3.4 Characterisation of PRB

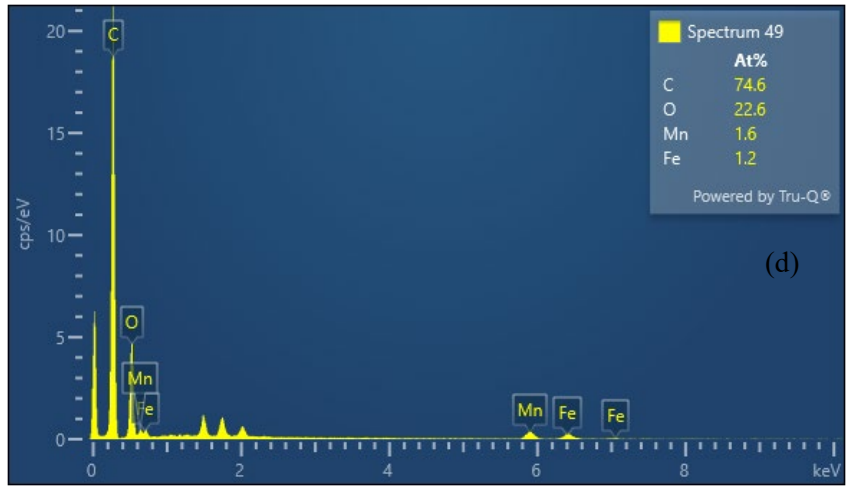
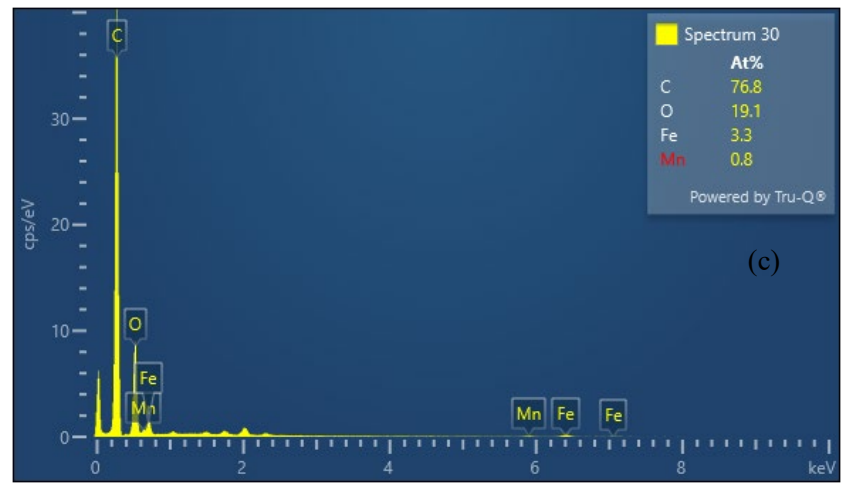
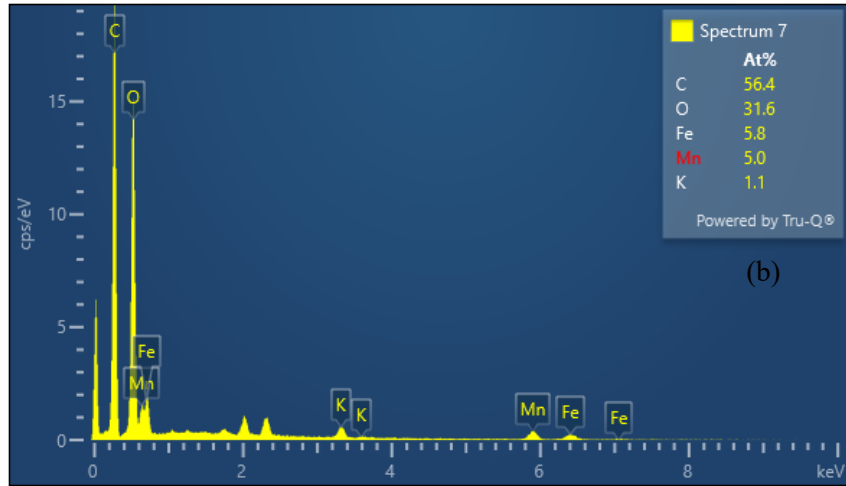
Further AC and FeAC PRBs were analysed to verify the experiments' results. The surface and the effectiveness of iron loading on the AC were analysed before and after coating on the AC, utilizing SEM-EDS. The PRBs were also analysed following EK testing to support the experimental findings that predicted iron loss from the PRB after the EK test and in the recycled FeAC PRB. **Figure 5.4b** shows Fe on the AC following the coating procedure. The Fe coating on the AC decreased from 5.8% to 3.3% after the EK test (**Figure 5.4b and 5.4c**). The iron concentration dropped at the end of experiment T5 with regenerated FeAC PRB, as seen in **Figure 5.4d**. These results are consistent with the experimental findings and removal efficiencies of FeAC PRB tests.

Furthermore, the BET measurement of the AC and FeAC surface area before and after coating with iron showed a decrease in the AC surface after iron loading, indicating that surface impregnation was successful. The AC surface area was initially 1200 m²/g, then decreased to 146.57 m²/g after iron loading. In previous studies where AC was impregnated with iron, it was reported that the surface area significantly decreased after coating (Suresh Kumar et al., 2017b). FTIR analysis also confirms the AC's surface changes after coating with iron. The FTIR spectra of AC and FeAC before the

electrokinetic (EK) experiments, as well as FeAC PRB after the EK tests, revealed distinct vibration peaks at 1650 cm⁻¹, 1100 cm⁻¹, and 670 cm⁻¹. These peaks are indicative of specific functional groups, namely -C=O, -C-O, and -C-O-C- bending, respectively. It can be seen from **Figure 5.4f** the FeAC PRB after coating, the peak intensity significantly changed. However, after the EK test, the intensity decreased, which could be attributed to the loss of Fe from the PRB surface.

The Zeta potential of PRBs before and after EK is illustrated in **Figure 5.4e**. The FeAC negative charge increased after the EK test due to the loss of Fe during the EK procedure. AC PRB becomes less negative after the EK test, possibly due to the adsorption of PFOA during the EK test or the change in the PRB pH due to the propagation of the acid front close to the PRB zone in the EK tests (**Figure 5.3a**).





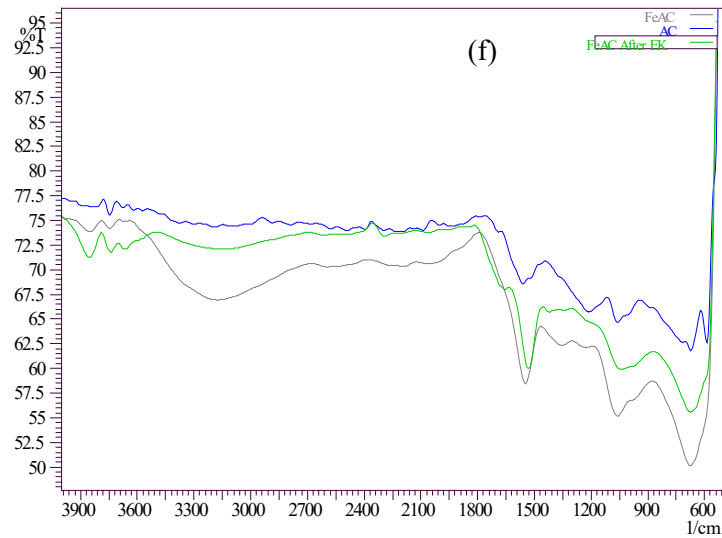
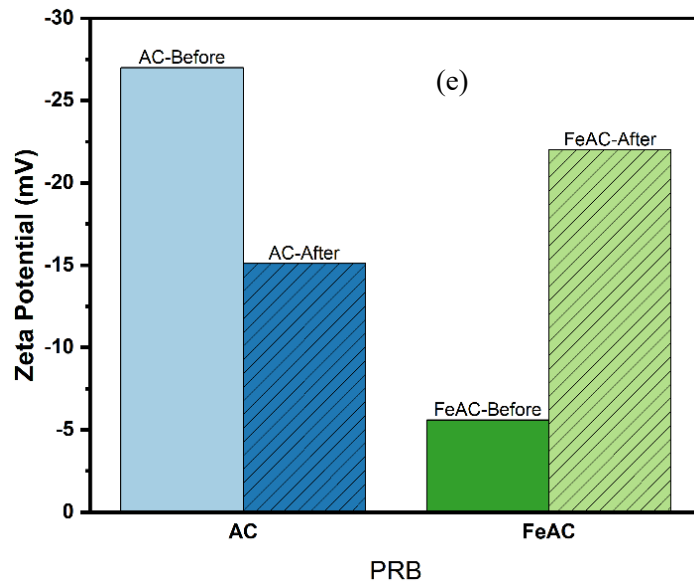


Figure 5.4: (a) AC EDS (b) FeAC EDS after iron loading (c) FeAC PRB after EK test (d) Recycled FeAC PRB after EK test (e) Zeta Potential of AC and FeAC PRB before and after EK tests (f) FTIR results of AC, FeAC before and after EK

5.3.5 Performance of Activated carbon and iron loaded activated carbon PRBs

Activated carbon has been widely investigated as an adsorbent for removing PFOA from aqueous medium and stabilising soil remediation processes. It has been known as the best adsorbent for long-chain PFAS compounds. Due to the hydrophobic chain and hydrophilic head functional group of PFOA, hydrophobic interactions and electrostatic attractions serve as the primary adsorption mechanisms of AC (Jin et al., 2021). Molecular diffusion was identified as the crucial factor of PFOA adsorption onto

powdered activated carbon (PAC), and the effectiveness of removing PFOA using PAC was about 99% (Barth et al., 2021). PFOA accumulated in sections S1 and S2 in the AC PRB enhanced EK process, as depicted in **Figure 5.5a**, indicating that electromigration is the predominant transportation mechanism in these tests.

In contrast, electroosmotic flow towards the cathode explains the presence of PFOA near the cathode region in the AC-EK tests. Also, PFOA was adsorbed onto the AC PRB due to its affinity to AC media. Near the cathode, where OH is constantly released due to water electrolysis causing soil pH increase, a high PFOA leachability occurred in the soil. Therefore, the concentration of PFOA is less in the soil section close to the cathode. However, as can be seen in **Figure 5.5b**, PFOA was transported towards sections S4 and S5, and the concentration of PFOA is less in soil sections near the anode. Contrary to the AC PRB test, most PFOA was transported to the cathode in the FeAC PRB test. This phenomenon can be hypothesized that PFOA forms a complex with Fe^{3+} , favouring the transportation towards the cathode.

As depicted in **Figure 5.5a** and **Figure 5.5b**, the change in pH and EC also differ in both tests. FeAC PRB exhibits higher EC than AC PRB, which can be attributed to the loading of Fe onto the AC. Moreover, the soil pH is higher in sections S3 to S6 of the FeAC EK test, which is above the initial pH level. The precipitation of iron compounds at alkaline pH near the cathode could explain the higher pH in the FeAC tests. In contrast, the pH was higher in sections S3 to S6 of the AC PRB EK but remained below the initial pH value.

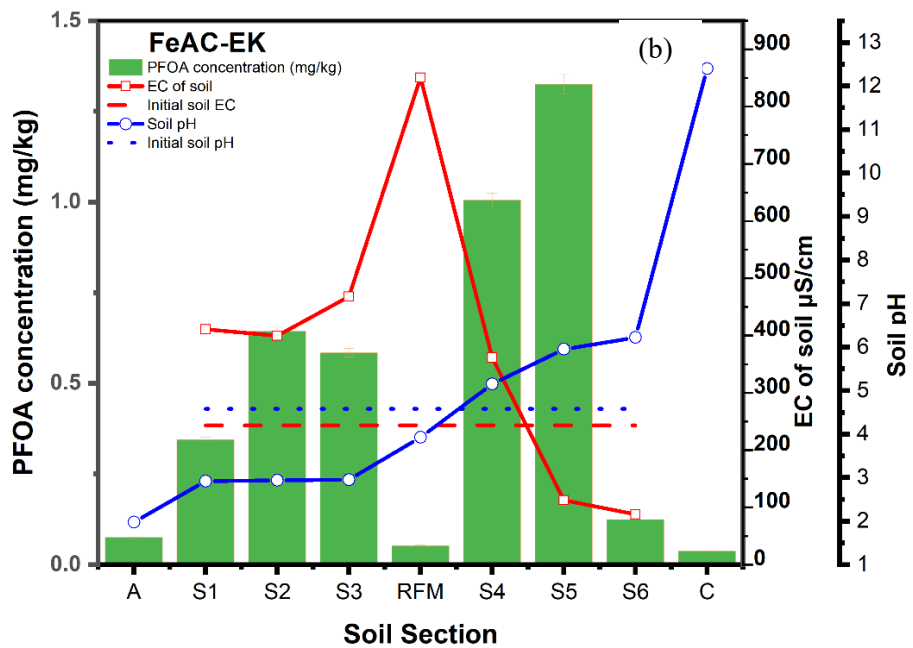
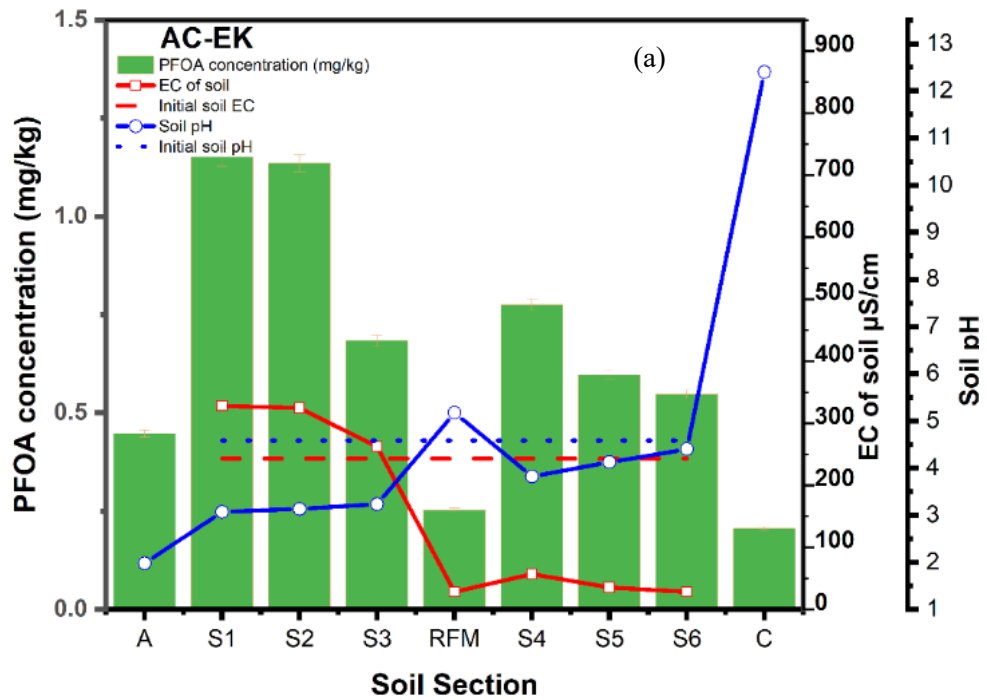


Figure 5.5: (a) AC-PRB EK test; (b) AC PRB EK test

5.3.6 Energy consumption and electroosmotic flow

Specific power consumption E_u (kWh kg^{-1}) was determined using **Equation 3.3** while considering remediation efficiency. The specific energy consumption exhibited variability across the experiments, with values ranging from $0.037 \text{ kWh kg}^{-1}$ in

experiment T5 and $0.076 \text{ kWh kg}^{-1}$ in experiment T6. Notably, an increase in the average electric current applied during the EK process resulted in a corresponding elevation in the specific energy consumption of the EK process. However, as shown in **Figure 5.6**, PFOA removal efficiency was not directly proportional or correlated with energy consumption (kWh kg^{-1}). High removal efficiency did not require higher energy consumption. As shown in **Figure 5.6** conventional EK process in experiment T1 consumed high SEC for soil treatment, which could be attributed to the higher soil resistivity and the voltage applied in the test. Compared to PRB-enhanced EK tests, the constant current of experiment T1 dropped rapidly and reached the maximum voltage in a shorter time. As a result, the voltage remained constant at a higher value for longer. Compared to all EK tests, the EK process with the FeAC PRB at the anode (experiment T6) consumed the highest electrical energy because experiment T6 had the longest elapsed constant current among all the tests; hence the average current for this test was the highest.

The highest average current resulted in the highest SEC in the EK treatment. The higher average current can be attributed to the presence and migration of the Fe to the cathode. This observation is consistent with the previous experimental results. Experiment T3, with the highest removal rate, had $0.689 \text{ kWh kg}^{-1} \text{ SEC}$, whereas experiment T2 had a slightly lower SEC of $0.585 \text{ kWh kg}^{-1}$. This is attributed to the prolonged constant current with increased elapsed time in experiment T3 compared to experiment T2, which resulted in a greater average current for the test.

The variation in electroosmotic flow (EOF) in EK tests is presented in **Figure 5.6**. To demonstrate the relationship between the variation of the EOF with energy consumption and overall removal rate. EOF depends on the fluid characteristics (dielectric constant and viscosity) and soil surface characteristics such as zeta potential and voltage gradient (Cameselle, 2015). The cumulative EOF was collected and measured at the end of the

experiment. The removal rate of PFOA post-remediation was not closely correlated with the EOF and the specific energy consumption (SEC), as seen in **Figure 5.6**. For all experiments, the EOF was generally high at the start of the EK test. It is explained by the ion production brought on by the electrolysis reaction at the electrode at the beginning of the EK test. Depending on the PRB applied, within the first 24 hours, 350–400 mL of EOF were generated and gradually declined over time. The EOF in experiment T1 started high before dropping sharply and producing the lowest EOF. This outcome may be related to the sharp decline in electric current in experiment T1, which slowed the EOF. In experiments T2 and T3, the increased EOF can be attributed to the longer constant current and high average voltage. In experiment T3, the constant current was stable for longer than in experiment T2. However, the maximum EOF was found in experiment T4 with a recycled AC, probably, due to the high average voltage and the changing zeta potential of the PRB. Experiment T5 EOF decreased drastically, which can also be attributed to the change in voltage and zeta potential of recycled FeAC PRB after regeneration. Although experiment T6 had a longer constant current during the remediation process, the EOF was low due to the increased soil resistivity and the accumulation of PFOA in the soil sections near the cathode.

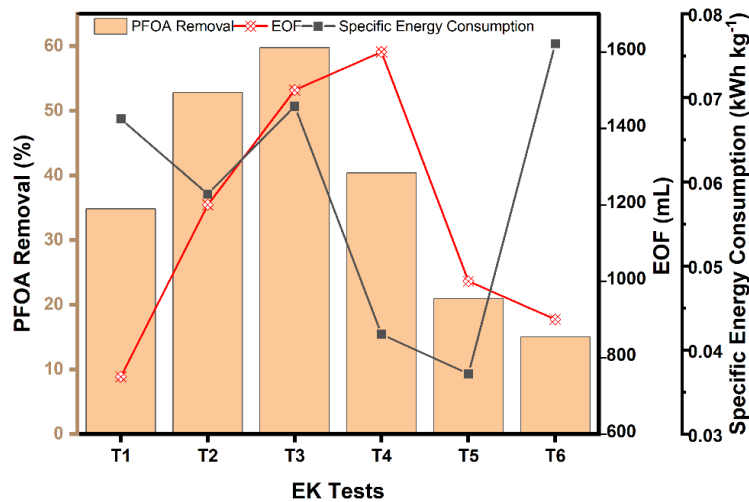


Figure 5.6: Specific Energy Consumption (kWh kg^{-1}), total PFOA removal of all EK tests and variation of EOF.

5.4 Conclusions

Based on mass balance and negligible concentration of intermediates in the soil section, it can be hypothesized that PFOA has not been degraded into shorter chain PFAS but is more likely transported and adsorbed onto the PRB in the EK test. The transportation of PFOA and accumulation in the sections near the anode in the AC PRB EK test and the accumulation of PFOA near the cathode region in the FeAC PRB EK test suggest the transportation mechanism in these tests was different. In AC PRB, enhanced EK PFOA migrated towards the anode by electromigration and electroosmosis transported to the cathode. FeAC EK tests hypothesized that PFOA formed a complex with Fe resulting in their transportation towards the cathode region. FeAC PRB enhanced EK test where PRB was placed in the middle of the EK cell resulted in 59% overall PFOA removal, whereas AC PRB enhanced EK test resulted in 54% removal. However, when PRBs were regenerated, AC PRB resulted in 40% removal, whereas FeAC regenerated PRB EK test resulted in a 24% removal rate. The low removal rate of FeAC suggests the loss of Fe during the EK test and the regeneration process, which affects the surface properties hence the dramatic change in the removal rate.

To better understand what occurs in the electrochemical cell during an experiment, more EK parameters need to be analysed and investigated in the future.

CHAPTER SIX

IRON SLAG PERMEABLE REACTIVE BARRIER FOR PFOA REMOVAL BY THE ELECTROKINETIC PROCESS

CHAPTER 6 : IRON SLAG PERMEABLE REACTIVE BARRIER FOR PFOA REMOVAL BY THE ELECTROKINETIC PROCESS

This chapter has been derived from the following published article:

Ganbat, N., et al. (2023) "Iron slag permeable reactive barrier for PFOA removal by the electrokinetic process" Journal of Hazardous Material

6.1 Background

PFAS are a group of environmental pollutants that have gained wide attention as emerging organic contamination of concern due to their potential adverse health effects and persistent, non-biodegradable accumulative nature in the soil and water. PFOA is one of the most prevalent PFAS compounds detected in the environment (Barth et al., 2021). PFOA has a hydrophobic fluorinated alkyl chain responsible for its thermal and chemical stability and polar functional group at the end, attributed to their solubility and affinity to transport in the environment. It can migrate through soil and water, potentially contaminating drinking water supplies and posing a risk to public health and wildlife (Schaefer et al., 2015). PFOA from AFFF (aqueous film-forming foam) is a significant concern, particularly in areas where AFFF has been extensively used, such as airports and military bases, since these locations frequently serve as firefighting training grounds (Brusseau et al., 2020). When PFOA containing AFFF is used to extinguish a fire, it releases PFOA and other types of PFAS into the environment, contaminating soils and groundwater. PFOA can also be released into the environment during production, as it has been used extensively in industrial and consumer goods (Ahmed et al., 2020). PFOA can also enter soil by disposing of products containing the chemical in landfills. PFOA can be transported through the air and deposited onto soil through atmospheric deposition. This can occur by releasing PFOA-containing aerosols from industrial processes or burning PFOA-containing materials (Bolan et al., 2021b). Due to their physicochemical properties, PFOA can persist in the environment for a long time and transport significant

distances from the source of contamination (Coggan et al., 2019). PFOA is particularly resistant to biodegradability, vaporization and highly bioaccumulative; hence, some plants may absorb them from the soil or water. In that situation, it enters the food chain posing a significant health risk to humans and wildlife. Most residents of industrialized nations will have some PFAS in their systems because of their widespread use (Epa Au, 2019). Exposure to PFOA has been linked to several health effects, including liver damage, immune system dysfunction, and an increased risk of cancer. However, long-term health has not been extensively studied (Longpré et al., 2020). As a result, efforts are being made to reduce the PFOA and other PFAS-containing products and remediate contaminated areas.

Recent technologies and remediation techniques for the removal of PFAS have been summarised in several review articles (Ahmed et al., 2020; Mahinroosta & Senevirathna, 2020b; Sima & Jaffé, 2021). Methods such as sorbent amendment, stabilisation, and solidification have been utilised to reduce PFAS mobility and leaching in contaminated sites, and destructive techniques such as thermal treatment, encapsulation, and capping have been investigated (Bolan et al., 2021b; Sleep & Juhasz, 2021; Söregård et al., 2020b). Typically, destructive methods involve the excavation of contaminated soil, which poses a safety risk during transport. The treatment procedure can be expensive and energy-intensive. Thermal heating is an inefficient, destructive, and costly process that consists of incinerating contaminated soil at high temperatures, resulting in industrial waste. Mechanochemical treatment reduced PFOA and PFOS levels in dry sand by 99% and 98%, respectively in AFFF contaminated soil (Turner et al., 2021). To remove PFASs from the soil, the soil washing plant utilised both physical and chemical processes, including fractionation of soil particles by size and partitioning of PFASs into the aqueous phase, followed by treatment of the contaminated water with granular activated carbon

and ion exchange resins, resulting in average removal efficiencies of 97.1% for PFOA and 94.9% for PFOS (Grimison et al., 2023). Excavation and transportation to treatment facilities are difficult and expensive processes. Hence, in situ soil washing method was investigated and compared to an excavated soil washing technique; a 76% removal efficiency was found for the in situ method (Høisæter et al., 2021). In a pilot scale study, 6 tons of AFFF-contaminated soil was used for stabilisation and solidification treatment, resulting in an average of 92% removal rate for PFOA and PFOS. However, the limitation of S/S treatment is the long-term assessment (Sörengård et al., 2021). Several lab-scale electrochemical treatments for PFAS removal have been evaluated for their viability. Electrokinetic treatment alone was insufficient to eliminate PFAS. However, the addition of enhancing agents to the EK process has increased the overall removal rate (Ganbat et al., 2022; Niarchos et al., 2022; Sörengård et al., 2019).

In electrokinetic remediation, contaminants are mobilised by the direct electric current, and the charged contaminants are transported toward the cathode or anode by electromigration and electroosmosis phenomenon (Acar & Alshawabkeh, 1993). Enhanced electrokinetic remediation processes have been used extensively to remove heavy metals and organic contaminations to improve the overall removal efficiency of contaminants (Alcántara et al., 2010; Colacicco et al., 2010). Enhanced EK processes include coupling the EK tests with surfactants and permeable reactive barriers (PRB) to improve contaminants removal from the soil. Many researchers have recently focused on an environmentally sustainable approach to improve EK processes (Ghobadi et al., 2021). PRB-enhanced EK studies have shown successful remediation results in several lab-scale experiments, especially the use of agricultural or industrial waste where the PRB media was an effective approach due to the sustainability and reuse of waste material (Ghobadi et al., 2021). In recent years PRB coupled EK process has gained much attention because

of their environmental compatibility, versatility, scale-up practice and cost-effectiveness. It has been used efficiently to increase the removal rate of contaminants in low-permeability soils (Andrade & dos Santos, 2020). Zero valent iron/Activated carbon enhanced EK coupled with biosurfactant has been applied to remove persistent organic pollutants and demonstrated a removal rate of 64.6% (Sun et al., 2017). Carbonized food waste has been used in the EK process to remove copper, with an average removal efficiency of 53.4%-84.6% (Han et al., 2010). Compost was applied as PRB in the EK process for the removal of copper in a lab scale study, and the experimental results were 84.09% removal and after two cycles of regeneration and reuse, the removal efficiency was 74.11% (Ghobadi, Altaee, Zhou, McLean, Ganbat, et al., 2020b). The advantages of PRB in the EK process include adsorption, degradation or immobilization of contaminants in situ without bringing them up to the surface (Cameselle & Reddy, 2012). PRB-enhanced EK tests have been successfully implemented in soil polluted with organic contaminations. In the EK process, surfactant-enhanced tests showed the potential to remove the contaminants from certain regions; however, the rest of the contaminants accumulated in the soil. PRB enhanced process on the other hand, can assist the beforementioned obstacles (Li et al., 2011). Research has reported that coupling various types of PRB with EK can greatly improve the removal efficiency (Ghobadi, Altaee, Zhou, McLean, Ganbat, et al., 2020b; Li et al., 2011; Ren et al., 2019; Zhou, Xu, et al., 2020). In these processes, the PRB was utilised in the soil chamber to adsorb, degrade, or precipitate contaminants transported via electroosmosis or electromigration. Activated carbon's high surface area and high adsorption capacity for organic contaminants and heavy metal ions make it a cost-effective PRB. Hence AC is often added to PRB for EK process. When choosing a PRB, it is essential to consider its cost-effectiveness and environmental resiliency.

Steel-making slag is an industrial waste. Steel-making slag is an industrial waste by-product of steel manufacturing (Díaz-Piloneta et al., 2022; Wang et al., 2021). Using slag as PRB is an environmentally sustainable approach for soil remediation in which waste materials enhance the EK performance for the PFOA treatment. To our knowledge, steel slag-PRB has not been used for PFOA removal from contaminated soils by the EK process. The main slag component is iron oxide, which has a high adsorption capacity for anionic compounds. Since PFOA is an anionic compound, it is hypothesized to have a high adsorption capacity towards PFOA. Sodium cholate (NaC) enhanced PFOA transport and concentration in the iron slag RFM (Ganbat et al., 2022). The study evaluated the feasibility of using a slag/activated carbon (AC) mixture PRB to enhance PFOA treatment and removal from contaminated kaolinite soil by the EK process. Different percentages of slag-to-AC ratios were used in the RFM, and PFOA removal was studied. The study also investigated the impact of the EK duration on PFOA removal by extending the EK duration from 2 to 3 weeks.

6.2 Materials and methods

6.2.1 Experimental set-up and analysis

From Sigma-Aldrich in Australia, PFOA with a purity level of > 99% was bought. Kaolin clay from Keane Ceramic Pty. in Australia was chosen as the model soil for the EK studies due to its weak cation exchange capacity, low carbon content, and low permeability. The physicochemical properties of the kaolin soil utilized in the EK experiments are the same as the previous study (Ganbat et al., 2022). All tests employed PFOA-spiked soil, with the initial concentration being 10 mg/kg. The spiked soil was kept at room temperature for at least 72 hours, and regular stirring ensured uniform distribution and homogenous PFOA adsorption. As PRB, slag was mixed with AC purchased from Sigma-Aldrich in Australia and was employed for each experiment. The saturated soil was then layered into

the reactor and compacted uniformly to ensure the uniform distribution of PFOA. A multimeter (Thermo Scientific model EUTECH PC 450) A slurry with a dry soil-to-DI water ratio of 1:5 (w:v) was prepared and utilized to measure the pH and electrical conductivity of the soil (Altaee et al., 2008). The PFOA concentration in the soil was analyzed before and after the EK tests using LC-MS as the analytical instrument. The morphological and chemical characteristics of the PRBs were determined through EDX, a chemical microanalysis technique. FTIR was employed to analyze the surface functional groups of PRBs before and after the EK tests. Additionally, the specific surface area of PRBs were determined using BET.

6.2.2 Electrokinetic cell setup and test design

Figure 6.1 displays the schematic setup diagram for the EK tests. The EK experiments were conducted at room temperature without pH control with an initial steady current of 20 mA. **Table 6.1** provides details on the six EK experiments. The anolyte was MQ water, and the catholyte was a 5% (w/w) NaC biosurfactant. The fluid level in the inflow reservoir was maintained at a constant level to maintain a continuous hydraulic gradient throughout the soil. The EK test was carried out for two weeks using PFOA-contaminated kaolin soil with an initial 10 mg/kg concentration.

To evaluate the effectiveness of the PRB-enhanced EK test, experiment E1 was conducted as a reference experiment to examine the removal of PFOA without a PRB with but only 5% w/w NaC biosurfactant introduced at the cathode. Experiment E2 examined the efficacy of slag/AC-PRB coupled with NaC biosurfactant, whereas experiment E3 investigated the effects of higher slag proportion, slag/AC-PRB coupled with a biosurfactant. Experiment E4 investigated the performance of regenerated slag/AC-PRB EK coupled with biosurfactant. Experiment E5 investigated the performance of slag/AC-PRB EK treatment without biosurfactant. Lastly, experiment E6 examined the effects of

the slag/AC-PRB EK test coupled with biosurfactant for 3 weeks. PRB was positioned in the middle of the reactor cell in all EK tests.

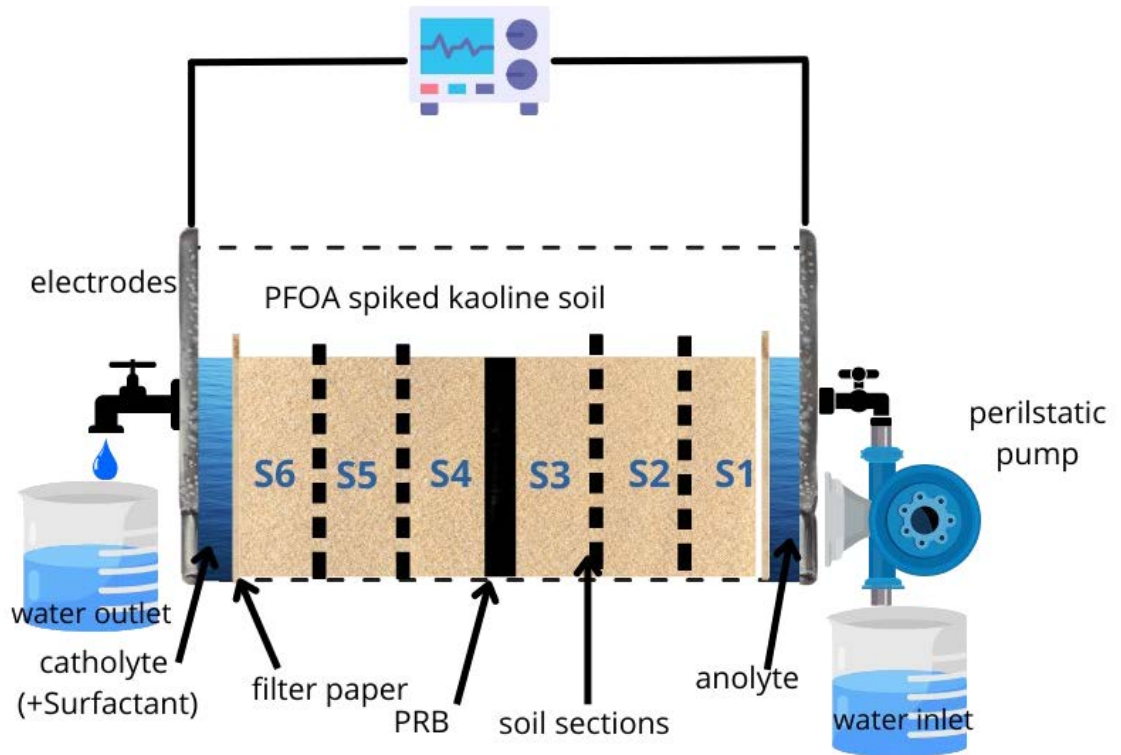


Figure 6.1: Electrokinetic test set-up of slag/AC PRB enhanced EK test.

Table 6.1: Biosurfactant enhanced EK tests coupled with Slag/AC PRB.

Ex p No.	Target Contamination	Concentration of PFOA (mg/kg)	Surfactant and dosing point	PRB type and position	Surfactant Concentration (% w/w) Catholyte	Duration (days)
E1	PFOA	10	NaC/cathode	NA	5	14
E2	PFOA	10	NaC/cathode	Slag/AC (50/50) in the middle	5	14
E3	PFOA	10	NaC/cathode	Slag/AC (70/30) in the middle	5	14
E4	PFOA	10	NaC/cathode	Regenerated Slag/AC (70/30) in the middle	5	14
E5	PFOA	10	NA	Slag/AC (70/30) in the middle	NA	14
E6	PFOA	10	NaC/cathode	Slag/AC (70/30) in the middle	5	21

6.2.3 PFOA analysis

After fourteen days experiments (E1-E5) and twenty-one days experiment (E6), the power supply was disconnected, and the test setup was disassembled. Aqueous solutions from the anode and cathode chambers were collected at the end of each test, and the PFOA concentration, pH, and EC were assessed. The soil sample was extracted into six equal sections (sections S1-S6, from anode to cathode), duplicate samples were obtained from each section, and the soil pore water was separated using a centrifuge. The remaining soil sample was then dried in an oven at 105°C for 12 hours. The previous study's methods were applied to extract PFOA from a soil sample (Ganbat et al., 2022). Triple methyl alcohol extraction was used to extract PFOA from each sample, and the extraction recovery for PFOA was around 92%. 5mL of methyl alcohol was added to 5g of dry soil,

shaken at 250 rpm, 25⁰C for 60 minutes, sonicated for 30 minutes at 30⁰C, and then centrifuged for 10 minutes at 9000 rpm (Zhan et al., 2020). After three extractions, the supernatants were collected, diluted, and filtered (using a PTFE syringe filter) and then transferred into vials for LC-MS/MS analysis (LC/MS 8060, Shimadzu, shim pack column 1.6 μ m, 2.0 mm \times 50 mm). PRB was also extracted same as soil samples. The removal efficacy was determined by equation 3.1. A 1:5 (w/v) ratio of dry mass to DI water slurry was prepared to measure the pH and EC of the soil and the PRB.

6.3 Results and discussion

6.3.1 Change in the current and voltage

The electric current mobilizes ionic species in the contaminated soil during the EK process. Water electrolysis reaction generates hydronium ions at the anode and hydroxide ions at the cathode electrode. The developed acid and alkaline front will migrate to the respective electrode in the soil. Charged molecules will be solubilized as the acid front advances in the soil and migrate to respective cathodes. **Figure 6.2** illustrates the variations in electric current and voltage within the soil across various EK experiments. In general, the electric current was directly correlated with the electric charge level passing through the soil pores, with the inverse direction of the electrons' movement (Guedes et al., 2019). The electric current was about 20 mA at the beginning of the EK experiment and progressively declined over time (Ghobadi et al., 2021; Guedes et al., 2019). Because of the electrolysis reaction at the anode and increasing dissolved ions in the pore solution, the electric current initially remained constant at 20 mA for several hours. The degree of electric current flowing through the soil cell is closely associated with the concentration of free ions, establishing it as a pivotal factor that significantly influences the transport of contaminants through the soil. The water electrolysis reaction and the migration of charged molecules to the opposite charge electrode can explain this

phenomenon. The current decreased after 48 to 240 hours due to reduced soil conductivity caused by acid and alkaline front meeting and charged molecules accumulation in the soil specimen (**Figure 6a**). Contaminants are transported towards the electrolytic chambers and removed during the EK process. As a result, the electric current drops due to fewer charged particles in the soil. The gradual decline in the electric current could also be due to the electrodes' fouling caused by soil particles accumulation, reducing the electrode surface area.

As illustrated in **Figure 6.2a**, experiments E1 to E3 exhibited a constant current that slowly dropped over time. However, in experiment E1, the current dropped rapidly after 48 hours, probably due to the faster-increased soil resistivity as PFOA was accumulated in the soil sections. As stated previously, the rapid drop in current could be related to the depolarization effect associated with the acid and alkaline front due to water electrolysis at the anode and cathode, leading to soil pore clogging (Acar & Alshwabkeh, 1993). During experiments E2 and E3, the electric current remained approximately constant at 20 mA for nearly 96 hours before experiencing fluctuations and eventually stabilizing at a constant value by the end of the experiment. In experiment E3, the electric current fluctuated more than in experiment E2 before it stabilized and decreased after 216 hours. A Comparison of the electric current indicates that tests with a slag PRB recorded higher currents than tests without a slag PRB (experiment E1). The slight increase in the current can explain this due to the high conductivity of the slag PRB. This observation agrees with previous studies where experiments conducted with a PRB recorded a higher electric current (Li et al., 2011; Wan et al., 2010). The ionic species were transported to the opposite charge electrolytic chambers over time, decreasing the soil's ionic conductivity and resulting in a sharp current drop. During experiments E4 and E5, the electric current maintained stable at around 20 mA for 336 and 240 hours, respectively. Experiment E5

was conducted without the NaC enhancement agent, which probably affected the transport of ionic species and accumulation in the soil, leading to an increased soil resistivity. The longer constant current in experiments E4 and E5 can be explained by flushing fluid compensating for the loss of ionic species, reducing the soil resistance and increasing the current intensity (Millán et al., 2020). The stable and constant current observed in experiment E4, where NaC was absent in the cathodic chamber, and experiment E5, where the slag PRB was regenerated, may be attributed to these factors. In these experiments, the migration of ions under the electric field occurred at a stable rate compared to other EK tests where fresh PRBs were used in combination with NaC. This stability can be attributed to the lower voltage values applied in experiments E4 and E5. The average current in experiment E4 was 19.75 mA and was 19.27 mA in experiment E5. Whereas in experiment E2, the average current was 10.51 mA, in experiment E3 was 13.39, and in experiment E6, it was 14.05 mA. However, the average voltage was higher in these tests. Experiment E6 was conducted for 3 weeks, and the current remained constant at 20 mA for 144 hours and gradually decreased, reaching 7 mA at the end of the experiment. Experiment E6 exhibited a steady decrease in the electric current over time. The reason could be PFOA accumulating in the PRB and less migration in the soil. Hence there are fewer mobilized species in the soil for transportation. As the PFOA accumulated in the PRB and the ions gradually depleted, reducing the soil conductivity and causing a decrease in the current. The sorption onto PRB may have induced a slow diffusion of PFOA in the EK cell.

As depicted in **Figure 6**, the change in electric current is inversely proportional to the change in voltage. When the current is stable at around 20 mA, the voltage remains low, but as soon as the current starts to decrease, the voltage increases. Generally, the voltage of PRB-enhanced EK tests was more stable than without a PRB. **Figure 6b** depicts the

change in voltage over time in the electrokinetic experiments E1 to E6. Experiment E1 reached the maximum voltage rapidly after 48 hours, indicating a sharp increase in soil resistivity. The greater voltage in experiment E3 than in experiment E2 reflected the fluctuation in the electric current in experiment E3. The voltage in experiments E4 and E5 remained stable for longer and slowly climbed up after almost 7 days due to the increased soil resistivity over time. The prolonged stable voltage could be because it was lower than the EK tests. The voltage increase in experiment E6 after 240 hours was due to the drop in the electric current (**Figure 6a**) due to the increased soil resistivity, causing a sharp increase in the voltage.

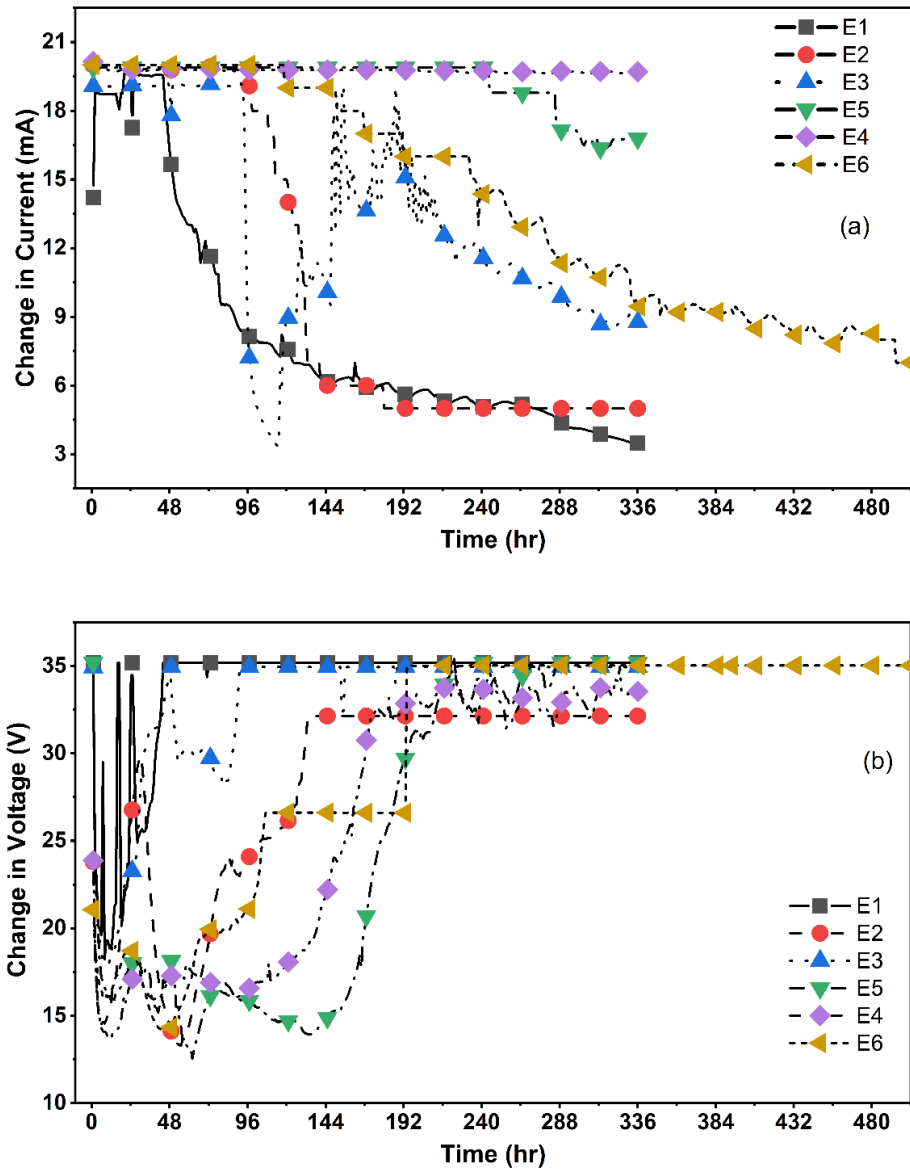


Figure 6.2. (a) change in current (b) change in voltage during the EK experiment

6.3.2 Soil pH and electric conductivity

Figure 6.3a illustrates the pH distribution across the soil, spanning from the anode to the cathode (sections S1 to S6), after the completion of the EK experiments. Notably, the EK experiments were conducted with no pH control. After the EK treatment, the soil pH in sections proximate to the anode compartment exhibited a decrease below the initial soil pH, gradually increasing as one progressed towards the cathode zone. As shown in **Figure 6.3a**, the soil pH in sections near the anode region, sections (S1 to S3) exhibited an acidic

nature, primarily attributed to the rapid migration of the acid front caused by the electrolysis reaction, which generates H^+ ions. This occurrence can be attributed to hydrogen ions' higher effective ionic mobility, approximately 1.8 times faster than hydroxide ions. (Acar & Alshawabkeh, 1993). **Figure 6.3a** clearly depicts the pH variations in the soil sections for both non-permeable reactive barrier-enhanced experiment E1 and PRB-enhanced experiments E2-E6. In experiment E1, the pH levels in soil sections S1 to S4 remain consistently acidic, with a minor increase observed near the cathode. This can be attributed to the faster migration of H^+ ions compared to OH^- ions. In contrast, in PRB-enhanced experiments E2 and E3, a noticeable increasing trend in pH are observed from the permeable reactive barrier towards soil sections S4 to S6. This trend can be attributed to the initial pH of the PRB, which is approximately 9, and its influence on the transportation of H^+ ions across the soil sections near the cathode. Notably, the pH at the cathode chamber remains around 12, while the pH values in the sections near the cathode (S4 to S6) fluctuate. Specifically, in experiment E2, the pH ranges across soil sections S1 to S3 are 2.94-3.00, while the pH ranges in sections S4 to S6 are 7.90-8.53. In experiment E3, the pH ranges across soil sections S1 to S3 are 2.54-2.92, while the pH ranges in sections S4 to S6 are 8.65-9.73. The pH values for the PRB in experiments E2 and E3 are 8.37 and 9.54, respectively. The slight increase in pH for the PRB can be attributed to a higher slag ratio within the PRB. In the regenerated PRB-enhanced (PRB-EK) test E4, a similar pH trend across the soil sections is evident, as observed in experiments E2/E3. In contrast, experiment E5 was conducted without using NaC biosurfactant, resulting in pH values ranging from 3.11 to 3.83 in sections S1 to S3 and from 9.81 to 10.26 in sections S4 to S5. Despite maintaining the same PRB (pH 8.12) ratio, the slight increase in pH across the soil sections can be attributed to the absence of biosurfactants. Lastly, experiment E6 was conducted over 3 weeks, revealing a pH range

of 3.72-3.80 in sections S1-S3 and 5.34-7.47 in sections S4-S6. Notably, experiment E6 demonstrated the lowest pH range in sections S4-S6. This observation can be attributed to the continuous generation and transportation of H⁺ ions across the soil sections over an extended period. The higher ionic mobility of H⁺ ions in the electrokinetic (EK) process could lead to their dominance and subsequent lower pH values in sections S4-S6 compared to other experiments. The higher pH in sections close to the cathode would impart a negative charge on the soil surface, decreasing PFOA adsorption on the soil. As the soil acquires a negative charge, PFOA adsorption on the soil decreases due to reducing the electrostatic interaction with the negatively charged PFOA compound (Wang & Shih, 2011). Previous studies observed that PFOA had higher adsorption affinity at acid soil pH (Oliver et al., 2019). The pH-dependent adsorption of PFOA agrees with earlier research where PFOS adsorption on kaolinite was studied, and experimental results observed decreased adsorption with an increase in pH (Johnson et al., 2007).

As shown in **Figure 6.3a**, the pH of experiment E1 without a PRB was acidic (pH3 to pH3.9) for soil sections S1 to S4 and slightly increased towards the cathode, reaching pH4.8 in section S5. In the E2 experiment, the soil pH in sections S1 to S3 was lower than the initial pH (pH 2.9 to 3), as shown in **Figure 6.3b**. It significantly increased in section S4, reaching pH 7.9 and gradually increased to pH 8.53 in section S6. As shown in **Figure 6.3c**, soil pH in sections S1 to S3 were 2.54 to 2.92 and significantly increased to 8.65 in soil section S4, and it continued to increase to section S6 with pH 9.73. The sudden increase in the soil pH in section S4 was probably attributed to the alkaline pH of the iron slag PRB (pH 9.5), which hindered the advancement of acid in the soil. Also, the advancement of OH⁻ ions from the cathode influenced the pH values in soil sections S4 to S6. In experiment E4, in sections S1 to S3, the recorded pH was pH3.02 to pH3.3 (**Figure 6.3d**) and drastically increased to 8.86 in soil section S4, then kept increasing to

9.35 in section S6 near the cathode. The higher pH in the cathode region for experiment E3 could be due to the higher slag content in the PRB. **Figure 6.3e** shows that the sections S1 to S3 pH was from pH3.11 to pH3.83 in experiment E5, and it increased significantly to pH 9.81 in the soil section S4. The highest soil pH in experiment E5 was pH10.26 in section S6, and it could be due to the absence of biosurfactants and the rapid advancement of OH⁻ in these soil sections. Experiment E6 also exhibited low pH3.72 to pH3.8 in sections S1 to S3 (**Figure 3f**) and increased to pH5.34 to pH 7.47 in sections S4 to S6. The increase in the soil pH from sections S3 to S4 was insignificant in experiment E6 due to the longer experimental time that allowed the acid to sweep across the soil specimen.

Soil conductivity, as seen in **Figure 6.3**, is inversely proportional to the pH of the soil. A similar trend was observed in the previous studies conducted (Söregård et al., 2019). Previous studies agree with these results that soil EC is inversely related to soil pH [21, 30]. The soil's electric conductivity (EC) plays a vital role in the EK treatment, which involves the movement of the contaminants and other charged particles under the direct electric current. During the EK process, the transportation of charged particles to the anode and cathode creates a concentration gradient that can result in soil resistivity and change in the soil pH. The soil has a more remarkable ability to transmit electrical charges when the EC of the soil is high; however, removing ionic species during the electrokinetic treatment can cause a decrease in electric conductivity. **Figure 6.3** suggests that the electric conductivity is lower in soil regions with high PFOA removal. The soil EC showed a progressive reduction from the anode to the cathode region in experiments E1 to E6, indicating that more free ions are in the anode than in the cathode region. In general, the EC is higher in sections S1 to S3 in all EK tests due to the concentration of the ionic species, which is correlated with free protons. In all experiments, the EC decreased in the soil sections S4 to S6 due to the acid and alkaline fronts meeting near the cathode region.

As shown in **Figures 6.3b and 6.3c**, there was a significant difference in the PRB EC of experiments E2 and E3 depending on the ratio of iron slag to AC in the PRB and the metal ions impurities captured by the PRB. For example, the PRB EC was 28.1 $\mu\text{S}/\text{cm}$ in experiment E2 and 850.3 $\mu\text{S}/\text{cm}$ in experiment E3. Furthermore, the EC of recycled PRB in experiment E4 (**Figure 6.3d**) was 79.3 $\mu\text{S}/\text{cm}$ and 356.6 $\mu\text{S}/\text{cm}$ in experiment E5 (**Figure 6.3e**). The highest EC in PRB was 3460 $\mu\text{S}/\text{cm}$ after 3 weeks of testing in experiment E6 (**Figure 6.3f**) and could be attributed to the longer experimental time and higher PFOA adsorption.

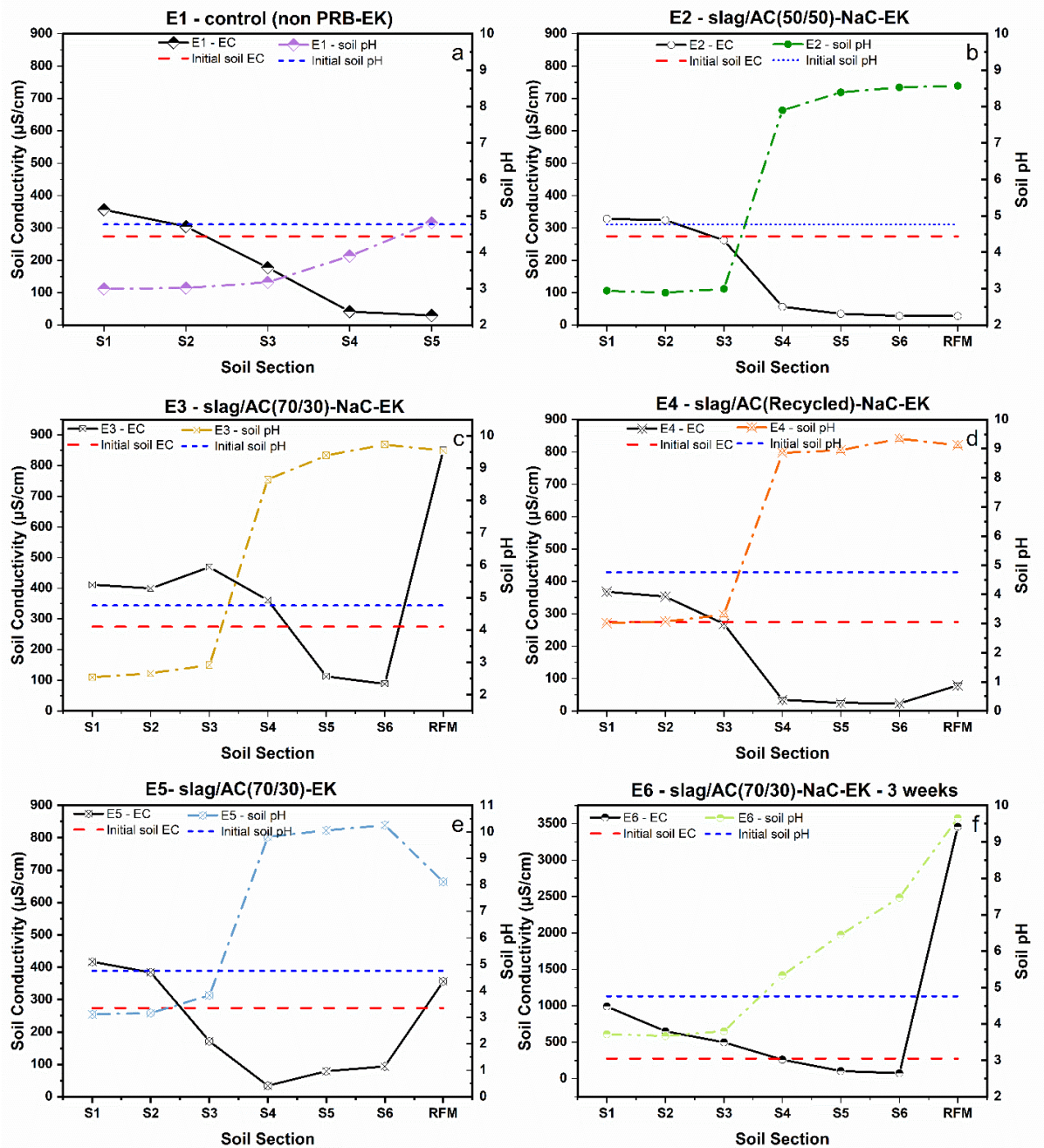


Figure 6.3: (a) the soil pH in all EK experiments (b) the soil EC in the soil section in all EK tests.

6.3.3 Removal efficiency

Figure 6.4a displays the residual concentration of perfluorooctanoic acid (PFOA) in each soil section and the permeable reactive barrier (PRB) after electrokinetic (EK) treatment. PFOA, characterized by a negatively charged nature and a hydrophilic functional group,

can migrate within soil pore water under the influence of an electric field throughout the EK process. In experiment E1 (without PRB), a notable observation can be made regarding the deposition of PFOA. A significant portion of the PFOA accumulated within the middle section. Due to the negative charge of PFOA, electromigration occurs in the anode direction, and electroosmosis occurs in the cathode direction. These mechanisms result in PFOA accumulation in the soil middle section. Previous experiments have also revealed PFOA deposition in the reactor's mid-area (Ganbat et al., 2022; Hou et al., 2022; Sörensén et al., 2019). Consequently, the PRBs were utilized in the reactor cell's centre to enhance the efficacy of EK remediation in conjunction with NaC.

Figure 6.4a clearly demonstrates significant PFOA adsorption by the PRB and the migration of PFOA towards the anode region. Notably, the cathode region exhibits lower PFOA levels, which can be attributed to the increased pH resulting in decreased PFOA adsorption. The observed relationship between pH and PFOA adsorption supports the understanding that the sorption of PFOA is influenced by soil pH (Wang & Shih, 2011). The charge of the soil is positive at pH values lower than the point of zero charge (pH_{Zpc}) and becomes negatively charged at pH values higher than the pH_{Zpc}. The adsorption of PFOA increases when the soil is positively charged near the anode region, as indicated by a pH value lower than the pH_{Zpc} (4.5). Conversely, PFOA adsorption on the soil decreases near the cathode region due to the high soil pH, with higher pH values than the pH_{Zpc}(4.5). Consequently, PFOA removal is more pronounced in the cathode zone due to two main factors: i) the electrostatic interaction between PFOA and the soil surface and ii) the electromigration of PFOA towards the anode. Another study reported a negative relationship between PFOA and pH, where an increase in pH led to decreased PFOA sorption in soil; the pH-PFOA adsorption relationship is consistent with earlier research (Groffen et al., 2019).

The non-PRB EK test E1 removal rate was 33%, as shown in **Figure 6.4b**. However, when combined with PRB, the overall removal rate was doubled, with an E2 experimental result of 78%. E3 examined the effect of increasing the slag-to-AC ratio and found that the overall removal rate increase was not too significant, at 79%. When the PFOA adsorption onto PRB in E2 and E3 was compared, the experimental results were not significantly different (**Table 6.2**). When comparing the PFOA prevalence in soil sections, the residual PFOA concentration in soil sections S4-S6 in experiment E3 was negligible. In addition, when the pH of two PRBs was compared, experiment E3 had a higher pH, which could be attributed to more slag. As a result, the residual PFOA concentration in soil sections after the EK process can be attributed to the slag content in the PRB. Experiment E4 evaluated the feasibility of recycled PRB in the EK process.

Additionally, the spent PRB was regenerated using methanol and subsequently reused in a subsequent cycle. The experimental findings demonstrate that the utilization of the spent PRB in the enhanced EK test resulted in a reduction of approximately 10% in the overall removal rate at 69%. The distribution of residual PFOA concentration in experiment E4 is illustrated in **Figure 6.4a**, where it can be observed that PFOA accumulated predominantly in sections S4 to S6 of the soil. This accumulation suggests that the PFOA migrated and deposited in these particular sections during the EK process. Experiment E4 PRB exhibited higher PFOA accumulation due to the reuse of spent material. In general, the reuse of PRB is feasible in the EK process, and the overall removal rate has remained relatively high.

To evaluate the importance of Sodium Cholate (NaC) in the PRB-enhanced EK process, experiment E5 was conducted without any surfactants. **Figure 6.4a** indicates the residual concentration of PFOA after the EK test E5; it can be seen that PFOA is distributed in the soil sections almost evenly, especially in S4-S6. NaC is an anionic surfactant facilitating

PFOA transportation towards the anode due to lower critical micelle concentration (CMC). As a result, the absence of the biosurfactant resulted in a decrease in the overall removal rate (70.38%) in experiment E5, and PFOA accumulation was observed in soil sections S4-S5. Previous research conducted by our team has indicated that including sodium cholate (NaC) facilitated the transfer of PFOA towards the anode. Sodium cholate has a negative charge (-COO-), while PFOA carries a negative charge on the carboxylate functional group, forming a strong electrostatic interaction. Also, PFOA's non-polar part strongly interacts with the hydrophobic segment of NaC. In addition to these interactions, hydrogen bonding can also play a role; both molecules possess hydrogen bonding capabilities. PFOA's functional group can form a hydrogen bond with NaC's hydroxyl group leading to an additional attraction. Due to these interactions, NaC enables PFOA's solubilization, mobilization and transport under an electric field in the EK process. Solubilization occurs by solubilizing PFOA by forming micelles. These micelles encapsulate the PFOA, effectively increasing their solubility in soil pore water and improving the contaminants' transportation by the EK process.

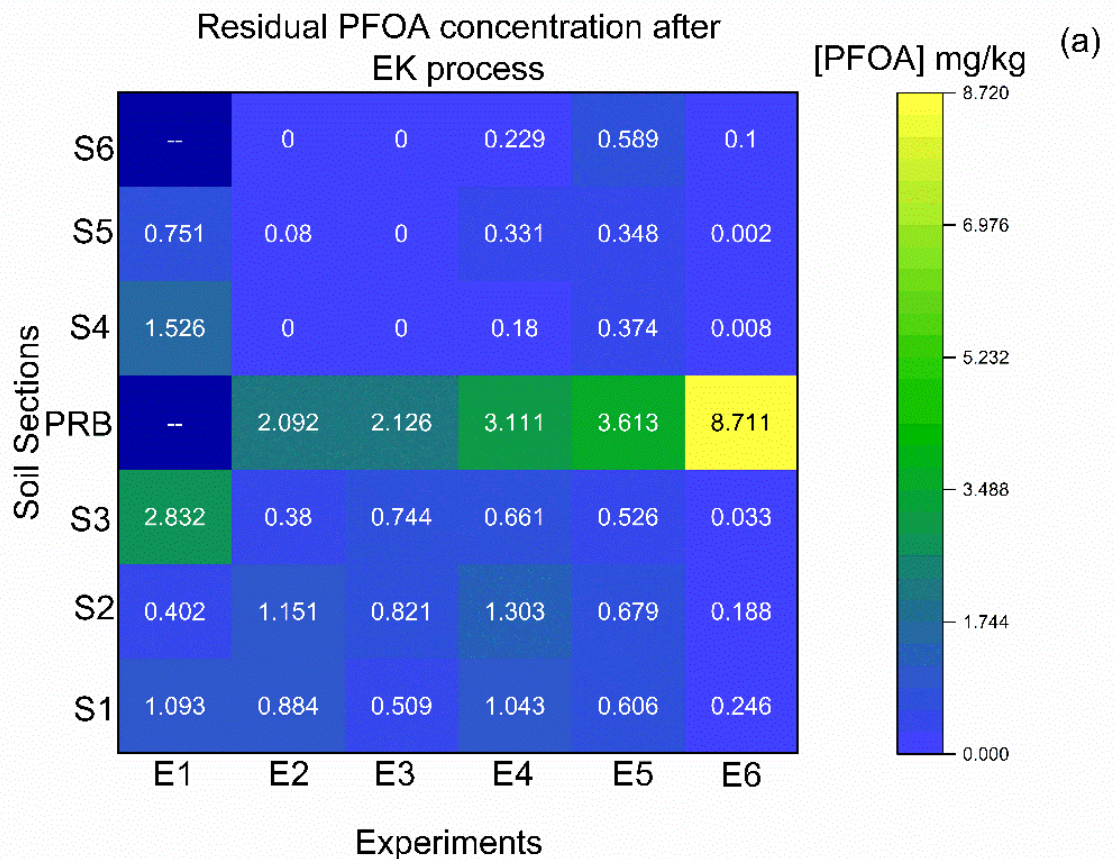
Furthermore, the results presented in **Figure 6.4** shed light on the effect of extending the experimental duration of the EK test to 3 weeks. The figure demonstrates a significant reduction in the residual concentration of PFOA in the soil sections compared to the 2-week experimental duration. This decrease in residual PFOA concentration signifies the successful adsorption of a substantial portion of PFOA onto the PRB employed in the EK system. **Figure 6.4a** depicts the experimental findings, showing that approximately 87% of the PFOA in the soil was effectively adsorbed onto the PRB, leading to an overall PFOA removal rate of 94% by the end of experiment E6 (**Table 6.2**). The residual concentration of PFOA in the soil was insignificant and primarily located near the anode region. This can be attributed to the acidic environment near the anode, which altered the

surface charge of the soil and facilitated PFOA adsorption. In contrast, the soil section close to the cathode exhibited lower PFOA concentrations compared to the anode region due to the alkaline environment and the negative charge of the soil near the cathode, which hindered the adsorption of PFOA.

The observed reduction in PFOA concentration in the soil near the cathode and the substantial PFOA capture by the PRB highlight the crucial roles of electromigration and electroosmosis in transporting PFOA under the applied electric field. While the primary mechanism of PFOA adsorption onto the PRB is anticipated to be electrostatic interaction, it is important to note that some PFOA may also form inner sphere Fe-carboxylate complexes through ligand exchange, as reported in aqueous solutions (Gao & Chorover, 2012). In a related study, an electrochemical process was employed to degrade PFOA and PFOS, resulting in approximately 51.7% and 33% removal rates, respectively (Hou et al., 2022). Our previous investigation focused on a surfactant-enhanced EK process, which successfully achieved around 75% PFOA removal with an initial concentration of 100 ppm (Ganbat et al., 2022). Furthermore, a novel setup combining extraction with stabilization in the EK system was explored, where a two-compartment configuration achieved 90% PFOA removal, whilst a single-compartment setup reached a removal rate of 75% (Niarchos et al., 2022). It is worth noting that the duration of the EK process played a significant role in PFOA removal. Longer processing times facilitated the transportation of PFOA and decreased its adsorption in the anode region, suggesting that an extended experimental duration enhances the efficiency of PFOA removal in the EK system.

Overall, incorporating iron slag/AC PRB in the EK improved PFOA removal, as demonstrated in experiments E1 and E2. The affinity of iron slag to PFOA enhances its removal during the EK process. Increasing the iron slag to AC ratio from 50%-50% in

experiment E2 to 70%-30% in experiment E3 slightly increased the PFOA removal from 75% to 79.25%. Comparing experiments E3 and E5 shows that PFOA removal was improved when NaC biosurfactant was dosed in the catholyte. PFOA removal was 79.25% and 70.35% in experiments E3 and E5 (**Figure 6.4a**). Regenerated iron slag/AC PRB use in the EK process decreased the PFOA removal from 79.25% in experiment E3 to 63.92% in experiment E4. The maximum PFOA removal was 94% in experiment E6 due to the longer process duration.



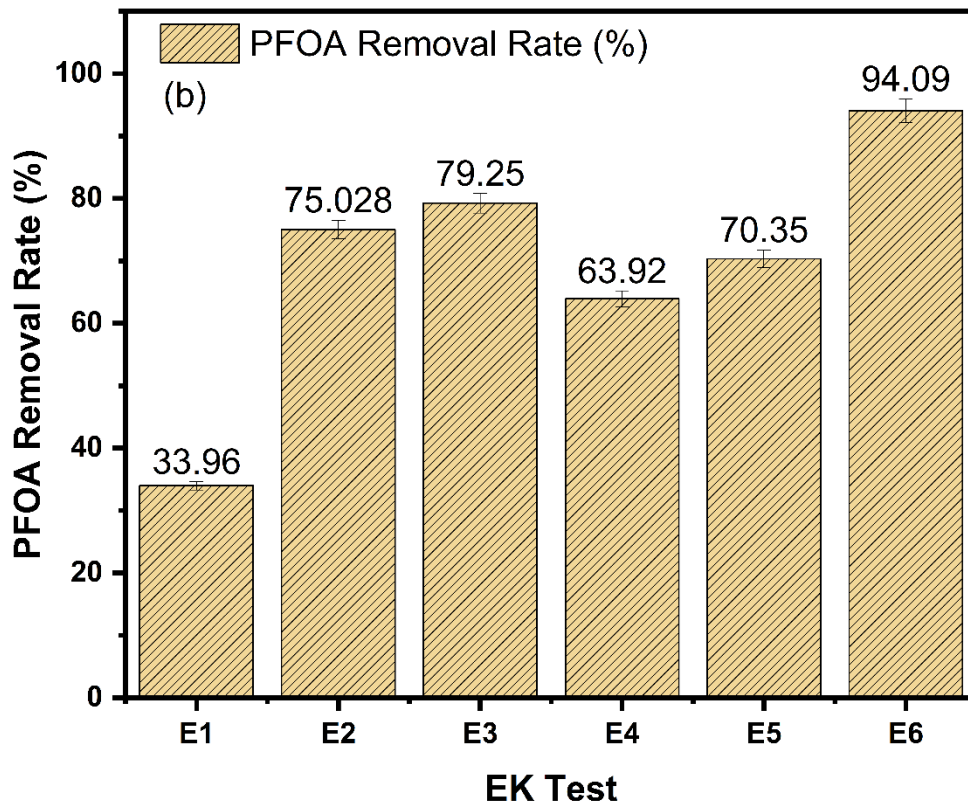


Figure 6.4: (a) E1 (b)E2 (c) E3 (d) E4 (e)E5 (f) E6 residual PFOA concentration(g) Removal Rate in all EK tests.

Table 6.2: Mass Balance and Removal efficiency of EK tests

Experiments	Initial PFOA in soil (mg)	Residual PFOA in treated soil (mg)	PFOA mass in PRB (mg)	PFOA mass in the electrolyte (mg)	Mass balance (%)	PFOA removal (%)
E1	10	6.8911	-	3.0725	99.65	33.16±0.11
E2	10	2.3806	2.0901	5.5293	98.04	78.93±0.09
E3	10	2.0749	2.1188	5.9576	101.12	79.25±0.15
E4	10	3.7491	3.1475	3.6199	101.21	69.91±0.12
E5	10	3.1223	3.6112	3.0888	98.36	70.38±0.09
E6	10	0.5904	8.7124	1.6004	109.07	94.09±0.16

6.3.4 Characteristics of PRB

Figure 6.5a exhibits the XRD result of the steel-making iron slag components. The results indicate that the main component of the slag is iron oxide, and iron oxide has an

adsorption capacity to remove contaminations (Díaz-Piloneta et al., 2022). PFOA's primary adsorption mechanism is electrostatic interaction, and PFOA forms inner sphere Fe-carboxylate complexes by ligand exchange (Ahn et al., 2022). pHzpc is the pH at which the net surface charge is zero. It determines the adsorbent's interaction with electrolytes and influences the ion exchange capacity (Pouretedal & Sadegh, 2014). The pHzpc was measured for the PRB used in the EK experiment to evaluate the PRB and PFOA adsorption mechanism, and the pHzpc of the PRB used was 9.5. Basic oxides possess a positive surface charge around pzc 9.4-9 (Tengvall, 2017). Because the surface charge of the PRB is positive and PFOA is anionic, the adsorption mechanism onto the PRB is most likely electrostatic interaction.

Furthermore, the analysis of adsorption kinetics revealed that both physical adsorption and chemical adsorption mechanisms contribute to the adsorption of PFOA onto PRB, where pseudo-second-order kinetics fitted well (R^2 : 0.99 for PRB) (**Figure 6.5c**).

Steel slag, a solid waste material, possesses favorable characteristics such as a high specific surface area and large porosity. It is a potential low-cost adsorbent for removing contaminants from water and soil (Shi et al., 2022). The capacity and efficiency of steel slag for pollutant removal are influenced by its surface physiochemical characteristics and chemical components. In the context of removing PFOA from contaminated water and soil, activated carbon has conventionally been employed as the adsorbent (Deng et al., 2015; Lee et al., 2020). Accordingly, our study used a mixture of activated carbon and slag as the permeable reactive barrier (PRB) to adsorb PFOA in the electrokinetic (EK) process. The components of the slag were analyzed using an X-ray diffraction (XRD) analyzer, as shown in **Figure 6.5a**. The interaction between iron oxide and PFOA is not yet fully understood; however, iron oxide can undergo adsorption or surface attachment reactions with PFOA in the environment. Due to its small particle size and high porosity,

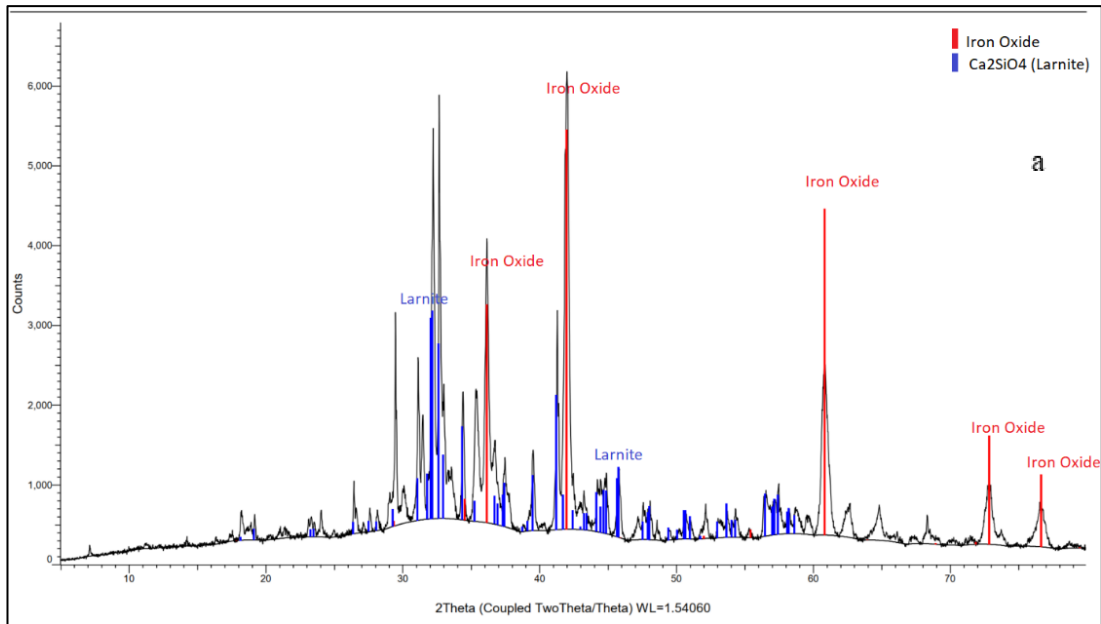
iron oxide exhibits a substantial surface area, rendering it an excellent adsorbent (Jain et al., 2018). The primary mechanism for the adsorption of PFOA onto iron oxide involves electrostatic interactions between PFOA molecules, with subsequent formation of inner-sphere Fe-carboxylate complexes through ligand exchange (Gao & Chorover, 2012). The adsorption of PFOA onto iron oxide particles can have several implications. Firstly, it can reduce the mobility of PFOA in the environment, thereby decreasing the likelihood of contaminating groundwater or leaching into the surrounding areas. Furthermore, the adsorption of PFOA onto iron oxide particles can affect the particle's behaviour and properties, such as stability and reactivity (Hassan et al., 2020).

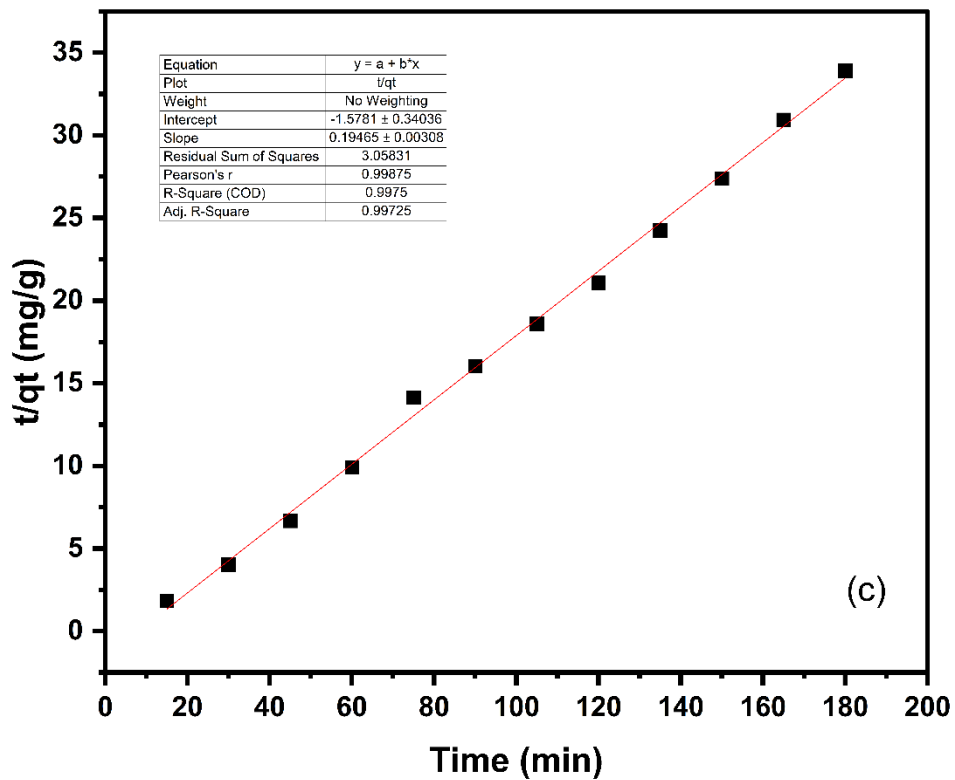
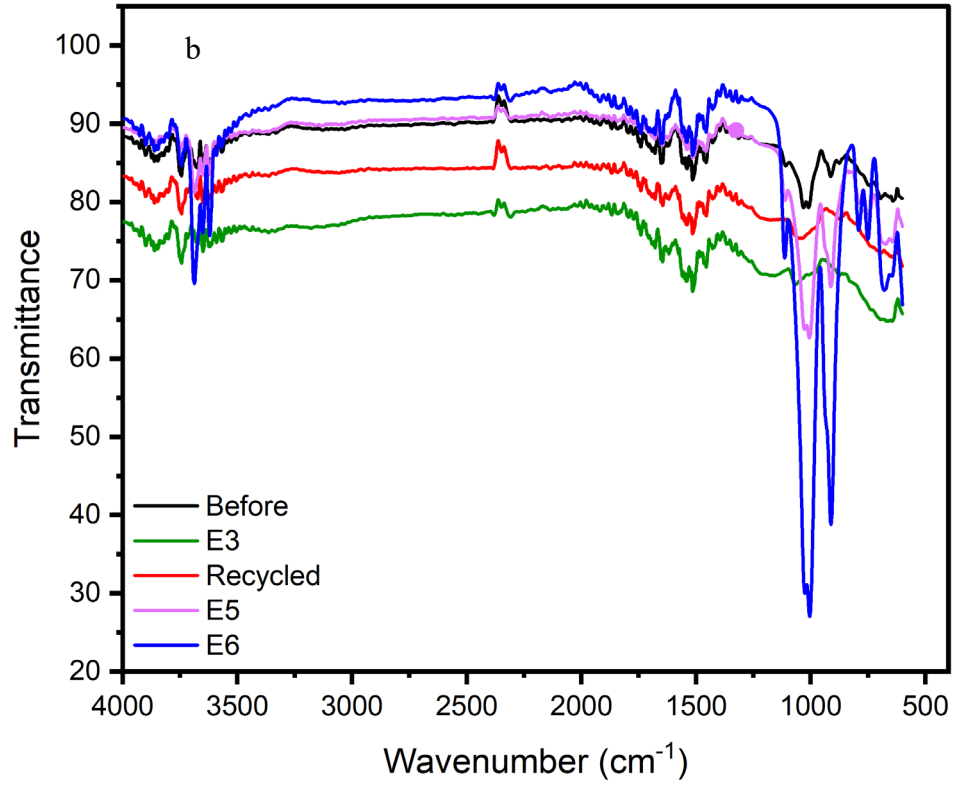
The Fourier-transform infrared spectroscopy (FTIR) results provide valuable insights into the functional groups present in the sample. As shown in **Figure 6.5b**, a strong band observed in the 1100-1000 cm^{-1} range corresponds to the C-O stretching vibrations. Additionally, a broad band around 3400-3200 cm^{-1} indicates the presence of O-H stretching vibrations. The band observed in the 1700-1600 cm^{-1} range corresponds to the C=O stretching vibrations of carboxylic acid. Another band observed in the 1600-1450 cm^{-1} range corresponds to the C=C stretching vibrations. These functional group vibrations are characteristic of activated carbon, as evidenced by the initial PRB FTIR spectrum. However, after conducting the electrokinetic (EK) experiments, these vibrations became more prominent, indicating the adsorption of PFOA in the PRB. In particular, a band around 1250-1180 cm^{-1} corresponds to the C-F stretching vibrations of the fluorinated carbon chain, while a band around 1000 cm^{-1} corresponds to the stretching vibrations of the ether group (-O-CF₂-). These bands confirm the presence of PFOA adsorbed by the PRB. The intensity and strength of these bands are higher in regions where the adsorption of PFOA is more pronounced.

BET of the PRB before and after the EK process was analyzed using the density functional theory (DFT) because, according to the literature, it has higher accuracy than Barrett-Joyner-Halenda (BJH) theory (Bardestani et al., 2019). The experimental findings revealed variations in the specific surface area of PRB before and after the EK tests. Prior to the EK test, the PRB exhibited a specific surface area of 243.06 m²/g. However, after experiment E2, the specific surface area decreased to 40.73 m²/g. In contrast, experiment E6, which spanned 3 weeks, further reduced the specific surface area to 18.927 m²/g. This decrease can be attributed to the accumulation of high levels of PFOA on the surface of the PRB following the EK test. It is noteworthy that the regenerated PRB, after the EK test, exhibited a BET result indicating a specific surface area of 52.459 m²/g. The slight increase in the BET of regenerated and reused PRB can be attributed to modifying the PRB surface during the recycling and EK treatment process.

The energy-dispersive X-ray spectroscopy (EDS) results of the PRB utilized in the EK tests are presented in **Figures 6.5c to 6.5f**. **Figure 6.5c** displays the EDS image of the PRB before undergoing EK treatment. **Figure 5d** exhibits the image of the PRB after 2 weeks of EK treatment, while **Figure 6.5e** represents the EDS image of the recycled PRB following 2 weeks of the EK process. **Figure 6.5f** illustrates the PRB after the 3-week EK experiment. Analyzing the EDS figures reveals variations in the iron content, particularly in experiment E6 (**Figure 6.5c**). This lower iron content can be attributed to the highest adsorption of PFOA onto the PRB, covering the iron surface. PRB analysis showed that 8.7 mg PFOA was adsorbed onto the iron slag PRB in experiment E6 compared to 2.118 g and 3.147 g in experiments E3 and E4 (Table 6.2). The higher PFOA adsorption in experiment E6 explains the EDS results in Figures 5e, 5f, and 5g. Compared to Figures 5e to 5g, the lower iron in Figure 5d could be due to more AC in the iron slag/AC sample. The EDS results provide visual evidence of the changes in elemental

composition resulting from the interaction between the PRB and the PFOA during the EK process.





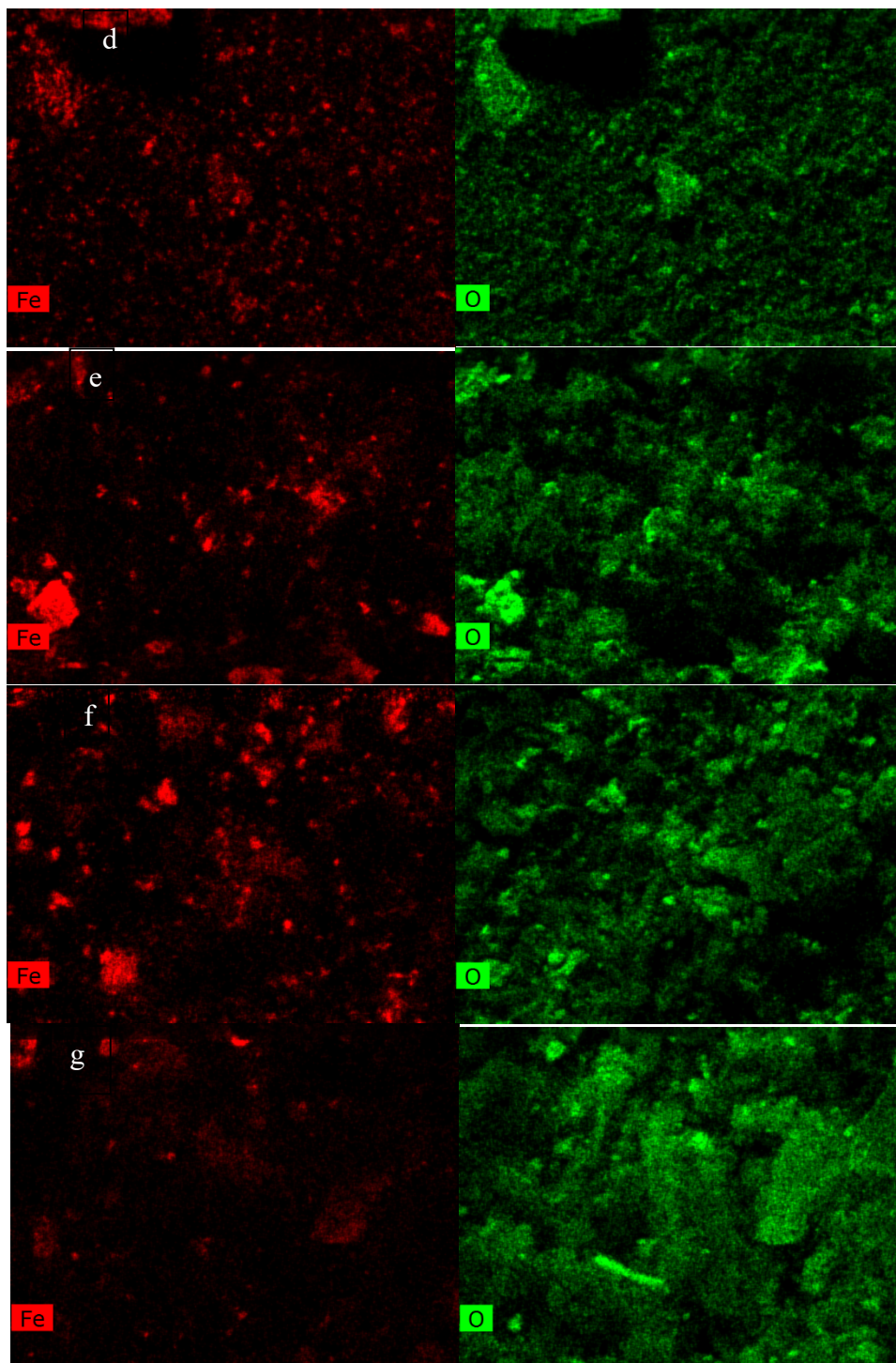


Figure 6.5: (a) Slag XRD spectrum (b) FTIR results of PRB before and after EK tests (c) Pseudo Second-order kinetic model (d) EDS results of PRB before EK tests (e) EDS results of PRB after EK test (E3) (f) EDS of PRB after E4 (g) EDS of PRB after E6.

6.3.5 Specific energy consumption

Calculating specific energy consumption is important in determining the overall energy consumption and treatment cost. The following equation calculated the SEC for all experiments using equation 3.3 (**Chapter 3**).

Figure 6.6 depicts the SEC in comparison with the overall removal rate. As can be seen, there is no direct relationship between the removal rate and energy consumption. However, the higher the average current of the EK test, the higher the SEC. Hence it is related to the energy it took to push the contaminants under an electric field. Experiment E3 had higher SEC (0.1059 kWh/kg) than E2 (0.0704 kWh/kg) due to having a higher average electric current, 10.51 mA and 13.39 mA, respectively. This result can be attributed to the slag content in the PRB. Higher slag content was more conducive. However, recycled slag PRB exhibited higher SEC (0.1214 kWh/kg), which was due to a higher average electric current (19.74 mA) which was similar to experiment E5 (19.27 mA) with SEC (0.1178 kWh/kg). The average higher current can be attributed to the lower average voltage and taking more energy to push through the contaminants across the soil medium. Increasing processing time has also increased the average current attributed to the higher SEC (0.1517 kWh/kg). However, considering the overall removal rate of 94.09% in experiment E6, the SEC is not significantly higher. The EK electroosmotic flow did not exhibit a direct correlation with the overall removal rate and the specific energy consumption of the EK process, as illustrated in Figure 6. Compared to PRB-enhanced EK tests E2 to E6, experiment E1 exhibited the lower electroosmotic flow due to low electric current (**Figure 6.2a**).

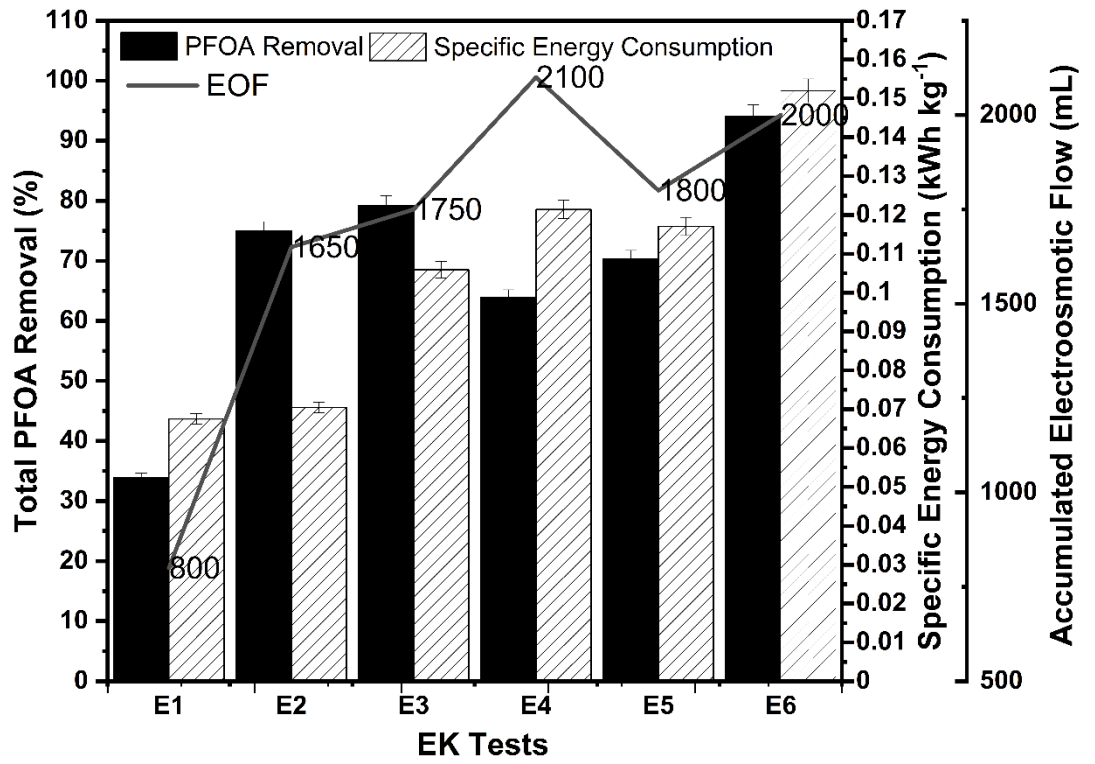


Figure 6: Specific Energy Consumption (SEC), accumulated electroosmotic flow (EOF) of all EK tests and the overall removal rate

6.4 Conclusion

This work confirms the applicability of iron slag/AC mixture as PRB in the EK process for PFOA treatment. The iron slag/AC PRB is inexpensive, available, has an excellent PFOA adsorption capacity and can be easily incorporated into the EK reactor. In the Ek process, PFOA was captured by the PRB and was easily recovered by a suitable solvent. Reusing slag in the EK process to capture PFOA from contaminated soil is an environmentally sustainable method with a promising future. Slag is typically disposed of in landfills because it is industrial waste. Slag/AC PRB enhanced EK test in conjunction with sodium cholate biosurfactant is an environmentally friendly method for PFOA removal. EK tests with 70/30 iron slag to AC PRB achieved the best PFOA removal from the kaolinite soil. After two weeks of treatment with 20mA constant current, the overall removal rate was 79%, with approximately 20% adsorbed onto PRB and the majority pushed into the catholyte overflow. However, when the experiment was extended to three weeks, the overall removal rate rose to 95%, and nearly 87% of PFOA was adsorbed onto PRB. The adsorbed PFOA was easily recovered from the PRB by methanol. The importance of biosurfactant was also assessed, and the results show that it plays an important role in the transport of PFOA towards the anode region or the PRB to be captured.

Generally, the iron slag/AC-enhanced EK process can potentially remove PFOA from real contaminated sites. The slag/AC PRB has strong adsorption to FPOA and can be extracted at the end of the EK process for PFOA extraction. The latter process will be quick due to the high iron slag permeability.

CHAPTER SEVEN

CONCLUSION AND FUTURE RESEARCH

DIRECTIONS

CHAPTER 7 : CONCLUSIONS AND FUTURE RESEARCH RECCOMENDATIONS

7.1 Conclusions

This research focused on an improved electrokinetic process for PFOA removal from the soil matrix. Initial studies concluded that the main transport mechanism of PFOA under an electric field is electromigration and electroosmosis. PFOA is an anionic compound with a carboxylic acid chain as a functional group; therefore, it is soluble in soil pore water. As a result, it can be transported by electromigration under an electric field in the EK process. However, the EK process as a single technique could not remove PFOA from kaolinite soil (as a model soil) because of the transportation mechanism it accumulated in the middle of the EK cell. Initial reference studies were consistent with previous research (Hou et al., 2022; Söregård et al., 2019). The researchers have also concluded that PFOA accumulated in the md section due to their transportation mechanism under an electric field. The overall removal rate of PFOA after 7 days of the EK test was 14-18% with an initial concentration of 100 mg/kg.

As a result of the reference tests, enhancement agents such as surfactants were added to the EK process to improve the removal rate of PFOA. Different types of surfactants were used to enhance the transportation of PFOA in the soil in the presence of an electric field. Anionic and non-ionic surfactants utilised the EK process to increase their removal efficiency. This study investigated the performance of the anionic surfactant sodium dodecyl sulphate (SDS), the non-ionic surfactant tween 80, and the biosurfactant sodium cholate (NaC). SDS and NaC improved removal efficiencies, whereas TW80 did not affect the PFOA removal rate. The NaC-enhanced EK experiment demonstrated 35% removal efficiency with an initial concentration of 100 mg/kg PFOA in one week at a constant current of 20 mA and the highest removal efficiency among all one-week

experiments. The efficiency of the EK system in removing PFOA was measured after two weeks to see if it had increased. The PFOA removal efficiency increased to 75.68% in the NaC-enhanced EK process. Extending the experimental duration from one to two weeks led to a notable improvement in the removal efficiency. The efficiency order of the EK-PRB experiments was as follows: EK-NaC (20 mA 2 WK) > EK-SDS (20 mA 2 WK) > EK-NaC (20mA 1 WK) > EK-NaC (10 mA 1WK) > EK (10 mA) > EK (20 mA) > EK-TW80. The advantages of NaC are low cost, biodegradable and environmentally sustainable. Non-ionic surfactant TW80 did not offer significant PFOA removal; the reason could be due to the low dielectric conductivity of TW80, as the electroosmotic flow is directly proportional to dielectric conductivity. In all EK tests, the centre region of the EK lab scale test had a significant PFOA content.

Lowering the initial concentration of PFOA from 100 mg/kg to 10 mg/kg, NaC enhanced EK test demonstrated removal efficiency of 39% after two weeks of the experiment. Hence, it was hypothesized that applying PRB in the surfactant-enhanced EK process would improve the overall removal rate. Activated carbon is a conventional adsorption material for the decontamination of environmental samples. It has been applied for stabilisation and solidification studies to remove PFAS in soil samples and used in adsorption studies to remove PFAS from water and wastewater. Hence, this study utilised AC and surface-modified AC as PRB in the EK system to improve the removal efficiency. Due to the accumulation of PFOA in the middle of the soil section, PRB was placed in the mid-section to capture the PFOA. In addition, PRB was put in various positions to evaluate the effect of PRB position shift in the EK cell. Based on mass balance and insignificant concentrations of intermediates in the soil section, it can be inferred that PFOA was not converted into shorter-chain PFAS but was transferred and adsorbed onto the PRB in the EK test. The transportation of PFOA and accumulation in the sections near

the anode in the AC PRB EK test and the accumulation of PFOA near the cathode region in the FeAC PRB EK test suggest the transportation mechanism in these tests was different. In AC PRB, enhanced EK PFOA migrated towards the anode by electromigration and electroosmosis transported to the cathode. FeAC EK tests hypothesized that PFOA formed a complex with Fe resulting in their transportation towards the cathode region. FeAC PRB enhanced EK test in which PRB was placed in the middle of the EK cell resulted in 59% overall PFOA removal, whereas AC PRB enhanced EK test resulted in 54% removal. However, when PRBs were regenerated, AC PRB resulted in 40% removal, whereas FeAC regenerated PRB EK test resulted in a 24% removal rate. The low FeAC removal rate indicates Fe loss during the EK test and regeneration process, which alters the surface characteristics and causes a significant change in the FeAC removal rate. More work should be performed on PRBs with high absorption capacities to PFOA in the soil.

Steel-making slag is an industrial waste, with the benefit of reusing the industrial waste in environmental clean-up. The experimental results have demonstrated great outcomes where after 3 weeks of EK test Slag/AC PRB enhanced EK test resulted in an overall 95% removal rate. However, after 2 weeks of testing, the results decreased to 79%. The results have shown that it can be recycled and reused for at least one cycle. After the regeneration and reuse of spent PRB, the removal rate dropped by around 10%. Changing the slag-to-AC ratio has also been investigated, and the results were insignificant. After 3 weeks of EK tests, PRB adsorption was 87%, which was the highest adsorption of PFOA onto PRB. The overall removal rate was recorded as the highest at 94.05%, with negligible residual PFOA concentration in the soil sections. It is hypothesized that the adsorption mechanism of PFOA onto PRB is by electrostatic and hydrophobic interactions.

7.2 The importance of the research and its impact on the field

The preliminary stage of this research encompassed the assessment of various surfactants to enhance the EK process aimed at removing PFOA from contaminated kaolin soil. Subsequently, normal and surface-modified activated carbon were assessed for their suitability in the EK process as PRBs. Activated carbon is widely recognized for its exceptional sorption affinity towards PFOA and has been extensively employed as an adsorbent in water treatment studies. Consequently, activated carbon was selected as the PRB to capture mobile PFOA within the EK cell effectively. In addition, iron-coated activated carbon was investigated. This particular form of activated carbon exhibits a significantly enhanced surface area and has successfully removed heavy metals and persistent organic pollutants in various previous applications. It is worth noting that PFOA possesses a great adsorption capacity towards AC.

Incorporating slag-mixed activated carbon as an enhancer in the EK process for PFOA removal has not been previously investigated. This study aimed to assess the efficacy of a slag/AC PRB in conjunction with the EK process, focusing on its impact on removal efficiency. Results revealed that the slag/AC PRB-enhanced EK system exhibited the highest overall removal efficiency, achieving an impressive rate of 94.05%. The PRB component demonstrated the ability to capture 87% of the PFOA, while the remaining fraction was transported to the catholyte. Notably, the EK process effectively reduced the residual PFOA concentration in the soil to negligible levels. Consequently, this study advances effective and sustainable approaches for employing enhancement agents in EK remediation of PFOA-contaminated soil.

Moreover, the proposed method holds promise for in situ application and scalability. In situ, EK remediation offers distinct advantages, including eliminating soil excavation and transportation requirements. Furthermore, using green energy sources can enhance cost-

effectiveness, and using environmentally friendly enhancers helps mitigate potential secondary contaminations.

7.3 Future studies

Drawing from the experimental findings in this study, the subsequent suggestions are put forward for future research:

- **Real soil testing:** Further investigations should conduct tests of the NaC-enhanced EK process on actual soil samples, such as soil contaminated with aqueous film-forming foam (AFFF), to assess the performance and efficacy of the technique under realistic conditions.
- **A pilot-scale study** is recommended to evaluate the effectiveness of the biosurfactant-enhanced electrokinetic (EK) process coupled with a slag/AC permeable reactive barrier (PRB) using actual contaminated soil, such as those found at defence sites or airport sites. This pilot-scale investigation will provide valuable insights into the practical application and performance of the proposed remediation approach under real-world conditions. The pilot-scale study should include comprehensive monitoring and analysis of key parameters, such as PFOA removal efficiency, concentration profiles, changes in soil properties, and potential leaching of contaminants. The system's effectiveness can be evaluated by comparing the results obtained from the pilot-scale study with the laboratory-scale findings.
- **Diverse PFAS evaluation:** The enhanced EK process should be tested with various per- and PFAS, including Perfluorooctane sulfonate (PFOS) and shorter-chain PFAS. Assessing the technique's effectiveness on different PFAS compounds can provide a broader understanding of its applicability.

- Lower initial concentration testing: Future research should investigate the performance of the enhanced EK process at lower initial concentrations of PFAS to determine the efficiency and effectiveness of the technique in treating the soil with lower contamination levels.
- Defluorination and PFOA degradation studies: It is recommended to include defluorination and PFOA degradation studies in future tests. Evaluating PFOA's defluorination potential and degradation pathways during the enhanced EK process can provide insights into the fate and transformation of PFAS in soil.
- Real soil testing with slag/AC PRB: Considering that the slag/AC PRB exhibited the highest removal rate, further research should apply this PRB configuration to real soil samples contaminated with a wider range of PFAS compounds. Assessing its performance in different soil contexts can help determine its efficacy and suitability for practical applications.
- Assessment of PFAS intermediates: Future investigations should focus on evaluating PFAS intermediates formed during the enhanced EK process in different soil sections. Understanding the formation and behaviour of these intermediates can contribute to a more comprehensive understanding of PFAS degradation pathways and potential by-products.
- Cost-effectiveness analysis: Conducting cost-effectiveness analyses of different EK configurations, surfactants, and PRB designs can help assess the economic feasibility and viability of the remediation approach. Evaluating the overall costs and benefits can guide decision-making in real-world applications.
- Long-term performance assessment: Future studies should investigate the long-term performance and stability of the EK process for PFOA removal. Assessing the process's effectiveness over extended durations and under various

environmental conditions can provide valuable insights into its practical applicability.

- Environmental fate and risk assessment: It is essential to conduct comprehensive assessments of the environmental fate and potential risks associated with PFOA and its degradation by-products during the EK process. Evaluating their fate, transport, and potential impacts on soil and groundwater can inform risk management strategies.

REFERENCES

- Abdel-Shafy, H. I., & Mansour, M. S. M. (2016). A review on polycyclic aromatic hydrocarbons: Source, environmental impact, effect on human health and remediation. *Egyptian Journal of Petroleum*, 25(1), 107-123. <https://doi.org/https://doi.org/10.1016/j.ejpe.2015.03.011>
- Acar, Y. B., & Alshawabkeh, A. N. (1993). Principles of electrokinetic remediation. *Environmental Science & Technology*, 27(13), 2638-2647. <https://doi.org/10.1021/es00049a002>
- Ahmed, M. B., Johir, M. A. H., McLaughlan, R., Nguyen, L. N., Xu, B., & Nghiem, L. D. (2020). Per- and polyfluoroalkyl substances in soil and sediments: Occurrence, fate, remediation and future outlook. *Science of The Total Environment*, 748, 141251-141251. <https://doi.org/10.1016/j.scitotenv.2020.141251>
- Ahn, S.-K., Park, K.-Y., Song, W.-j., Park, Y.-m., & Kweon, J.-H. (2022). Adsorption mechanisms on perfluorooctanoic acid by FeCl₃ modified granular activated carbon in aqueous solutions. *Chemosphere*, 303, 134965. <https://doi.org/https://doi.org/10.1016/j.chemosphere.2022.134965>
- Alcántara, M. T., Gómez, J., Pazos, M., & Sanromán, M. A. (2008). Combined treatment of PAHs contaminated soils using the sequence extraction with surfactant–electrochemical degradation. *Chemosphere*, 70(8), 1438-1444. <https://doi.org/https://doi.org/10.1016/j.chemosphere.2007.08.070>
- Alcántara, M. T., Gómez, J., Pazos, M., & Sanromán, M. A. (2010). Electrokinetic remediation of PAH mixtures from kaolin. *Journal of Hazardous Materials*, 179(1), 1156-1160. <https://doi.org/https://doi.org/10.1016/j.jhazmat.2010.03.010>
- Alshawabkeh, A. N. (2009). Electrokinetic Soil Remediation: Challenges and Opportunities. *Separation Science and Technology*, 44(10), 2171-2187. <https://doi.org/10.1080/01496390902976681>
- Altaee, A., Smith, R., & Mikhalovsky, S. (2008). The feasibility of decontamination of reduced saline sediments from copper using the electrokinetic process. *Journal of Environmental Management*, 88(4), 1611-1618. <https://doi.org/https://doi.org/10.1016/j.jenvman.2007.08.008>
- Altarawneh, M., Almatarneh, M. H., & Dlugogorski, B. Z. (2022). Thermal decomposition of perfluorinated carboxylic acids: Kinetic model and theoretical requirements for PFAS incineration. *Chemosphere*, 286, 131685. <https://doi.org/https://doi.org/10.1016/j.chemosphere.2021.131685>
- Anawar, H. M., Akter, F., Solaiman, Z. M., & Strezov, V. (2015). Biochar: an emerging panacea for remediation of soil contaminants from mining, industry and sewage wastes. *Pedosphere*, 25(5), 654-665.
- Andrade, D. C., & dos Santos, E. V. (2020). Combination of electrokinetic remediation with permeable reactive barriers to remove organic compounds from soils. *Current Opinion in Electrochemistry*, 22, 136-144. <https://doi.org/https://doi.org/10.1016/j.coelec.2020.06.002>
- Angelstam, P. K. (1998). Maintaining and restoring biodiversity in European boreal forests by developing natural disturbance regimes. *Journal of vegetation science*, 9(4), 593-602.
- Ballesteros, S., Rincón, J. M., Rincón-Mora, B., & Jordán, M. M. (2017). Vitrification of urban soil contamination by hexavalent chromium. *Journal of Geochemical Exploration*, 174, 132-139. <https://doi.org/https://doi.org/10.1016/j.gexplo.2016.07.011>
- Bamforth, S. M., & Singleton, I. (2005). Bioremediation of polycyclic aromatic hydrocarbons: current knowledge and future directions. 80(7), 723-736. <https://doi.org/10.1002/jctb.1276>
- Bardestani, R., Patience, G. S., & Kaliaguine, S. (2019). Experimental methods in chemical engineering: specific surface area and pore size distribution measurements—BET, BJH,

- and DFT. *The Canadian Journal of Chemical Engineering*, 97(11), 2781-2791.
<https://doi.org/https://doi.org/10.1002/cjce.23632>
- Barth, E., McKernan, J., Bless, D., & Dasu, K. (2021). Investigation of an immobilization process for PFAS contaminated soils. *Journal of Environmental Management*, 296, 113069-113069. <https://doi.org/10.1016/J.JENVMAN.2021.113069>
- Bautista-Baños, S., Romanazzi, G., & Jiménez-Aparicio, A. (2016). Preface. In S. Bautista-Baños, G. Romanazzi, & A. Jiménez-Aparicio (Eds.), *Chitosan in the Preservation of Agricultural Commodities* (pp. xv-xvii). Academic Press.
<https://doi.org/https://doi.org/10.1016/B978-0-12-802735-6.00018-5>
- Bolan, N., Sarkar, B., Yan, Y., Li, Q., Wijesekara, H., Kannan, K., Tsang, D. C. W., Schauerte, M., Bosch, J., Noll, H., Ok, Y. S., Scheckel, K., Kumpiene, J., Gobindlal, K., Kah, M., Sperry, J., Kirkham, M. B., Wang, H., Tsang, Y. F., Hou, D., & Rinklebe, J. (2021a). Remediation of poly- and perfluoroalkyl substances (PFAS) contaminated soils – To mobilize or to immobilize or to degrade? *Journal of Hazardous Materials*, 401, 123892.
<https://doi.org/https://doi.org/10.1016/j.jhazmat.2020.123892>
- Bolan, N., Sarkar, B., Yan, Y., Li, Q., Wijesekara, H., Kannan, K., Tsang, D. C. W., Schauerte, M., Bosch, J., Noll, H., Ok, Y. S., Scheckel, K., Kumpiene, J., Gobindlal, K., Kah, M., Sperry, J., Kirkham, M. B., Wang, H., Tsang, Y. F., Hou, D., & Rinklebe, J. (2021b). Remediation of poly- and perfluoroalkyl substances (PFAS) contaminated soils – To mobilize or to immobilize or to degrade? *Journal of Hazardous Materials*, 401, 123892-123892.
<https://doi.org/10.1016/j.jhazmat.2020.123892>
- Boulakradeche, M. O., Akretche, D. E., Cameselle, C., & Hamidi, N. (2015). Enhanced Electrokinetic Remediation of Hydrophobic Organics contaminated Soils by the Combinations of Non-Ionic and Ionic Surfactants. *Electrochimica Acta*, 174, 1057-1066.
<https://doi.org/10.1016/j.electacta.2015.06.091>
- Bradl, H. B. (2005). Sources and origins of heavy metals. In (Vol. 6, pp. 1-27). Elsevier.
- Braud, A., Hannauer, M., Mislin, G. L. A., & Schalk, I. J. (2009). The Pseudomonas aeruginosa pyochelin-iron uptake pathway and its metal specificity. *Journal of bacteriology*, 191(11), 3517-3525.
- Brusseau, M. L., Anderson, R. H., & Guo, B. (2020). PFAS concentrations in soils: Background levels versus contaminated sites. *Science of The Total Environment*, 740, 140017-140017. <https://doi.org/10.1016/J.SCITOTENV.2020.140017>
- Cameselle, C. (2015). Enhancement Of Electro-Osmotic Flow During The Electrokinetic Treatment Of A Contaminated Soil. *Electrochimica Acta*, 181, 31-38.
<https://doi.org/https://doi.org/10.1016/j.electacta.2015.02.191>
- Cameselle, C., & Gouveia, S. (2018). Electrokinetic remediation for the removal of organic contaminants in soils. *Current Opinion in Electrochemistry*, 11, 41-47.
<https://doi.org/10.1016/j.coelec.2018.07.005>
- Cameselle, C., & Reddy, K. R. (2012). Development and enhancement of electro-osmotic flow for the removal of contaminants from soils. *Electrochimica Acta*, 86, 10-22.
<https://doi.org/10.1016/j.electacta.2012.06.121>
- Celary, P., & Sobik-Szołtysek, J. (2014). Vitrification as an alternative to landfilling of tannery sewage sludge. *Waste Management*, 34(12), 2520-2527.
<https://doi.org/https://doi.org/10.1016/j.wasman.2014.08.022>
- Chen, M., Xu, P., Zeng, G., Yang, C., Huang, D., & Zhang, J. (2015). Bioremediation of soils contaminated with polycyclic aromatic hydrocarbons, petroleum, pesticides, chlorophenols and heavy metals by composting: applications, microbes and future research needs. *Biotechnology advances*, 33(6), 745-755.
- Chen, R., Zhou, L., Wang, W., Cui, D., Hao, D., & Guo, J. (2022). Enhanced Electrokinetic Remediation of Copper-Contaminated Soil by Combining Steel Slag and a Permeable Reactive Barrier. *Applied Sciences*, 12(16).

- Chen, W., Parette, R., Zou, J., Cannon, F. S., & Dempsey, B. A. (2007). Arsenic removal by iron-modified activated carbon. *Water Research*, 41(9), 1851-1858. <https://doi.org/https://doi.org/10.1016/j.watres.2007.01.052>
- Cheng, M., Zeng, G., Huang, D., Yang, C., Lai, C., Zhang, C., & Liu, Y. (2017). Advantages and challenges of Tween 80 surfactant-enhanced technologies for the remediation of soils contaminated with hydrophobic organic compounds. *Chemical Engineering Journal*, 314, 98-113. <https://doi.org/10.1016/j.cej.2016.12.135>
- Coggan, T. L., Moodie, D., Kolobaric, A., Szabo, D., Shimeta, J., Crosbie, N. D., Lee, E., Fernandes, M., & Clarke, B. O. (2019). An investigation into per- and polyfluoroalkyl substances (PFAS) in nineteen Australian wastewater treatment plants (WWTPs). *Heliyon*, 5(8), e02316-e02316. <https://doi.org/10.1016/j.heliyon.2019.e02316>
- Colacicco, A., De Gioannis, G., Muntoni, A., Pettinao, E., Polettini, A., & Pomi, R. (2010). Enhanced electrokinetic treatment of marine sediments contaminated by heavy metals and PAHs. *Chemosphere*, 81(1), 46-56. <https://doi.org/https://doi.org/10.1016/j.chemosphere.2010.07.004>
- Cordner, A., De La Rosa, V. Y., Schaidler, L. A., Rudel, R. A., Richter, L., & Brown, P. (2019). Guideline levels for PFOA and PFOS in drinking water: the role of scientific uncertainty, risk assessment decisions, and social factors. *Journal of Exposure Science and Environmental Epidemiology*, 29(2), 157-171. <https://doi.org/10.1038/s41370-018-0099-9>
- Crownover, E., Oberle, D., Kluger, M., & Heron, G. (2019). Perfluoroalkyl and polyfluoroalkyl substances thermal desorption evaluation. *Remediation*, 29(4), 77-81. <https://doi.org/10.1002/rem.21623>
- Deng, S., Nie, Y., Du, Z., Huang, Q., Meng, P., Wang, B., Huang, J., & Yu, G. (2015). Enhanced adsorption of perfluorooctane sulfonate and perfluorooctanoate by bamboo-derived granular activated carbon. *Journal of Hazardous Materials*, 282, 150-157. <https://doi.org/10.1016/j.jhazmat.2014.03.045>
- Dermont, G., Bergeron, M., Mercier, G., & Richer-Lafleche, M. (2008). Soil washing for metal removal: a review of physical/chemical technologies and field applications. *Journal of Hazardous Materials*, 152(1), 1-31.
- Díaz-Piloneta, M., Ortega-Fernández, F., Terrados-Cristos, M., & Álvarez-Cabal, J. V. (2022). Application of Steel Slag for Degraded Land Remediation. *Land*, 11(2).
- Dong, L., Witkowski, C. M., Craig, M. M., Greenwade, M. M., & Joseph, K. L. (2009). Cytotoxicity effects of different surfactant molecules conjugated to carbon nanotubes on human astrocytoma cells. *Nanoscale research letters*, 4(12), 1517-1523. <https://doi.org/10.1007/s11671-009-9429-0>
- Du, Z., Deng, S., Bei, Y., Huang, Q., Wang, B., Huang, J., & Yu, G. (2014). Adsorption behavior and mechanism of perfluorinated compounds on various adsorbents—a review. *J Hazard Mater*, 274, 443-454. <https://doi.org/10.1016/j.jhazmat.2014.04.038>
- 10.1016/j.jhazmat.2014.04.038. Epub 2014 Apr 25.
- Du, Z., Deng, S., Bei, Y., Huang, Q., Wang, B., Huang, J., & Yu, G. (2014). Adsorption behavior and mechanism of perfluorinated compounds on various adsorbents—A review. *Journal of Hazardous Materials*, 274, 443-454. <https://doi.org/https://doi.org/10.1016/j.jhazmat.2014.04.038>
- ECHA. (2022). *Proposal for a restriction* https://echa.europa.eu/view-article/-/journal_content/title/9109026-217#scientific-committees-take-more-time-to-conclude-on-restricting-pfass-in-firefighting-foams
- Environment, D. o. (2021). *Canada Gazette, Part I, Volume 155, Number 17: GOVERNMENT NOTICES* <https://canadagazette.gc.ca/rp-pr/p1/2021/2021-04-24/html/notice-avis-eng.html#n15>

- Epa Au, N. Z. (2019). *PFAS National Environmental Management Plan VERSION 2.0 CONSULTATION DRAFT*. <https://www.epa.vic.gov.au/your-environment/land-and-groundwater/pfas-in-victoria/pfas-nemp-2-0>
- European, C. (2020a). Poly- and perfluoroalkyl substances (PFAS): Chemicals Strategy for Sustainability Towards a Toxic-Free Environment. *Commission Staff Working Document*, 1-22. <https://www.oecd.org/chemicalsafety/portal-perfluorinated-chemicals/aboutpfass/Figure1-classification-of-per-and->
- European, C. (2020b). Regulation (EU) 2019/1021 of the European Parliament and of the Council of 20 June 2019 on Persistent Organic Pollutants. PFOA has been listed in Annex I of the POPs Regulation with Regulation (EU) 2020/784. (793), 1-5.
- Falciglia, P. P., Giustra, M. G., & Vagliasindi, F. G. A. (2011). Low-temperature thermal desorption of diesel polluted soil: Influence of temperature and soil texture on contaminant removal kinetics. *Journal of Hazardous Materials*, 185(1), 392-400. <https://doi.org/https://doi.org/10.1016/j.jhazmat.2010.09.046>
- Fardin, A. B., Jamshidi-Zanjani, A., & Darban, A. K. (2021). Application of enhanced electrokinetic remediation by coupling surfactants for kerosene-contaminated soils: Effect of ionic and nonionic surfactants. *Journal of Environmental Management*, 277, 111422-111422. <https://doi.org/10.1016/J.JENVMAN.2020.111422>
- Figuerola, A., Cameselle, C., Gouveia, S., & Hansen, H. K. (2016). Electrokinetic treatment of an agricultural soil contaminated with heavy metals. *Journal of environmental science and health. Part A, Toxic/hazardous substances & environmental engineering*, 51(9), 691-700. <https://doi.org/10.1080/10934529.2016.1170425>
- Ganbat, N., Altaee, A., Zhou, J. L., Lockwood, T., Al-Juboori, R. A., Hamdi, F. M., Karbassiyazdi, E., Samal, A. K., Hawari, A., & Khabbaz, H. (2022). Investigation of the effect of surfactant on the electrokinetic treatment of PFOA contaminated soil. *Environmental Technology & Innovation*, 102938. <https://doi.org/https://doi.org/10.1016/j.eti.2022.102938>
- Gao, X., & Chorover, J. (2012). Adsorption of perfluorooctanoic acid and perfluorooctanesulfonic acid to iron oxide surfaces as studied by flow-through ATR-FTIR spectroscopy. *Environmental Chemistry*, 9(2), 148-157. <https://doi.org/https://doi.org/10.1071/EN11119>
- Ghobadi, R., Altaee, A., Zhou, J. L., Karbassiyazdi, E., & Ganbat, N. (2021). Effective remediation of heavy metals in contaminated soil by electrokinetic technology incorporating reactive filter media. *Science of The Total Environment*, 794, 148668-148668. <https://doi.org/10.1016/j.scitotenv.2021.148668>
- Ghobadi, R., Altaee, A., Zhou, J. L., McLean, P., Ganbat, N., & Li, D. (2020a). Enhanced copper removal from contaminated kaolinite soil by electrokinetic process using compost reactive filter media. *Journal of Hazardous Materials*, 402, 123891.
- Ghobadi, R., Altaee, A., Zhou, J. L., McLean, P., Ganbat, N., & Li, D. (2020b). Enhanced copper removal from contaminated kaolinite soil by electrokinetic process using compost reactive filter media. *Journal of Hazardous Materials*, 402, 123891-123891.
- Ghobadi, R., Altaee, A., Zhou, J. L., McLean, P., & Yadav, S. (2020a). Copper removal from contaminated soil through electrokinetic process with reactive filter media. *Chemosphere*, 126607-126607.
- [Record #476 is using a reference type undefined in this output style.]
- Giannis, A., Gidaracos, E., & Skouta, A. (2007). Application of sodium dodecyl sulfate and humic acid as surfactants on electrokinetic remediation of cadmium-contaminated soil. *Desalination*, 211(1-3), 249-260. <https://doi.org/10.1016/j.desal.2006.02.097>
- Giri, A. K. (2012). *Removal of arsenic (III) and chromium (VI) from the water using phytoremediation and bioremediation techniques*
- Gobelius, L., Lewis, J., & Ahrens, L. (2017). Plant Uptake of Per- and Polyfluoroalkyl Substances at a Contaminated Fire Training Facility to Evaluate the Phytoremediation Potential of

- Various Plant Species. *Environmental Science and Technology*, 51(21), 12602-12610. <https://doi.org/10.1021/acs.est.7b02926>
- Gong, Z., Alef, K., Wilke, B.-M., & Li, P. (2007). Activated carbon adsorption of PAHs from vegetable oil used in soil remediation. *Journal of Hazardous Materials*, 143(1), 372-378. <https://doi.org/https://doi.org/10.1016/j.jhazmat.2006.09.037>
- Grimison, C., Knight, E. R., Nguyen, T. M. H., Nagle, N., Kabiri, S., Bräunig, J., Navarro, D. A., Kookana, R. S., Higgins, C. P., McLaughlin, M. J., & Mueller, J. F. (2023). The efficacy of soil washing for the remediation of per- and poly-fluoroalkyl substances (PFASs) in the field. *Journal of Hazardous Materials*, 445, 130441. <https://doi.org/https://doi.org/10.1016/j.jhazmat.2022.130441>
- Groffen, T., Rijnders, J., Verbrigghe, N., Verbruggen, E., Prinsen, E., Eens, M., & Bervoets, L. (2019). Influence of soil physicochemical properties on the depth profiles of perfluoroalkylated acids (PFAAs) in soil along a distance gradient from a fluorochemical plant and associations with soil microbial parameters. *Chemosphere*, 236, 124407-124407. <https://doi.org/10.1016/J.CHEMOSPHERE.2019.124407>
- Guedes, P., Lopes, V., Couto, N., Mateus, E. P., Pereira, C. S., & Ribeiro, A. B. (2019). Electrokinetic remediation of contaminants of emergent concern in clay soil: Effect of operating parameters. *Environmental Pollution*, 253, 625-635. <https://doi.org/10.1016/j.envpol.2019.07.040>
- Hahladakis, J. N., Latsos, A., & Gidaracos, E. (2016). Performance of electroremediation in real contaminated sediments using a big cell, periodic voltage and innovative surfactants. *Journal of Hazardous Materials*, 320, 376-385. <https://doi.org/https://doi.org/10.1016/j.jhazmat.2016.08.003>
- Han, J.-G., Hong, K.-K., Kim, Y.-W., & Lee, J.-Y. (2010). Enhanced electrokinetic (E/K) remediation on copper contaminated soil by CFW (carbonized foods waste). *Journal of Hazardous Materials*, 177(1), 530-538. <https://doi.org/https://doi.org/10.1016/j.jhazmat.2009.12.065>
- Hansen, H. K., Ottosen, L. M., & Ribeiro, A. B. (2016). Electrokinetic Soil Remediation: An Overview. In A. B. Ribeiro, E. P. Mateus, & N. Couto (Eds.), *Electrokinetics Across Disciplines and Continents: New Strategies for Sustainable Development* (pp. 3-18). Springer International Publishing. https://doi.org/10.1007/978-3-319-20179-5_1
- Hassan, M., Liu, Y., Naidu, R., Du, J., & Qi, F. (2020). Adsorption of Perfluorooctane sulfonate (PFOS) onto metal oxides modified biochar. *Environmental Technology and Innovation*, 19, 100816-100816. <https://doi.org/10.1016/j.eti.2020.100816>
- Herlem, G., Picaud, F., Girardet, C., & Micheau, O. (2019). Chapter 16 - Carbon Nanotubes: Synthesis, Characterization, and Applications in Drug-Delivery Systems. In S. S. Mohapatra, S. Ranjan, N. Dasgupta, R. K. Mishra, & S. Thomas (Eds.), (pp. 469-529). Elsevier. <https://doi.org/https://doi.org/10.1016/B978-0-12-814033-8.00016-3>
- Høisæter, Å., Arp, H. P. H., Slinde, G., Knutsen, H., Hale, S. E., Breedveld, G. D., & Hansen, M. C. (2021). Excavated vs novel in situ soil washing as a remediation strategy for sandy soils impacted with per- and polyfluoroalkyl substances from aqueous film forming foams. *Science of The Total Environment*, 794, 148763. <https://doi.org/https://doi.org/10.1016/j.scitotenv.2021.148763>
- Hou, J., Li, G., Liu, M., Chen, L., Yao, Y., Fallgren, P. H., & Jin, S. (2022). Electrochemical destruction and mobilization of perfluorooctanoic acid (PFOA) and perfluorooctane sulfonate (PFOS) in saturated soil. *Chemosphere*, 287(P3), 132205-132205. <https://doi.org/10.1016/j.chemosphere.2021.132205>
- HSPH. (2020, 15/08/2022). PFAS exposure linked with worse COVID-19 outcomes. <https://www.hsph.harvard.edu/news/hsph-in-the-news/pfas-exposure-linked-with-worse-covid-19->

[outcomes/#:~:text=People%20who%20had%20elevated%20blood%20levels%20of%20a,by%20Harvard%20T.H.%20Chan%20School%20of%20Public%20Health.](#)

- Huang, S., & Jaffé, P. R. (2019). Defluorination of Perfluorooctanoic Acid (PFOA) and Perfluorooctane Sulfonate (PFOS) by Acidimicrobium sp. Strain A6 [Article]. *Environmental Science and Technology*. <https://doi.org/10.1021/acs.est.9b04047>
- [Record #95 is using a reference type undefined in this output style.]
- Jain, M., Yadav, M., Kohout, T., Lahtinen, M., Garg, V. K., & Sillanpää, M. (2018). Development of iron oxide/activated carbon nanoparticle composite for the removal of Cr(VI), Cu(II) and Cd(II) ions from aqueous solution. *Water Resources and Industry*, 20(March), 54-74. <https://doi.org/10.1016/j.wri.2018.10.001>
- Jiang, D., Zeng, G., Huang, D., Chen, M., Zhang, C., Huang, C., & Wan, J. (2018). Remediation of contaminated soils by enhanced nanoscale zero valent iron. *Environmental Research*, 163, 217-227. <https://doi.org/https://doi.org/10.1016/j.envres.2018.01.030>
- Jin, T., Peydayesh, M., & Mezzenga, R. (2021). Membrane-based technologies for per- and polyfluoroalkyl substances (PFASs) removal from water: Removal mechanisms, applications, challenges and perspectives. *Environment International*, 157, 106876. <https://doi.org/https://doi.org/10.1016/j.envint.2021.106876>
- Johnson, D. B., Okibe, N., Wakeman, K., & Yajie, L. (2008). Effect of temperature on the bioleaching of chalcopyrite concentrates containing different concentrations of silver. *Hydrometallurgy*, 94(1-4), 42-47.
- Johnson, R. L., Anschutz, A. J., Smolen, J. M., Simcik, M. F., & Penn, R. L. (2007). The Adsorption of Perfluorooctane Sulfonate onto Sand, Clay, and Iron Oxide Surfaces. *Journal of Chemical & Engineering Data*, 52(4), 1165-1170. <https://doi.org/10.1021/je060285g>
- Kabiri, S., Centner, M., & McLaughlin, M. J. (2021). Durability of sorption of per- and polyfluorinated alkyl substances in soils immobilised using common adsorbents: 1. Effects of perturbations in pH. *Science of The Total Environment*, 766, 144857-144857. <https://doi.org/10.1016/j.scitotenv.2020.144857>
- Khalid, S., Shahid, M., Niazi, N. K., Murtaza, B., Bibi, I., & Dumat, C. (2017). A comparison of technologies for remediation of heavy metal contaminated soils. *Journal of Geochemical Exploration*, 182, 247-268.
- Kim, H.-C., Lee, C.-G., Park, J.-A., & Kim, S.-B. (2010). Arsenic removal from water using iron-impregnated granular activated carbon in the presence of bacteria. *Journal of Environmental Science and Health, Part A*, 45(2), 177-182. <https://doi.org/10.1080/10934520903429832>
- Kim, H. C., Lee, C. G., Park, J. A., & Kim, S. B. (2010). Arsenic removal from water using iron-impregnated granular activated carbon in the presence of bacteria. *Journal of Environmental Science and Health - Part A Toxic/Hazardous Substances and Environmental Engineering*, 45(2), 177-182. <https://doi.org/10.1080/10934520903429832>
- Ko, S.-O., Schlautman, M. A., & Carraway, E. R. (2000). Cyclodextrin-Enhanced Electrokinetic Removal of Phenanthrene from a Model Clay Soil. *Environmental Science & Technology*, 34(8), 1535-1541. <https://doi.org/10.1021/es990223t>
- Koul, B., & Taak, P. (2018). In Situ Soil Remediation Strategies. In B. Koul & P. Taak (Eds.), (pp. 59-75). Springer Singapore. https://doi.org/10.1007/978-981-13-2420-8_3
- Kumar, R., Dada, T. K., Whelan, A., Cannon, P., Sheehan, M., Reeves, L., & Antunes, E. (2023). Microbial and thermal treatment techniques for degradation of PFAS in biosolids: A focus on degradation mechanisms and pathways. *Journal of Hazardous Materials*, 452, 131212. <https://doi.org/https://doi.org/10.1016/j.jhazmat.2023.131212>
- Kuppusamy, S., Thavamani, P., Venkateswarlu, K., Lee, Y. B., Naidu, R., & Megharaj, M. (2017). Remediation approaches for polycyclic aromatic hydrocarbons (PAHs) contaminated

- soils: Technological constraints, emerging trends and future directions. *Chemosphere*, 168, 944-968. <https://doi.org/10.1016/j.chemosphere.2016.10.115>
- Kwon, B. G., Lim, H. J., Na, S. H., Choi, B. I., Shin, D. S., & Chung, S. Y. (2014). Biodegradation of perfluorooctanesulfonate (PFOS) as an emerging contaminant [Article]. *Chemosphere*, 109, 221-225. <https://doi.org/10.1016/j.chemosphere.2014.01.072>
- Lakshmanan, V. I., Roy, R., & Gorain, B. (2019). Recycling of Gold and Silver. In (pp. 175-198). Springer.
- Lal, K. (2019). Potential Pollutants in Soil System: Impacts and Remediation. In (pp. 407-422). Springer.
- Lee, Y. C., Li, Y. f., Chen, M. J., Chen, Y. C., Kuo, J., & Lo, S. L. (2020). Efficient decomposition of perfluorooctanic acid by persulfate with iron-modified activated carbon. *Water Research*, 174. <https://doi.org/10.1016/j.watres.2020.115618>
- Lei, Y.-J., Tian, Y., Sobhani, Z., Naidu, R., & Fang, C. (2020). Synergistic degradation of PFAS in water and soil by dual-frequency ultrasonic activated persulfate. *Chemical Engineering Journal*, 388, 124215. <https://doi.org/10.1016/j.cej.2020.124215>
- Lenka, S. P., Kah, M., & Padhye, L. P. (2021). A review of the occurrence, transformation, and removal of poly- and perfluoroalkyl substances (PFAS) in wastewater treatment plants. *Water Research*, 199, 117187-117187. <https://doi.org/10.1016/j.watres.2021.117187>
- Li, J., Li, X., Da, Y., Yu, J., Long, B., Zhang, P., Bakker, C., McCarl, B. A., Yuan, J. S., & Dai, S. Y. (2022). Sustainable environmental remediation via biomimetic multifunctional lignocellulosic nano-framework. *Nature communications*, 13(1), 4368. <https://doi.org/10.1038/s41467-022-31881-5>
- Li, Y., Bräunig, J., Angelica, G. C., Thai, P. K., Mueller, J. F., & Yuan, Z. (2021). Formation and partitioning behaviour of perfluoroalkyl acids (PFAAs) in waste activated sludge during anaerobic digestion. *Water Research*, 189, 116583. <https://doi.org/10.1016/j.watres.2020.116583>
- Li, Z., Yuan, S., Wan, J., Long, H., & Tong, M. (2011). A combination of electrokinetics and Pd/Fe PRB for the remediation of pentachlorophenol-contaminated soil. *Journal of Contaminant Hydrology*, 124(1), 99-107. <https://doi.org/10.1016/j.jconhyd.2011.03.002>
- Limmer, M., & Burken, J. (2016). Phytovolatilization of Organic Contaminants. <https://doi.org/10.1021/acs.est.5b04113>
- Liu, C. J., Werner, D., & Bellona, C. (2019). Removal of per- And polyfluoroalkyl substances (PFASs) from contaminated groundwater using granular activated carbon: A pilot-scale study with breakthrough modeling. *Environmental Science: Water Research and Technology*, 5(11), 1844-1853. <https://doi.org/10.1039/c9ew00349e>
- Liu, D., Xiu, Z., Liu, F., Wu, G., Adamson, D., Newell, C., Vikesland, P., Tsai, A.-L., & Alvarez, P. J. (2013). Perfluorooctanoic acid degradation in the presence of Fe(III) under natural sunlight. *Journal of Hazardous Materials*, 262, 456-463. <https://doi.org/10.1016/j.jhazmat.2013.09.001>
- Liu, H., Xu, Q., Yan, C., & Qiao, Y. (2011). Corrosion behavior of a positive graphite electrode in vanadium redox flow battery [Article]. *Electrochimica Acta*, 56(24), 8783-8790. <https://doi.org/10.1016/j.electacta.2011.07.083>
- Liu, L., Li, W., Song, W., & Guo, M. (2018). Remediation techniques for heavy metal-contaminated soils: Principles and applicability. *Science of The Total Environment*, 633, 206-219. <https://doi.org/10.1016/j.scitotenv.2018.03.161>
- Liu, X., Chen, B. W., & Wen, J. K. (2009). Acidithiobacillus played important role in Zijinshan commercial low-grade copper bioleaching heap.
- Longpré, D., Lorusso, L., Levicki, C., Carrier, R., & Cureton, P. (2020). PFOS, PFOA, LC-PFCAS, and certain other PFAS: A focus on Canadian guidelines and guidance for contaminated sites

- management. *Environmental Technology and Innovation*, 18, 100752-100752. <https://doi.org/10.1016/j.eti.2020.100752>
- López-Vizcaíno, R., Sáez, C., Cañizares, P., & Rodrigo, M. A. (2012). The use of a combined process of surfactant-aided soil washing and coagulation for PAH-contaminated soils treatment. *Separation and Purification Technology*, 88, 46-51. <https://doi.org/https://doi.org/10.1016/j.seppur.2011.11.038>
- Lu, W.-B., Shi, J.-J., Wang, C.-H., & Chang, J.-S. (2006). Biosorption of lead, copper and cadmium by an indigenous isolate *Enterobacter* sp. J1 possessing high heavy-metal resistance. *Journal of Hazardous Materials*, 134(1-3), 80-86.
- Luthy, R. G., Aiken, G. R., Brusseau, M. L., Cunningham, S. D., Gschwend, P. M., Pignatello, J. J., Reinhard, M., Traina, S. J., Weber, W. J., & Westall, J. C. (1997). Sequestration of hydrophobic organic contaminants by geosorbents. *Environmental Science & Technology*, 31(12), 3341-3347.
- Ma, Y., Rajkumar, M., Vicente, J. A. F., & Freitas, H. (2010). Inoculation of Ni-resistant plant growth promoting bacterium *Psychrobacter* sp. strain SRS8 for the improvement of nickel phytoextraction by energy crops. *International journal of phytoremediation*, 13(2), 126-139.
- [Record #394 is using a reference type undefined in this output style.]
- Mahinroosta, R., & Senevirathna, L. (2020b). A review of the emerging treatment technologies for PFAS contaminated soils. *Journal of Environmental Management*, 255(June 2019), 109896-109896. <https://doi.org/10.1016/j.jenvman.2019.109896>
- Mathew, M. (2017). *Optimum Co-product Utilization from Hydrothermal Liquefaction of Microalgae*. Arizona State University.
- Matos, M. P. S. R., Correia, A. A. S., & Rasteiro, M. G. (2017). Application of carbon nanotubes to immobilize heavy metals in contaminated soils. *Journal of Nanoparticle Research*, 19(4), 126-126. <https://doi.org/10.1007/s11051-017-3830-x>
- Mena, E., Villaseñor, J., Rodrigo, M. A., & Cañizares, P. (2016). Electrokinetic remediation of soil polluted with insoluble organics using biological permeable reactive barriers: Effect of periodic polarity reversal and voltage gradient. *Chemical Engineering Journal*, 299, 30-36. <https://doi.org/https://doi.org/10.1016/j.cej.2016.04.049>
- Meng, F., Xue, H., Wang, Y., Zheng, B., & Wang, J. (2018). Citric-acid preacidification enhanced electrokinetic remediation for removal of chromium from chromium-residue-contaminated soil. *Environmental Technology*, 39(3), 356-362. <https://doi.org/10.1080/09593330.2017.1301565>
- Meng, F., Xue, H., Wang, Y., Zheng, B., Wang, J., Song, Y., Cang, L., Zuo, Y., Yang, J., Zhou, D., Duan, T., Wang, R., Rezaee, M., Asadollahfardi, G., Gomez-Lahoz, C., Villen-Guzman, M., Paz-Garcia, J. M., Falciglia, P. P., Giustra, M. G., Vagliasindi, F. G. A., Taube, F., Pommer, L., Larsson, T., Shchukarev, A., Nordin, A., Zhang, S., He, Y., Wu, L., Wan, J., Ye, M., Long, T., Yan, Z., Jiang, X., Lin, Y., Lu, X., Abdel-Shafy, H. I., & Mansour, M. S. M. (2019). Remediation of Organochlorine Pesticide-Contaminated Soils by Surfactant-Enhanced Washing Combined with Activated Carbon Selective Adsorption. *Journal of Hazardous Materials*, 29(1), 125439-125439. <https://doi.org/10.1080/09593330.2017.1301565>
- Merino, N., Wang, M., Ambrocio, R., Mak, K., O'Connor, E., Gao, A., Hawley, E. L., Deeb, R. A., Tseng, L. Y., & Mahendra, S. (2018). Fungal biotransformation of 6:2 fluorotelomer alcohol [Article]. *Remediation*, 28(2), 59-70. <https://doi.org/10.1002/rem.21550>
- Millán, M., Bucio-Rodríguez, P. Y., Lobato, J., Fernández-Marchante, C. M., Roa-Morales, G., Barrera-Díaz, C., & Rodrigo, M. A. (2020). Strategies for powering electrokinetic soil remediation: A way to optimize performance of the environmental technology. *Journal of Environmental Management*, 267, 110665-110665. <https://doi.org/https://doi.org/10.1016/j.jenvman.2020.110665>

- Mishra, V. K., & Tripathi, B. D. (2008). Concurrent removal and accumulation of heavy metals by the three aquatic macrophytes. *Bioresource technology*, 99(15), 7091-7097.
- Montinaro, S., Concas, A., Pisu, M., & Cao, G. (2007). Remediation of heavy metals contaminated soils by ball milling. *Chemosphere*, 67(4), 631-639. <https://doi.org/10.1016/j.chemosphere.2006.11.009>
- Nason, S. L., Stanley, C. J., PeterPaul, C. E., Blumenthal, M. F., Zuverza-Mena, N., & Silliboy, R. J. (2021). A community based PFAS phytoremediation project at the former Loring Airforce Base. *iScience*, 24(7), 102777-102777. <https://doi.org/10.1016/J.ISCI.2021.102777>
- [Record #678 is using a reference type undefined in this output style.]
- Niarchos, G., Söregård, M., Fagerlund, F., & Ahrens, L. (2022). Electrokinetic remediation for removal of per- and polyfluoroalkyl substances (PFASs) from contaminated soil. *Chemosphere*, 291, 133041. <https://doi.org/https://doi.org/10.1016/j.chemosphere.2021.133041>
- Nie, L., Shah, S., Rashid, A., Burd, G. I., Dixon, D. G., & Glick, B. R. (2002). Phytoremediation of arsenate contaminated soil by transgenic canola and the plant growth-promoting bacterium *Enterobacter cloacae* CAL2. *Plant Physiology and Biochemistry*, 40(4), 355-361.
- O'Brien, P. L., DeSutter, T. M., Casey, F. X. M., Khan, E., & Wick, A. F. (2018). Thermal remediation alters soil properties – a review. *Journal of Environmental Management*, 206, 826-835. <https://doi.org/https://doi.org/10.1016/j.jenvman.2017.11.052>
- Oliver, D. P., Li, Y., Orr, R., Nelson, P., Barnes, M., McLaughlin, M. J., & Kookana, R. S. (2019). The role of surface charge and pH changes in tropical soils on sorption behaviour of per- and polyfluoroalkyl substances (PFASs). *Science of The Total Environment*, 673, 197-206. <https://doi.org/10.1016/J.SCITOTENV.2019.04.055>
- Ortiz-Soto, R., Leal, D., Gutierrez, C., Aracena, A., Rojo, A., & Hansen, H. K. (2019). Electrokinetic remediation of manganese and zinc in copper mine tailings. *Journal of Hazardous Materials*, 365, 905-911. <https://doi.org/https://doi.org/10.1016/j.jhazmat.2018.11.048>
- Pan, G., Jia, C., Zhao, D., You, C., Chen, H., & Jiang, G. (2009). Effect of cationic and anionic surfactants on the sorption and desorption of perfluorooctane sulfonate (PFOS) on natural sediments. *Environmental Pollution*, 157(1), 325-330. <https://doi.org/https://doi.org/10.1016/j.envpol.2008.06.035>
- Pardo, F., Santos, A., & Romero, A. (2016). Fate of iron and polycyclic aromatic hydrocarbons during the remediation of a contaminated soil using iron-activated persulfate: A column study. *Science of The Total Environment*, 566-567, 480-488. <https://doi.org/https://doi.org/10.1016/j.scitotenv.2016.04.197>
- Pelch, K. E., Reade, A., Wolffe, T. A. M., & Kwiatkowski, C. F. (2019). PFAS health effects database: Protocol for a systematic evidence map. *Environment International*, 130, 104851. <https://doi.org/https://doi.org/10.1016/j.envint.2019.05.045>
- Peluffo, M., Pardo, F., Santos, A., & Romero, A. (2016). Use of different kinds of persulfate activation with iron for the remediation of a PAH-contaminated soil. *Science of The Total Environment*, 563-564, 649-656. <https://doi.org/https://doi.org/10.1016/j.scitotenv.2015.09.034>
- Pierpaoli, M., Szopińska, M., Wilk, B. K., Sobaszek, M., Łuczkiwicz, A., Bogdanowicz, R., & Fudala-Książek, S. (2021). Electrochemical oxidation of PFOA and PFOS in landfill leachates at low and highly boron-doped diamond electrodes. *Journal of Hazardous Materials*, 403, 123606-123606. <https://doi.org/10.1016/j.jhazmat.2020.123606>
- Ponz, F., Hauser, M.-T., Suman, J., Uhlik, O., Viktorova, J., & Macek, T. (2018). Phytoextraction of Heavy Metals: A Promising Tool for Clean-Up of Polluted Environment? *Frontiers in Plant Science* | www.frontiersin.org, 9, 1476-1476. <https://doi.org/10.3389/fpls.2018.01476>

- Pouretedal, H. R., & Sadegh, N. (2014). Effective removal of Amoxicillin, Cephalexin, Tetracycline and Penicillin G from aqueous solutions using activated carbon nanoparticles prepared from vine wood. *Journal of Water Process Engineering*, 1, 64-73. <https://doi.org/https://doi.org/10.1016/j.jwpe.2014.03.006>
- Qiao, M. X., Zhang, Y., Zhai, L. F., & Sun, M. (2018). Corrosion of graphite electrode in electrochemical advanced oxidation processes: Degradation protocol and environmental implication [Article]. *Chemical Engineering Journal*, 344, 410-418. <https://doi.org/10.1016/j.cej.2018.03.105>
- Qin, F., Peng, Y., Song, G., Fang, Q., Wang, R., Zhang, C., Zeng, G., Huang, D., Lai, C., & Zhou, Y. (2020). Degradation of sulfamethazine by biochar-supported bimetallic oxide/persulfate system in natural water: Performance and reaction mechanism. *Journal of Hazardous Materials*, 122816-122816.
- Rai, P. K. (2008). Heavy metal pollution in aquatic ecosystems and its phytoremediation using wetland plants: an ecosustainable approach. *International journal of phytoremediation*, 10(2), 133-160.
- Ramesha, V., Praveen, H. G., & Madhushree, A. (2017). Polycyclic hydrocarbon degradation by bacteria: a review. *Trends in Biosciences*, 10(14), 2465-2473.
- Reddy, K. R., & Cameselle, C. (2009). *Electrochemical remediation technologies for polluted soils, sediments and groundwater*. John Wiley & Sons.
- Ren, D., Li, S., Wu, J., Fu, L., Zhang, X., & Zhang, S. (2019). Remediation of Phenanthrene-Contaminated Soil by Electrokinetics Coupled with Iron/Carbon Permeable Reactive Barrier. *Environmental Engineering Science*, 36(9), 1224-1235. <https://doi.org/10.1089/ees.2019.0066>
- Ren, Y., Zhang, M., & Zhao, D. (2008). Synthesis and properties of magnetic Cu(II) ion imprinted composite adsorbent for selective removal of copper. *Desalination*, 228(1), 135-149. <https://doi.org/https://doi.org/10.1016/j.desal.2007.08.013>
- Rezaee, M., Asadollahfardi, G., Gomez-Lahoz, C., Villen-Guzman, M., & Paz-Garcia, J. M. (2019). Modeling of electrokinetic remediation of Cd- and Pb-contaminated kaolinite. *Journal of Hazardous Materials*, 366, 630-635. <https://doi.org/https://doi.org/10.1016/j.jhazmat.2018.12.034>
- Rodowa, A. E., Knappe, D. R. U., Chiang, S. Y. D., Pohlmann, D., Varley, C., Bodour, A., & Field, J. A. (2020). Pilot scale removal of per- and polyfluoroalkyl substances and precursors from AFFF-impacted groundwater by granular activated carbon. *Environmental Science: Water Research and Technology*, 6(4), 1083-1094. <https://doi.org/10.1039/c9ew00936a>
- Ruiz, C., Mena, E., Cañizares, P., Villaseñor, J., & Rodrigo, M. A. (2014). Removal of 2,4,6-Trichlorophenol from Spiked Clay Soils by Electrokinetic Soil Flushing Assisted with Granular Activated Carbon Permeable Reactive Barrier. *Industrial & Engineering Chemistry Research*, 53(2), 840-846. <https://doi.org/10.1021/ie4028022>
- Saichek, R. E., & Reddy, K. R. (2003). Effect of pH control at the anode for the electrokinetic removal of phenanthrene from kaolin soil. *Chemosphere*, 51(4), 273-287. [https://doi.org/https://doi.org/10.1016/S0045-6535\(02\)00849-4](https://doi.org/https://doi.org/10.1016/S0045-6535(02)00849-4)
- Saifuddin, N., Wong, C. W., & Yasumira, A. A. (2009). Rapid biosynthesis of silver nanoparticles using culture supernatant of bacteria with microwave irradiation. *Journal of Chemistry*, 6(1), 61-70.
- Salt, D. E., Blaylock, M., Kumar, N. P. B. A., Dushenkov, V., Ensley, B. D., Chet, I., & Raskin, I. (1995). Phytoremediation: A novel strategy for the removal of toxic metals from the environment using plants. *Bio/Technology*, 13(5), 468-474. <https://doi.org/10.1038/nbt0595-468>
- Schaefer, C. E., Andaya, C., Urriaga, A., McKenzie, E. R., & Higgins, C. P. (2015). Electrochemical treatment of perfluorooctanoic acid (PFOA) and perfluorooctane sulfonic acid (PFOS)

- in groundwater impacted by aqueous film forming foams (AFFFs). *Journal of Hazardous Materials*, 295, 170-175. <https://doi.org/10.1016/j.jhazmat.2015.04.024>
- Senevirathna, S. T. M. L. D., Mahinroosta, R., Li, M., & KrishnaPillai, K. (2021). In situ soil flushing to remediate confined soil contaminated with PFOS- an innovative solution for emerging environmental issue. *Chemosphere*, 262, 127606-127606. <https://doi.org/10.1016/j.chemosphere.2020.127606>
- Sharma, S., Shetti, N. P., Basu, S., Nadagouda, M. N., & Aminabhavi, T. M. (2022). Remediation of per- and polyfluoroalkyls (PFAS) via electrochemical methods. *Chemical Engineering Journal*, 430, 132895. <https://doi.org/https://doi.org/10.1016/j.ccej.2021.132895>
- Shaw, D. M. J., Munoz, G., Bottos, E. M., Duy, S. V., Sauvé, S., Liu, J., & Van Hamme, J. D. (2019). Degradation and defluorination of 6:2 fluorotelomer sulfonamidoalkyl betaine and 6:2 fluorotelomer sulfonate by *Gordonia* sp. strain NB4-1Y under sulfur-limiting conditions [Article]. *Science of The Total Environment*, 647, 690-698. <https://doi.org/10.1016/j.scitotenv.2018.08.012>
- Shi, C., Wang, X., Zhou, S., Zuo, X., & Wang, C. (2022). Mechanism, application, influencing factors and environmental benefit assessment of steel slag in removing pollutants from water: A review. *Journal of Water Process Engineering*, 47, 102666. <https://doi.org/https://doi.org/10.1016/j.jwpe.2022.102666>
- Shih, Y.-J., Wu, P.-C., Chen, C.-W., Chen, C.-F., & Dong, C.-D. (2020). Nonionic and anionic surfactant-washing of polycyclic aromatic hydrocarbons in estuarine sediments around an industrial harbor in southern Taiwan. *Chemosphere*, 127044-127044. <https://doi.org/https://doi.org/10.1016/j.chemosphere.2020.127044>
- Shtripling, L. O., Kholkin, E. G., & Larionov, K. S. (2016). The Technology Refinement of Soil Decontamination Contaminated with Petroleum Products by the Reagent Capsulation Method. *Procedia Engineering*, 152, 13-17. <https://doi.org/https://doi.org/10.1016/j.proeng.2016.07.609>
- [Record #478 is using a reference type undefined in this output style.]
- Silva, A., Delerue-Matos, C., & Fiúza, A. (2005). Use of solvent extraction to remediate soils contaminated with hydrocarbons. *Journal of Hazardous Materials*, 124(1), 224-229. <https://doi.org/https://doi.org/10.1016/j.jhazmat.2005.05.022>
- Sima, M. W., & Jaffé, P. R. (2021). A critical review of modeling Poly- and Perfluoroalkyl Substances (PFAS) in the soil-water environment. *Science of The Total Environment*, 757, 143793-143793. <https://doi.org/10.1016/j.scitotenv.2020.143793>
- Singer, E., Emerson, D., Webb, E. A., Barco, R. A., Kuenen, J. G., Nelson, W. C., Chan, C. S., Comolli, L. R., Ferriera, S., & Johnson, J. (2011). *Mariprofundus ferrooxydans* PV-1 the first genome of a marine Fe (II) oxidizing Zetaproteobacterium. *PloS one*, 6(9), e25386-e25386.
- Sleep, J. A., & Juhasz, A. L. (2021). A Review of Immobilisation-Based Remediation of Per- and Poly-Fluoroalkyl Substances (PFAS) in Soils. *Current Pollution Reports*, 7(4), 524-539. <https://doi.org/10.1007/s40726-021-00199-z>
- Song, Y., Cang, L., Zuo, Y., Yang, J., Zhou, D., Duan, T., & Wang, R. (2020). EDTA-enhanced electrokinetic remediation of aged electroplating contaminated soil assisted by combining dual cation-exchange membranes and circulation methods. *Chemosphere*, 243, 125439-125439. <https://doi.org/https://doi.org/10.1016/j.chemosphere.2019.125439>
- Song, Y., Tang, H., Yan, Y., Guo, Y., Wang, H., & Bian, Z. (2022). Combining electrokinetic treatment with modified zero-valent iron nanoparticles for rapid and thorough dechlorination of trichloroethene. *Chemosphere*, 292, 133443. <https://doi.org/https://doi.org/10.1016/j.chemosphere.2021.133443>
- Sörensård, M., Gago-Ferrero, P., B. Kleja, D., & Ahrens, L. (2021). Laboratory-scale and pilot-scale stabilization and solidification (S/S) remediation of soil contaminated with per- and

- polyfluoroalkyl substances (PFASs). *Journal of Hazardous Materials*, 402(July 2020), 123453-123453. <https://doi.org/10.1016/j.jhazmat.2020.123453>
- Söregård, M., Lindh, A. S., & Ahrens, L. (2020a). Thermal desorption as a high removal remediation technique for soils contaminated with per- and polyfluoroalkyl substances (PFASs). *PloS one*, 15(6), e0234476. <https://doi.org/10.1371/journal.pone.0234476>
- Söregård, M., Lindh, A. S., & Ahrens, L. (2020b). Thermal desorption as a high removal remediation technique for soils contaminated with per- and polyfluoroalkyl substances (PFASs). *PloS one*, 15(6), e0234476-e0234476. <https://doi.org/10.1371/journal.pone.0234476>
- Söregård, M., Niarchos, G., Jensen, P. E., & Ahrens, L. (2019). Electrolytic per- and polyfluoroalkyl substances (PFASs) removal mechanism for contaminated soil. *Chemosphere*, 232, 224-231. <https://doi.org/10.1016/j.chemosphere.2019.05.088>
- Sørmo, E., Silvani, L., Bjerkli, N., Hagemann, N., Zimmerman, A. R., Hale, S. E., Hansen, C. B., Hartnik, T., & Cornelissen, G. (2021). Stabilization of PFAS-contaminated soil with activated biochar. *Science of The Total Environment*, 763. <https://doi.org/10.1016/j.scitotenv.2020.144034>
- Stokes, A., Douglas, G. B., Fourcaud, T., Giadrossich, F., Gillies, C., Hubble, T., Kim, J. H., Loades, K. W., Mao, Z., & McIvor, I. R. (2014). Ecological mitigation of hillslope instability: ten key issues facing researchers and practitioners. *Plant and Soil*, 377(1-2), 1-23.
- Su, H., Fang, Z., Tsang, P. E., Zheng, L., Cheng, W., Fang, J., & Zhao, D. (2016). Remediation of hexavalent chromium contaminated soil by biochar-supported zero-valent iron nanoparticles. *Journal of Hazardous Materials*, 318, 533-540. <https://doi.org/https://doi.org/10.1016/j.jhazmat.2016.07.039>
- Suanon, F., Tang, L., Sheng, H., Fu, Y., Xiang, L., Wang, Z., Shao, X., Mama, D., Jiang, X., & Wang, F. (2020). Organochlorine pesticides contaminated soil decontamination using TritonX-100-enhanced advanced oxidation under electrokinetic remediation [Article]. *Journal of Hazardous Materials*, 393, Article 122388. <https://doi.org/10.1016/j.jhazmat.2020.122388>
- Sugioka, H., Matsuoka, K., & Moroi, Y. (2003). Temperature effect on formation of sodium cholate micelles. *Journal of Colloid and Interface Science*, 259(1), 156-162. [https://doi.org/10.1016/S0021-9797\(02\)00191-1](https://doi.org/10.1016/S0021-9797(02)00191-1)
- Sui, H., Rong, Y., Song, J., Zhang, D., Li, H., Wu, P., Shen, Y., & Huang, Y. (2018). Mechanochemical destruction of DDTs with Fe-Zn bimetal in a high-energy planetary ball mill. *Journal of Hazardous Materials*, 342, 201-209. <https://doi.org/10.1016/j.jhazmat.2017.08.025>
- Sun, M., Cui, J. n., Guo, J., Zhai, Z., Zuo, P., & Zhang, J. (2020). Fluorochemicals biodegradation as a potential source of trifluoroacetic acid (TFA) to the environment. *Chemosphere*, 254, 126894. <https://doi.org/https://doi.org/10.1016/j.chemosphere.2020.126894>
- Sun, Y., Gao, K., Zhang, Y., & Zou, H. (2017). Remediation of persistent organic pollutant-contaminated soil using biosurfactant-enhanced electrokinetics coupled with a zero-valent iron/activated carbon permeable reactive barrier. *Environmental Science and Pollution Research*, 24(36), 28142-28151. <https://doi.org/10.1007/s11356-017-0371-x>
- Sunil, K., Karunakaran, G., Yadav, S., Padaki, M., Zadorozhnyy, V., & Pai, R. K. (2018). Al-Ti2O6 a mixed metal oxide based composite membrane: A unique membrane for removal of heavy metals. *Chemical Engineering Journal*, 348, 678-684. <https://doi.org/https://doi.org/10.1016/j.cej.2018.05.017>
- Suresh Kumar, P., Prot, T., Korving, L., Keesman, K. J., Dugulan, I., van Loosdrecht, M. C. M., & Witkamp, G.-J. (2017a). Effect of pore size distribution on iron oxide coated granular activated carbons for phosphate adsorption – Importance of mesopores. *Chemical Engineering Journal*, 326, 231-239. <https://doi.org/https://doi.org/10.1016/j.cej.2017.05.147>

- Suresh Kumar, P., Prot, T., Korving, L., Keesman, K. J., Dugulan, I., van Loosdrecht, M. C. M., & Witkamp, G. J. (2017b). Effect of pore size distribution on iron oxide coated granular activated carbons for phosphate adsorption – Importance of mesopores. *Chemical Engineering Journal*, 326, 231-239. <https://doi.org/10.1016/j.cej.2017.05.147>
- Taube, F., Pommer, L., Larsson, T., Shchukarev, A., & Nordin, A. (2008). Soil Remediation – Mercury Speciation in Soil and Vapor Phase During Thermal Treatment. *Water, Air, and Soil Pollution*, 193(1), 155-163. <https://doi.org/10.1007/s11270-008-9679-y>
- Teaf, C. M., Garber, M. M., Covert, D. J., & Tuovila, B. J. (2019). Perfluorooctanoic Acid (PFOA): Environmental Sources, Chemistry, Toxicology, and Potential Risks. *Soil and Sediment Contamination*, 28(3), 258-273. <https://doi.org/10.1080/15320383.2018.1562420>
- Tengvall, P. (2017). 4.6 Protein Interactions With Biomaterials ☆. In P. Ducheyne (Ed.), *Comprehensive Biomaterials II* (pp. 70-84). Elsevier. <https://doi.org/https://doi.org/10.1016/B978-0-12-803581-8.10110-9>
- Turner, L. P., Kueper, B. H., Jaansalu, K. M., Patch, D. J., Battye, N., El-Sharnouby, O., Mumford, K. G., & Weber, K. P. (2021). Mechanochemical remediation of perfluorooctanesulfonic acid (PFOS) and perfluorooctanoic acid (PFOA) amended sand and aqueous film-forming foam (AFFF) impacted soil by planetary ball milling. *Science of The Total Environment*, 765, 142722-142722. <https://doi.org/10.1016/j.scitotenv.2020.142722>
- van Asselt, E. D., Rietra, R. P. J. J., Römkens, P. F. A. M., & van der Fels-Klerx, H. J. (2011). Perfluorooctane sulphonate (PFOS) throughout the food production chain. *Food Chemistry*, 128(1), 1-6. <https://doi.org/https://doi.org/10.1016/j.foodchem.2011.03.032>
- Vidonish, J. E., Zygourakis, K., Masiello, C. A., Sabadell, G., & Alvarez, P. J. J. (2016). Thermal Treatment of Hydrocarbon-Impacted Soils: A Review of Technology Innovation for Sustainable Remediation. *Engineering*, 2(4), 426-437. <https://doi.org/10.1016/J.ENG.2016.04.005>
- Viet, P. V., Nguyen, H. T., Cao, T. M., & Hieu, L. V. (2016). Fusarium antifungal activities of copper nanoparticles synthesized by a chemical reduction method. *Journal of Nanomaterials*, 2016.
- Villen-Guzman, M., Paz-Garcia, J. M., Rodriguez-Maroto, J. M., Garcia-Herruzo, F., Amaya-Santos, G., Gomez-Lahoz, C., & Vereda-Alonso, C. (2015). Scaling-up the acid-enhanced electrokinetic remediation of a real contaminated soil. *Electrochimica Acta*, 181, 139-145. <https://doi.org/https://doi.org/10.1016/j.electacta.2015.02.067>
- Virkutyte, J., Sillanpää, M., & Latostenmaa, P. (2002). Electrokinetic soil remediation — critical overview. *Science of The Total Environment*, 289(1), 97-121. [https://doi.org/https://doi.org/10.1016/S0048-9697\(01\)01027-0](https://doi.org/https://doi.org/10.1016/S0048-9697(01)01027-0)
- Vunain, E., Mishra, A. K., & Mamba, B. B. (2016). Dendrimers, mesoporous silicas and chitosan-based nanosorbents for the removal of heavy-metal ions: A review. *International Journal of Biological Macromolecules*, 86, 570-586. <https://doi.org/https://doi.org/10.1016/j.ijbiomac.2016.02.005>
- Wan, J., Li, Z., Lu, X., & Yuan, S. (2010). Remediation of a hexachlorobenzene-contaminated soil by surfactant-enhanced electrokinetics coupled with microscale Pd/Fe PRB. *Journal of Hazardous Materials*, 184(1), 184-190. <https://doi.org/https://doi.org/10.1016/j.jhazmat.2010.08.022>
- Wang, F., & Shih, K. (2011). Adsorption of perfluorooctanesulfonate (PFOS) and perfluorooctanoate (PFOA) on alumina: influence of solution pH and cations. *Water Res*, 45(9), 2925-2930. <https://doi.org/10.1016/j.watres.2011.03.007>
- Wang, J., Lin, Z., He, X., Song, M., Westerhoff, P., Doudrick, K., & Hanigan, D. (2022). Critical Review of Thermal Decomposition of Per- and Polyfluoroalkyl Substances: Mechanisms and Implications for Thermal Treatment Processes. *Environmental Science & Technology*, 56(9), 5355-5370. <https://doi.org/10.1021/acs.est.2c02251>

- Wang, K., Huang, D., Wang, W., Ji, Y., & Niu, J. (2020). Enhanced perfluorooctanoic acid degradation by electrochemical activation of peroxymonosulfate in aqueous solution. *Environment International*, 137, 105562-105562. <https://doi.org/10.1016/J.ENVINT.2020.105562>
- Wang, X., Li, X., Yan, X., Tu, C., & Yu, Z. (2021). Environmental risks for application of iron and steel slags in soils in China: A review. *Pedosphere*, 31(1), 28-42. [https://doi.org/https://doi.org/10.1016/S1002-0160\(20\)60058-3](https://doi.org/https://doi.org/10.1016/S1002-0160(20)60058-3)
- Wang, Y., Fang, Z., Kang, Y., & Tsang, E. P. (2014). Immobilization and phytotoxicity of chromium in contaminated soil remediated by CMC-stabilized nZVI. *Journal of Hazardous Materials*, 275, 230-237. <https://doi.org/https://doi.org/10.1016/j.jhazmat.2014.04.056>
- Wen, D., Fu, R., & Li, Q. (2021). Removal of inorganic contaminants in soil by electrokinetic remediation technologies: A review. *Journal of Hazardous Materials*, 401, 123345. <https://doi.org/https://doi.org/10.1016/j.jhazmat.2020.123345>
- Wen, D. D., Fu, R. B., Zhang, W., & Gu, Y. Y. (2017). Enhanced Electrokinetic Remediation of Heavy Metals Contaminated Soils by Stainless Steel Electrodes as well as the Phenomenon and Mechanism of Electrode Corrosion and Crystallization [Article]. *Huanjing Kexue/Environmental Science*, 38(3), 1209-1217. <https://doi.org/10.13227/j.hjx.201608195>
- Yadav, A., Chowdhary, P., Kaithwas, G., & Bharagava, R. N. (2017). 9 Toxic Metals in the Environment. *Handbook of Metal-Microbe Interactions and Bioremediation*.
- Yan, D., Gang Daniel, D., Zhang, N., & Lin, L. (2013). Adsorptive Selenite Removal Using Iron-Coated GAC: Modeling Selenite Breakthrough with the Pore Surface Diffusion Model. *Journal of Environmental Engineering*, 139(2), 213-219. [https://doi.org/10.1061/\(ASCE\)EE.1943-7870.0000633](https://doi.org/10.1061/(ASCE)EE.1943-7870.0000633)
- Yan, Y., Xue, F., Muhammad, F., Yu, L., Xu, F., Jiao, B., Shiao, Y. C., & Li, D. (2018). Application of iron-loaded activated carbon electrodes for electrokinetic remediation of chromium-contaminated soil in a three-dimensional electrode system. *Scientific Reports*, 8(1), 1-11. <https://doi.org/10.1038/s41598-018-24138-z>
- Yang, Y., Zeng, G., Huang, D., Zhang, C., He, D., Zhou, C., Wang, W., Xiong, W., Li, X., & Li, B. (2020). Molecular engineering of polymeric carbon nitride for highly efficient photocatalytic oxytetracycline degradation and H₂O₂ production. *Applied Catalysis B: Environmental*, 118970.
- Yuan, S., Tian, M., & Lu, X. (2006). Electrokinetic movement of hexachlorobenzene in clayed soils enhanced by Tween 80 and beta-cyclodextrin. *Journal of Hazardous Materials*, 137(2), 1218-1225. <https://doi.org/10.1016/j.jhazmat.2006.04.014>
- Zegzouti, Y., Boutafda, A., Ezzariai, A., El Fels, L., El Hadek, M., Hassani, L. A. I., & Hafidi, M. (2020). Bioremediation of landfill leachate by *Aspergillus flavus* in submerged culture: Evaluation of the process efficiency by physicochemical methods and 3D fluorescence spectroscopy. *Journal of Environmental Management*, 255, 109821-109821.
- Zeng, Q., Peng, S., Liu, M., Song, Z., Wang, X., Zhang, X., & Hong, S. (2013). Solubilization and adsorption behaviors of 2,4,6-trichlorophenol in the presence of surfactants. *Chemical Engineering Journal*, 230, 202-209. <https://doi.org/10.1016/J.CEJ.2013.06.058>
- Zhan, J., Zhang, A., Héroux, P., Guo, Y., Sun, Z., Li, Z., Zhao, J., & Liu, Y. (2020). Remediation of perfluorooctanoic acid (PFOA) polluted soil using pulsed corona discharge plasma. *Journal of Hazardous Materials*, 387, 121688. <https://doi.org/https://doi.org/10.1016/j.jhazmat.2019.121688>
- Zhang, J., Zhang, G., Cai, D., & Wu, Z. (2015). Immediate remediation of heavy metal (Cr(VI)) contaminated soil by high energy electron beam irradiation. *Journal of Hazardous Materials*, 285, 208-211. <https://doi.org/10.1016/j.jhazmat.2014.11.007>

- Zhang, Z., Sarkar, D., Biswas, J. K., & Datta, R. (2022). Biodegradation of per- and polyfluoroalkyl substances (PFAS): A review. *Bioresource technology*, 344, 126223. <https://doi.org/https://doi.org/10.1016/j.biortech.2021.126223>
- Zhou, H., Liu, Z., Li, X., & Xu, J. (2020). Remediation of lead (II)-contaminated soil using electrokinetics assisted by permeable reactive barrier with different filling materials. *Journal of Hazardous Materials*, 124885.
- Zhou, H., Xu, J., Lv, S., Liu, Z., & Liu, W. (2020). Removal of cadmium in contaminated kaolin by new-style electrokinetic remediation using array electrodes coupled with permeable reactive barrier. *Separation and Purification Technology*, 239, 116544-116544. <https://doi.org/10.1016/J.SEPPUR.2020.116544>
- Zhu, J., Chen, Y., Gu, Y., Ma, H., Hu, M., Gao, X., & Liu, T. (2022). Feasibility study on the electrochemical reductive decomposition of PFOA by a Rh/Ni cathode. *Journal of Hazardous Materials*, 422, 126953. <https://doi.org/https://doi.org/10.1016/j.jhazmat.2021.126953>